# Framework to Analyze Interactions between Transmission and Distribution (T&D) Systems with High Distributed Energy Resource (DER) Penetrations

*Final Project Report*

T-60

**Power Systems Engineering Research Center**
*Empowering Minds to Engineer*
*the Future Electric Energy System*

# Framework to Analyze Interactions between Transmission and Distribution (T&D) Systems with High Distributed Energy Resource (DER) Penetrations

**Final Project Report**

**Project Team**
Anamika Dubey, Project Leader
Washington State University

P.K. Sen
Colorado School of Mines

**Graduate Students**
Gayathri Krishnamoorthy
Washington State University

Yaswanth Nag Velaga
Aoxia (Kevin) Chen
Colorado School of Mines

**PSERC Publication 19-03**

September 2019

**For information about this project, contact:**

Anamika Dubey
Assistant Professor
Department of Electrical Engineering and Computer Science
Washington State University
355 NE Spokane St, Pullman, WA 99163
Office: EME 23
Phone: (509) 335-1865
Email: anamika.dubey@wsu.edu

**Power Systems Engineering Research Center**

The Power Systems Engineering Research Center (PSERC) is a multi-university Center conducting research on challenges facing the electric power industry and educating the next generation of power engineers. More information about PSERC can be found at the Center's website: http://www.pserc.org.

**For additional information, contact:**

Power Systems Engineering Research Center
Arizona State University
527 Engineering Research Center
Tempe, Arizona 85287-5706
Phone: 480-965-1643
Fax: 480-727-2052

# Acknowledgements

We express our appreciation for the support provided by PSERC's industry members and thank the industry advisors for this project:

- Lei Fan, Devin T Van Zandt (General Electric Energy)
- Sakshi Mishra, Larry E Anderson II, Pankaj Kansal, Beverly Laios, Tom Weaver III (American Electric Power)
- Anupam Thatte (Midcontinent Independent System Operator)
- Yohan Sutjandra (The Energy Authority)
- S. Kolluri (Entergy)
- Aftab Alam (California Independent System Operator)
- Angel Aquino (Power World)
- Bill Middaugh, Chris Pink (Tri-State Generation and Transmission)
- Fei Ding, B Palmintier, Murali Baggu, Ben Kroposki, Santosh Veda (National Renewable Energy Laboratory)
- Dan Hamai (Western Area Power Administration)
- Deepak Ramasubramanian, Anish Gaikwad, Parag Mitra, Jens Boemer, Evangelos Farantatos (Electric Power Research Institute)
- Francisco G Velez-Cedeno (Virginia Power)
- Di Shi, Xi Chen (Global Energy Interconnection Research Institute)
- Orlando Ciniglio, Milorad Papic (Idaho Power)
- Francisco G Velez-Cedeno, Gefei "Derek" Kou (Dominion Virginia Power)

# Executive Summary

With the growing levels of DER deployment, it is imperative to analyze the interactions between electric power transmission and distribution (T&D) systems, especially the impacts of distribution system connected DERs on the transmission systems operations. This project develops an iteratively coupled T&D analysis framework through co-simulation approach to address the future requirements for modeling and analysis of the large-scale integrated T&D systems with high levels of DER penetrations. The impacts of DERs on T&D system may manifest as steady-state concerns (voltage regulation, variability, voltage unbalance), dynamic concerns (frequency regulation), or in its transient response (angle and voltage stability during faults). Depending upon the requirements for DER impact study, we present three types of co-simulation methods: *quasi-static co-simulation* to evaluate steady-state concerns; *hybrid co-simulation* to evaluate and mitigate frequency regulation concerns, and *dynamic co-simulation* to model T&D system response during transients/faults.

The proposed framework utilizes dedicated software modules to solve the decoupled T&D models. The T&D interactions are captured by exchanging network solutions at the point of common coupling (PCC). An iterative coupling approach is adopted for co-simulation that results in a co-simulation model that closely approximates the behavior of a stand-alone unified T&D simulation platform. The iterative vs. non-iterative coupling of T&D systems are thoroughly evaluated using rigorous simulation studies. It is observed that a non-iterative coupling for quasi-static T&D co-simulation study may lead to significant errors for cases with significant DER variability and unbalanced loading conditions. However, a non-iterative coupling may be able to accurately model hybrid co-simulation cases if simulation time is advanced in small steps. Finally, it is validated that a coupled T&D model with a three-sequence transmission system model and power flow solver is more accurate compared to a positive-sequence model, especially when DERs introduce significant phase unbalance.

**Need for Co-Simulation**

Several exploratory studies and field demonstrations have pointed out that the new and recent developments, including the integration of DERs, electric vehicle loads, and energy storage units are increasing the stress on power delivery systems. Unfortunately, most of the existing DER interconnection studies evaluate the integrational challenges of DERs either only at the distribution level or on a decoupled T&D system. The decoupled T&D system analysis models (1) distribution system as lumped loads and (2) transmission system as a constant power source. The potential impacts on the transmission grid are either ignored given low penetrations of DERs or are non-representative due to the decoupled T&D model. It is expected that the ongoing and future large-scale DER deployment projects can potentially affect the regional transmission grid operations. The situation worsens in rural areas where the distribution system is lightly loaded and covers an extended area with low load density. Specifically, in the lightly loaded areas, with the increase in DER penetrations, the distributed generation may exceed the local consumption needs, resulting in a reverse power flow condition from individual consumers through the feeders back to the distribution substation and possibly into the transmission system. Therefore, a decoupled analysis of T&D system is no longer adequate, calling for new tools capable of capturing the interactions between T&D systems with high-levels of DER penetrations.

**Summary of the Research Contributions**

As discussed before, in this project, three co-simulation models are developed to evaluate the impacts of DERs on the integrated T&D systems. These are quasi-static co-simulation (suitable for voltage regulation and power flow studies), hybrid co-simulation (to simulate frequency regulation concerns and AGC response from DERs), and dynamic co-simulation (to model system response during transients and faults).

In Chapter 1, we detail an iteratively coupled *quasi-static T&D co-simulation* framework where both the transmission and distribution systems are simulated in quasi-static mode. This part is the major emphasis of this project, and the work is jointly conducted by Washington State University and Colorado School of Mines. In Chapter 2, a *hybrid co-simulation* framework is developed to study DER variability and its effects on the bulk grid frequency and AGC response. In *hybrid co-simulation approach*, we model the transmission system in dynamic simulation mode while distribution system is modeled in a quasi-static mode; this part of the study is mainly conducted by Washington State University. In Chapter 3, a *dynamic T&D co-simulation* framework is introduced by Colorado School of Mines where both transmission and distribution systems are simulated in dynamic mode. The objective is to study the integrated system response during faults and transients with high-levels of DER penetrations.

**Chapter 1 – Quasi-Static T&D Co-Simulation Framework**

The focus of this chapter is the development of an iteratively coupled co-simulation framework for the quasi-static analysis of T&D systems. Therefore, the transmission and distribution systems are simulated in the quasi-static mode of operation. Recently, several T&D co-simulation frameworks for the quasi-static analysis have been proposed in the literature, including, but not limited to FNCS, IGMS, HELICS. The existing quasi-static T&D co-simulation frameworks, however, are limited in accurately modeling T&D interactions as these conduct transmission system analyses using a balanced positive sequence power flow approach that does not account for unbalanced load conditions. Furthermore, the existing co-simulation methods loosely couple T&D systems introducing errors in the solutions. To address these concerns, an approach to iteratively couple the T&D systems using a co-simulation approach is proposed. The proposed framework is comprised of three modules: a three-sequence ac power flow for the transmission system, a three-phase power flow solver for the distribution system, and an iterative coupling approach at the T&D interface. The co-simulation approach is implemented using MATLAB coupled with OpenDSS. The proposed framework is suitable for the integrated analysis of T&D systems subject to unbalanced load conditions and significant variations in load demand.

An analytical formulation for the boundary variable updates that represent the coupled T&D system with interface constraint equations is developed. This analytical model characterizes the convergence of the proposed iterative co-simulation framework as a function of T&D system conditions. The developed non-linear interface constraint equations are solved using the first-order and second-order convergent techniques based on Fixed-Point Iteration (FPI) and Quasi-Newton method, respectively. The proposed iteratively coupled quasi-static T&D co-simulation framework is used to evaluate the impacts of distribution-connected PVs on both transmission and distribution system voltages.

The developed framework is tested using IEEE 9-bus and IEEE 39-bus transmission system models coupled with multiple EPRI Ckt-24 distribution feeder model. The conditions for convergence by exchanging the boundary variables at the PCC are examined in detail using several case studies with varying levels of distribution load unbalance and PV penetrations. The simulation results highlight the need for co-simulation when evaluating DER impacts for the cases with high levels of distributed PV deployment and their utility in supporting the grid via active voltage regulation methods. A case study in which multiple distribution systems coupled to the transmission load points is also presented to demonstrate the scalability of the approach. The results obtained using co-simulation approach are validated against a standalone T&D system simulated in OpenDSS. It is demonstrated that the iteratively coupled T&D model closely approximates the stand-alone T&D model for highly stressed system conditions.

The main take away here is that the iteratively coupled co-simulation framework provides accurate convergence characteristics at the T&D boundary when compared to the existing loosely coupled co-simulation models. It is also shown that the boundary variable update rules (also called co-iteration rules) using Quasi Newton method results in faster convergence than the FPI method; the improvements in the number of iterations and the time taken to converge are more pronounced for stressed system conditions.

**Chapter 2– Hybrid T&D Co-Simulation Framework**

The increasing penetrations of renewable resources such as solar and wind resources with high variability in generation patterns may result in increased uncertainty in the supply and demand unbalance. In the bulk grid, the frequency regulation services performed by automatic generation control (AGC) plays a critical role in maintaining the supply-demand balance. Traditionally, the majority of frequency regulation capability is provided by specially equipped generators. As technologies evolve, the participation of new types of flexible energy resources such as battery energy storage systems (BESS) and flywheels, with their significantly faster ramping capabilities, can reduce the need to procure additional regulation capacity for variable generation resources. In order to successfully integrate BESS technologies in the grid for frequency regulation services, they must be included in the distribution system planning process, and their impacts should be evaluated at both transmission and distribution levels.

Owing to these emerging concerns, there is a need for integrated modeling and analysis of transmission and distribution systems for the AGC simulation studies. A high-level of DER penetrations in the distribution system may lead to reverse power flow from distribution to transmission systems that may adversely affect the transmission system operations resulting in frequency regulation problems. Furthermore, with frequent load changes and BESS responding to RegD (fast responding AGC signals) from the ISO, an aggregate battery model at the T&D coupling point is no longer adequate to represent actual system response. The ISOs should be aware of the BESS availability at every connecting point in the distribution system to perform planning studies for AGC response from BESS requiring an integrated T&D system analysis. While a fully dynamic T&D model can capture these scenarios, it is unnecessarily complicated. This is because, although the transmission system needs to be modeled in a dynamic mode to fully study the bulk grid AGC response, for frequency regulation concerns, the effects of distribution-connected DER generation variability can be captured using quasi-static simulations for distribution systems. This calls for a hybrid co-simulation platform that can appropriately model the bulk grid frequency response due to variable DERs.

In this chapter, an iteratively coupled T&D hybrid co-simulation framework is developed to study the effects of distribution-connected DERs/PVs on AGC response and the utility of BESS in maintaining supply-demand balance for scenarios with highly variable DER/PV generation profiles. The proposed hybrid co-simulation framework is demonstrated using IEEE 9-bus transmission system model coupled with multiple EPRI Ckt-24 distribution system models. The generator dynamic model for the IEEE 9-bus transmission system is available in PSAT MATLAB toolbox. The quasi-static model for distribution system is developed using OpenDSS. The interactions between transmission and distribution systems at the point of common coupling (PCC) are captured using a tightly-coupled co-simulation interface developed in MATLAB. The developed hybrid T&D co-simulation platform is used to understand the PV integration impacts at both transmission and distribution levels, specifically, the effects of PV generation variability on the AGC dispatch signals. The utility of distribution-connected BESS on improving the AGC response by providing frequency regulation services is also detailed.

**Chapter 3 – Dynamic T&D Co-Simulation Framework**

The existing dynamic co-simulation studies focus on studying the stability issues for the bulk grid when subjected to a transient event such as transmission line faults. The high-levels of DER penetrations can potentially aggravate or reduce the stability concerns during and post transient period. For example, the revised interconnection standard IEEE 1547-2018 allows the DERs to provide ride-through capabilities for dynamic voltage and frequency support that can help mitigate stability concerns for the bulk grid. The primary objective of this chapter is to develop a framework to understand the effects of high DER penetrations during faults on the bulk grid. Towards this goal, we present a loosely coupled T&D co-simulation framework for dynamic studies along with a model for DER ride-through requirements for distribution-connected DERs. The proposed framework leverages the stand-alone programs for dynamic simulation of T&D systems by coupling the solutions at the T&D interface. An integrated T&D dynamic model is developed using a positive-sequence simulation for the transmission system and a three-phase approach for the distribution systems. The T&D dynamic co-simulation is developed using PSAT & OpenDSS with MATLAB interface; transmission positive sequence dynamic model is developed in PSAT and distribution systems dynamics are simulated using the dynamic simulation mode in OpenDSS. The control of DER smart inverters is modeled using the IEEE 1547-2018 standard. Preliminary studies are presented to assess the impacts of DERs on the bulk grid system.

**Project Publications:**

[1] Krishnamoorthy, Gayathri, and Anamika Dubey. "A framework to analyze interactions between transmission and distribution systems." In *2018 IEEE Power & Energy Society General Meeting (PESGM),* pp. 1-5. IEEE, 2018.

[2] Yaswanth Nag Velaga, Aoxia Chen, P. K. Sen, Gayathri Krishnamoorthy, and Anamika Dubey. "Transmission-Distribution Co-Simulation: Model Validation with Standalone Simulation." In *2018 North American Power Symposium (NAPS)*, pp. 1-6. IEEE, 2018. (second best paper)

[3] G. Krishnamoorthy and A. Dubey, "Transmission–Distribution Cosimulation: Analytical Methods for Iterative Coupling," in *IEEE Systems Journal*.

[4] Krishnamoorthy, Gayathri, and Anamika Dubey. "Iteratively-Coupled Co-simulation Framework for Unbalanced Transmission-Distribution System," *accepted for publication in IEEE PES PowerTech Milano 2019.*

[5] Gayathri Krishnamoorthy, and Anamika Dubey. " Distributed PV Penetration Impact Analysis on Transmission System Voltages using Co-Simulation" accepted for presentation in *2019 North American Power Symposium (NAPS).*

[6] Yaswanth Nag Velaga, Aoxia Chen, P.K. Sen, Gayathri Krishnamoorthy, and Anamika Dubey "Advancements in Co-Simulation Techniques in Combined Transmission & Distribution Systems Analysis," *accepted for publication in The Journal of Engineering*.

[7] Yaswanth Nag, Aoxia Chen, Gayathri Krishnamoorthy, Anamika Dubey, and P.K. Sen, "Trends and Future of Rural Electric Utilities: Challenges and Opportunities," *accepted for publication in IEEE IAS REPC Conference (2019)*.

[8] Rabayet Sadnan, Gayathri Krishnamoorthy, and Anamika Dubey "Comparison of different coupling method used in transmission and distribution (T&D) co-simulation', *submitted to IET GT&D.*

[9] Gayathri Krishnamoorthy, and Anamika Dubey, "Hybrid Transmission Distribution (T&D) Co-simulation Platform: Frequency Regulation Services using Battery Energy Storage Systems," submitted to PSCC 2020.

[10] Gayathri Krishnamoorthy, and Anamika Dubey, "Co-optimization of T&D system operations by optimal scheduling of Battery Energy Storage Systems (BESS)," (in preparation).

**Student Thesis:**

[1] Gayathri Krishnamoorthy, "An Iterative Co-simulation Framework for the Integrated Transmission and Distribution System Analysis," M.S. Thesis, Washington State University, May 2018.

[2] Yaswanth Nag Velaga, "Co-simulation Framework for Integrated Transmission and Distribution (T&D) Analysis with High Distributed Energy Resource (DER) Penetrations" Ph.D. dissertation, Colorado School of Mines (in progress).

# Table of Contents

# List of Figures

# List of Tables

# 1. Quasi-Static T&D Co-Simulation Framework and Impacts of Integrating Distributed Energy Resources (DERs)

## 1.1 Introduction

### 1.1.1 Background

The electric power grid is one of the nation's most critical infrastructures, and virtually every system in modern society depends on the reliable delivery of electricity. At present, the U.S. power grid has more than 9,200 electric generating units with 1 million megawatts of generating capacity and more than 600,000 miles of transmission lines. The electric infrastructure today is significantly stressed due to dramatically changing load and generation characteristics [1]. The grid was originally designed for unidirectional power flow using dispatchable generation units for predictable customer loads. However, with the integration of distributed energy resources (DERs), the grid is experiencing bidirectional power flows, variable and uncertain generation, and stochastic load demands [2]. A significant effort has been lately directed towards grid modernization using advanced sensing and control devices to address these concerns [3]. Several smart grid demonstration projects have worked on improving the grid functionalities using smart devices and controls such as phasor measurement units (PMUs) that allows operators to assess the grid stability, relays that can quickly recover the system from faults, advanced digital meters that can automatically report outages, renewables that can support peak consumer demands, and batteries that can store excess energy to improve grid operations [4]. To this regard, a smart grid is characterized by the integration of information and communication technologies into the traditional power systems using intelligent electronic devices (IEDs) for sensing and monitoring purposes, and integration of DERs and demand response for advanced system control and operations. Integration of smart grid technologies is focused on providing systematic emergency response, better restoration practices, and intelligent optimization and control methodologies.

With the incentivized rapid decarbonization of electric power generation industry and the aggressive renewable portfolio standards (RPS) (see Figure 1.1), the electric power delivery system, i.e. the integrated transmission and distribution (T&D) systems are expected to transform rapidly in the foreseeable future [5]. Also, federal policymakers have put forward proposals to establish a national RPS, that makes technological developments an immediate requirement for the existing grid. Although low-levels of DER penetrations can be easily integrated, accommodating more than 30% generation from these renewable sources will require new techniques to operating and interacting within the grid [6]. With the increasing integration of DERs, technical changes are expected both on generation and load ends [7]. The generation end is likely to have changes that will include efficient use of variable-generation forecasting in standard grid operation practices, more flexible operating characteristics with high tolerance to frequency ramping and part-load efficiencies and providing possible modifications to base-load units. Electric vehicle loads, load-shifting encouragement with distribution market practices, increased flexibility in loads driven by utility demand-response programs are some of the changes expected on the load end. Therefore, in order to achieve renewable energy goals, innovations are called for reliably integrating new generation resources into the existing grid.

Given recent changes in T&D systems, another line of research has focused on evaluating the impacts of integrating new technologies, especially DERs into the existing T&D systems. This includes the development of software platforms and simulation studies to perform quantitative analysis of DER impacts on T&D systems. However, the existing models evaluate the impacts of DERs separately for transmission and distribution systems. The objective of this chapter is to address this concern by developing an integrated T&D framework using co-simulation approach that accurately models the two systems in their dedicated software platforms to perform DER integration analysis.

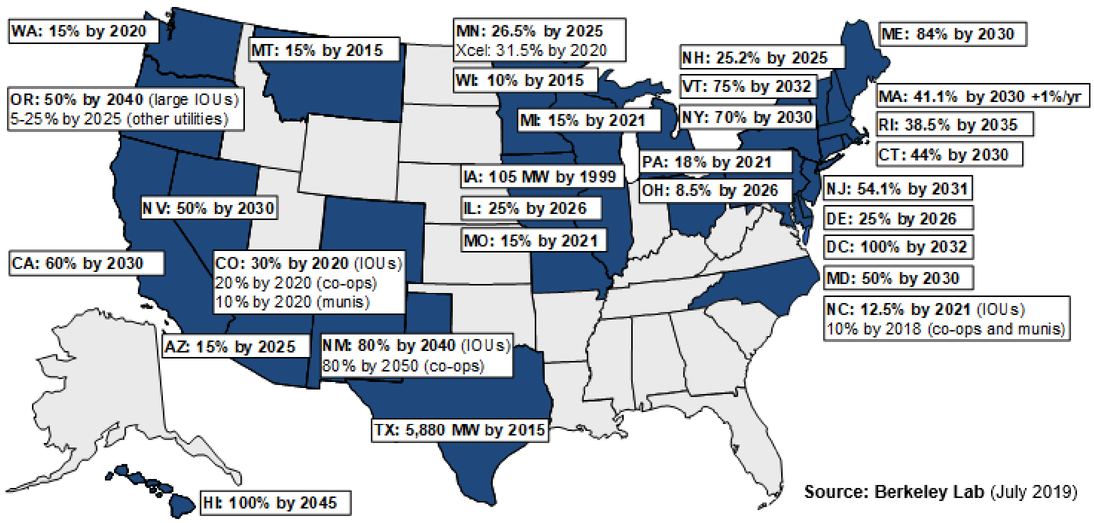


Figure 1.1 RPS 2019 report on the integration of renewable resources to the grid in the U.S.

### 1.1.2 Literature Review

Most of the traditional approaches that model the integrated framework decouple the T&D systems while conducting DER interconnection studies. In the decoupled framework, the distribution system is modeled as a lumped load for transmission system analysis, and transmission system is modeled as an ideal power supply for distribution system analysis. This decoupled model cannot capture the interactions between the transmission and distribution systems accurately. In literature, multiple frameworks to model T&D interactions have been proposed to address this concern [8-17]. Based on the existing methods, these frameworks are primarily categorized as the following:

A. Standalone unified tools using an integrated power system modeling in one platform
B. Co-simulation methods to combine multiple interacting domains for an integrated T&D system modeling and analysis.

#### A. Standalone Unified Models

The "standalone" unified framework models the entire T&D system on a single simulation platform. The example of standalone T&D modeling tools includes Energynet Platform by New Power Technologies [8] and GridLAB-D by PNNL [9]. The Energynet project was dedicated to developing an approach to integrate distribution and transmission operations to evaluate the regional grid impacts of wholesale PV projects. The results from this project show that a new level of modeling capability was needed to visualize the impacts of DERs, particularly in those where distribution connected systems have impacts extending beyond a single feeder through the substation and into the transmission systems. This indicates that the impacts of PVs deployed on the distribution system is reflected in transmission systems operations and using the integrated T&D platform, it is possible to achieve coordinated control of T&D systems. Similarly, the GridLAB-D project from PNNL integrated the distribution systems, transactive markets, and other end-use load models using an agent-based simulation framework. Since GridLAB-D is an open-source software platform, several smart grid problems in renewable integration and demand response were studied. The article in [9] details how the integrated T&D models are developed using an agent-based paradigm. This model has potential applications in Volt-VAR optimization, providing demand response for renewables integration and real-time pricing demonstrations. This study was done to simplify the integration of multiple simulation environments by modeling all the components on a single platform using GridLAB-D.

The major limitation of the standalone unified modeling approach is the cost of simulating a unified T&D model. Given each distribution feeder includes 100s-1000s of nodes and multiple such feeders may be connected at the point-of-common coupling (PCC) for the T&D systems, a standalone model is usually too expensive to simulate and analyze. It is tedious and time-consuming to build all the components of a complex electric power generation and distribution systems on a single platform. Moreover, the unified model fails to take advantage of legacy software tools that are dedicated to modeling individual domains. These legacy tools have specialized functional capabilities corresponding to their operational domains, i.e. transmission or distribution systems. Therefore, it is usually unnecessary and inefficient to bring together all of those functionalities in a single environment to model a stand-alone T&D system.

### B. Co-Simulation Models

The "co-simulation" approach models the interactions between multiple domains while simultaneously solving the individual systems, in this case transmission and distribution systems, in their respective solvers. Essentially, in a co-simulation approach, a hierarchical model is developed where single transmission-level representation connects to a large number of distribution systems that are run in parallel. The major advantage is that it can integrate the existing simulators available in different domains to make the interconnection studies scalable. One of the limitations of the co-simulation framework is the inherent complexity of each interacting domains. Simulating the detailed model while including several operations carried out in multiple timescales and obtaining the coupling is a complicated task requiring time synchronization and efficient convergence protocols. A few examples of co-simulation framework in the literature are Framework for Network Co-Simulation (FNCS) from PNNL [10], GridSpice [11], Integrated Grid Modeling System (IGMS) by NREL [12], and HELICS platform [13].

#### Framework for Network Co-Simulation (FNCS)

The FNCS platform by PNNL integrates simulators in multiple domains using a common communication platform. For instance, the transmission system in MATPOWER, distribution system in GridLAB-D, and wholesale markets in MATPOWER are interconnected through network simulator-3. This integrated platform is called "FNCS." This platform helps provide time synchronization and interchange of messages between various simulators. FNCS is programmed in C++ and easily interfaces with C, JAVA, Fortran, etc. The major design goal is to re-use the existing simulators, as shown in Figure 1.2. This platform has potential applications in various domains, including real-time market pricing, transmission, distribution and market communications, etc. Reference [10] provides detailed information on the design of the platform and its endless expandability to multiple applications.

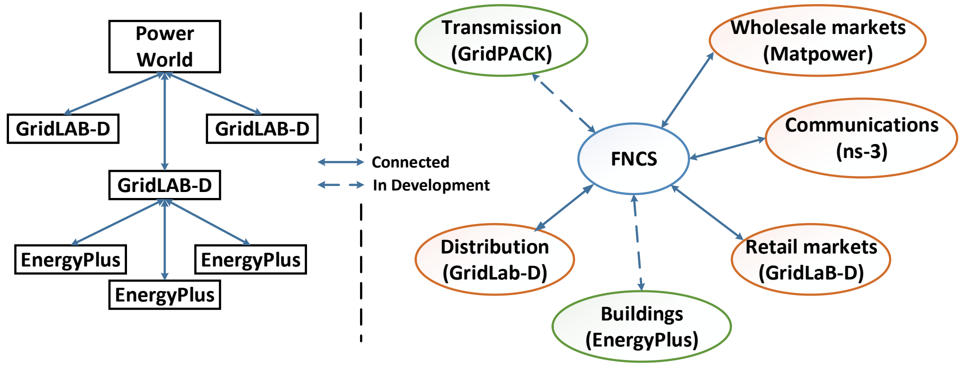


Figure 1.2 FNCS co-simulation framework

## GridSpice

GridSpice is an open-source co-simulation platform with a cloud-based architecture that is managed with a representational state transfer API, as presented in Figure 1.3 (a). It provides a browser-based interface for new users and can be run on a python interface. The first implementation of GridSpice was done to integrate GridLAB-D and MATPOWER simulators to identify the optimal placement of distributed resources and to develop optimal dispatch schedules for the flexible loads [11].

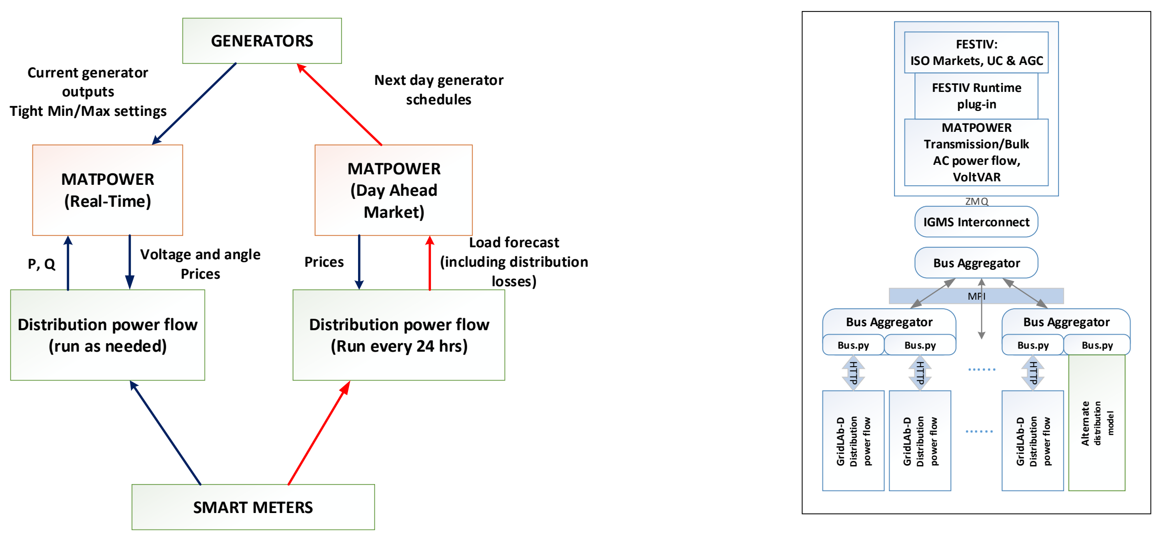


(a) (b)

Figure 1.3 Co-simulation frameworks a) Grid Spice b) IGMS

### Integrated Grid Modeling System (IGMS)

Another software model in this domain is the IGMS tool from NREL, as shown in Figure 1.3 (b). This is a hierarchical co-simulation framework that was built on High-Performance Computing (HPC) platform and integrates distribution systems with 1000's of nodes with transmission systems, detailed ISO markets, and AGC level reserve deployments [12]. The transmission level operation is based on MATPOWER and distribution systems in modeled using GridLAB-D. Here, each transmission or sub-transmission load bus is assigned to an aggregator which connects to multiple distribution loads modeled on GridLAB-D. A Message Passing Interface (MPI) paradigm is used to establish communication between the simulators. IGMS tool has been extensively used to evaluate the impacts of distribution connected PVs on transmission level operations.

### Work from Academia

Recently, several methods have also been proposed in academia for the integration of T&D systems [14-17]. For example, the study in [14] proposed a tightly coupled framework for combined T&D system analysis to assess the impacts of bulk Volt/VAR control on the transmission system. This work exchanges the positive sequence transmission parameters and three-phase distribution system parameters at the interface (PCC). For exchange, the distribution parameters are converted from three-phase to positive sequence components at the boundary. The study done in [15] uses a similar framework in [14] at the interface for load parameter estimation. Here, the converged distribution parameters obtained at the distribution bus is fitted through a constrained linear least-squares optimization technique to obtain the equivalent load models of the distribution system. The study in [16] models transmission system operation using sequence component analysis and also iteratively couples the T&D system interface for dynamic system simulation. Another recent article in [17] performs a comparative study of iterative and non-iterative interfacing techniques of T&D co-simulation environment. This study also compares the responses of the integrated T&D system by using both a balanced positive sequence model and three-sequence model for the transmission system analysis. Table 1.1 compares all the co-simulation models discussed, along with their advantages and limitations.

### Existing Gaps in the Literature

Unfortunately, a majority of the above-mentioned co-simulation platforms for integrated T&D system analysis use a balanced positive sequence AC power flow for transmission system analysis and loosely couple the T&D networks. In a loosely coupled model, the T&D boundary variables are exchanged only once. That is, the simulation time step is advanced without making the boundary variables converge. A loosely coupled model assumes that the changes in T&D simulations are relatively slow and the integrated T&D model converges over multiple time stamps. This limits the expandability of the existing framework to the operations with faster dynamics. This also limits both implementation and advanced mitigation actions involving coordinated control of the T&D systems. Also, with the increasing levels of system unbalance in the distribution system resulting from single-phase small-scale DER integration, analysis done using three-phase balanced positive sequence approach and loosely coupled interface may not be sufficient to evaluate the power quality impacts. This calls for an iterative interfacing framework that can model and solve transmission system in three-phase details and tightly couple the interface of T&D systems. Articles in [16] and [17] addresses the above two concerns by modeling transmission system operation using sequence component analysis and by iteratively coupling the T&D system interface. However, they use a small distribution network with 8 nodes for the analysis. It is required to evaluate the convergence properties for T&D coupling with the increased levels of system unbalance for a large-scale distribution system. In addition to this, the existing literature does not provide a mathematical analysis for T&D coupling and the associated convergence properties. For larger T&D systems with rapidly varying load and generation profiles, it is important to characterize the convergence of the co-simulation framework as a function of T&D system conditions at the interface.

Table 1.1 Comparison of Existing Co-simulation Platforms

| **Approach** | **Platforms** | **Advantages** | **Limitations** |
|---|---|---|---|
| **Standalone integrated model** | EnergyNet | • Provides a new level of visibility to coordinated control of T&D systems.<br>• Does not rely on the use of representative feeder models | • expensive to simulate<br>• do not take advantage of existing analysis tools |
| | GridLAB-D | | |
| **Co-simulation approach** | FNCS | Uses network simulator (ns-3) for communication between simulators making the framework highly scalable. | • Positive sequence model for transmission system<br>• Loosely coupled interface model |
| | GridSpice | Open source cloud-based architecture for simulation with common user interfaces like python | |
| | IGMS | • Uses HPC tools for integration<br>• Includes AGC reserves and flexible scheduling tool for PV integration | |
| | Frameworks from academia | • Tightly coupled boundary<br>• Iterative interfacing for exchange of variables<br>• Three sequence transmission system analysis | • Smaller test systems<br>• Simplified transmission system operations<br>• Mathematical model is missing |

### 1.1.3 Problem Statement – Need for Co-Simulation

As discussed previously, the combined T&D simulation can be achieved using 1) Stand-alone T&D system models and 2) Co-simulation approach. The major limitation of the standalone unified modeling approach is the cost of simulation. Given that the detailed model of a typical distribution feeder includes 1000s of buses/nodes, a stand-alone T&D model is usually too complex to simulate and analyze using a single tool. In addition, the stand-alone models do not take advantage of legacy power systems modeling and simulation platform. It should be noted that the electric power transmission systems and distribution systems are significantly different. While transmission systems are largely balanced with low R/X ratio and highly meshed, a typical distribution feeder is highly unbalanced, include single-phase loads and laterals, and is radial in the configuration. Owing to these differences, the solution approach used for the two networks also differ. The Newton-Raphson method is adopted to solve the power flow model for transmission systems while distribution systems are solved using forward-backward sweep or current injection methods. There are multiple other functional differences between the two systems making it impractical and inefficient to bring together all of the functionalities of individual legacy software tools into a single simulation environment. Consequently, it is more efficient to use co-simulation methods that bring the individual legacy tools together to perform the combined T&D simulation studies without having to make changes to the individual legacy platforms.

Next, we discuss the need for an iteratively/tightly coupled T&D co-simulation approach. The loosely coupled co-simulation methods are accurate only when the changes in distribution system loading characteristics, both during load unbalance and demand variability, are slower than the simulation time-step at which the two systems are solved, and the solutions are exchanged. Otherwise, the loosely coupled model introduces simulation errors [13]. This is because, in the loosely coupled models, the time step for individual T&D simulators is advanced without making the boundary variables converge. The primary assumption is that the changes in power system loads are rather slow, and the system converges over multiple time steps. This limits the applicability of the existing framework when modeling faster load/DER variations. In an actual co-simulation platform, the simulation time step must not advance until the boundary variables for both transmission and distribution systems have converged. This requires an iteratively or tightly coupled co-simulation approach.

### 1.1.4 Co-simulation Approach Proposed in this Work

To address the aforementioned gaps in the literature, this study presents a co-simulation framework that is close to the standalone T&D model by accurately modeling the system unbalance and by tightly coupling the T&D networks using an iterative approach. The framework for the proposed iterative co-simulation approach is presented in Figure 1.5.

The sequence component transmission system modeling and operations are carried out in MATLAB, and the modeling of the three-phase distribution system is done using OpenDSS. The T&D interface module is designed using MATLAB. This iterative framework based on "co-simulation approach" gives an understanding of the T&D system operation as a whole and eliminates the uncertainties from using the decoupled model for interaction. In this framework, the T&D systems are solved independently, i.e., they are decoupled at their operational level and solved using their dedicated software modules. The T&D interactions are captured by interchanging the solutions obtained from the two simulators at the point of common coupling (PCC) and making them converge. The key idea here is to simulate existing and/or potential interactions between the T&D networks. Also, this co-simulation approach assists in comprehending both the subsystem level operations and the convergence at the PCC. This leads to a co-simulation model that closely approximates a stand-alone unified model for the two systems.

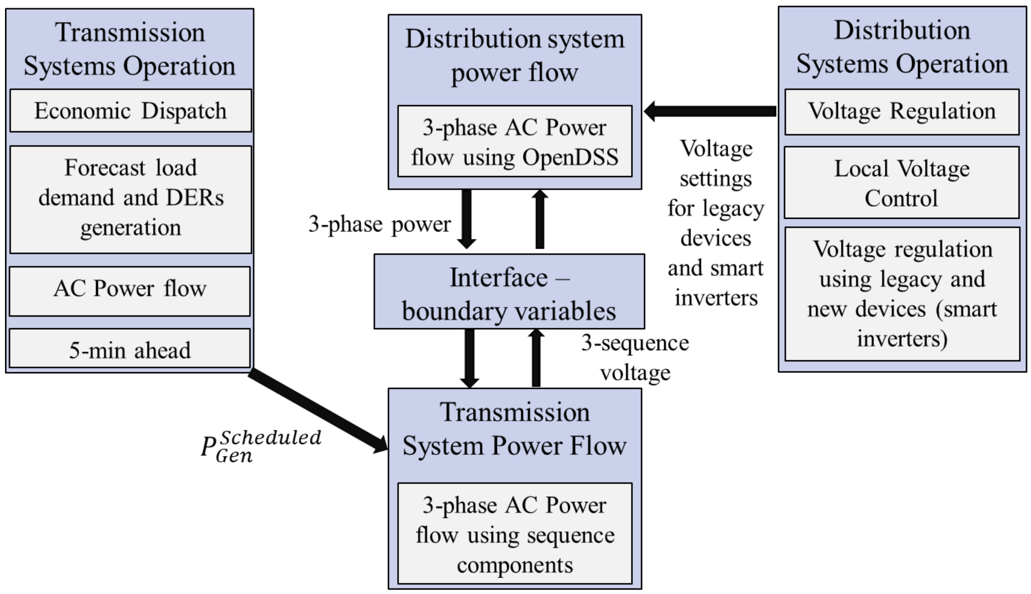


Figure 1.4 Proposed integrated T&D framework

### 1.1.5 Specific Contributions

The following specific contributions are made in this part of the project:

1. *Transmission system operational framework:* A three-phase transmission power flow framework is developed in MATLAB that uses three-sequence power flow method [18]. An integration of transmission system operational framework is demonstrated by interfacing a transmission system ACOPF economic dispatch program.
2. *Iteratively coupled co-simulation framework:* An iterative framework to tightly couple the T&D networks at each iteration is developed using MATLAB. The proposed iterative method results in a T&D co-simulation approach that is comparable to that of the stand-alone unified T&D model.
3. *Mathematical representation of T&D co-simulation interface:* The co-simulation interface is represented using a set of nonlinear equations that appropriately represents the interface coupling and individual subsystem equations. The developed non-linear interface constraint equations are solved using the first-order, and second-order convergence techniques and the results from two methods are compared.
4. *Comparison of T&D coupling methods:* Different methods of T&D coupling, namely decoupled (DC), loosely coupled (LC), and tightly coupled (TC) are compared for their accuracy in modeling the integrated T&D system in a quasi-static simulation for different DER integration scenarios. In addition, a stand-alone T&D model is developed to validate the results from the TC co-simulation model.
5. *Accurate simulation during system unbalance and variability:* A stochastic PV deployment scenario is developed using the Monte-Carlo method. The three co-simulation models (DC, LC, and TC) are evaluated for their performance by analyzing the error at T&D PCC by simulating multiple test cases with different levels of PV variability, PV penetrations, load unbalances, and the number of T&D coupling points.

6. *Significance of three-sequence transmission system analysis:* The strength of the developed tightly coupled framework with three-sequence TS analysis is demonstrated using comparisons against a single-phase TS analysis employing other coupling models, mainly LC model. It is validated that the three-sequence transmission model accurately represents system unbalances.
7. *Overall impact studies on transmission and distribution Systems:* This study utilizes the developed TC T&D co-simulation framework to understand the impacts of high levels of PV penetrations and resulting operational challenges on the entire transmission and distribution systems.

### 1.1.6 Chapter Organization

This chapter of the report is organized as follows:

- Section 1.2 provides the modeling details on all components of the quasi-static co-simulation framework. It provides a background on the existing transmission and distribution system modeling practices and the changes that are needed in the modeling of T&D systems to support DER interconnection studies. This section provides the ACOPF economic dispatch formulation for the time-series simulation of the proposed integrated T&D framework. The three-sequence transmission system model is detailed along with three-sequence analysis done in MATLAB to run the transmission system load flow. It provides information about the OpenDSS simulator used in creating the distribution system model and explains the three-phase power flow methods used by the software. It presents the PV deployment cases using the Monte-Carlo approach. A detailed explanation of the three coupling methods (DC, LC, and TC) for the quasi-static co-simulation platform is also presented.
- Section 1.3 details the mathematical model at the interface to understand the characteristics and convergence of the TC T&D integrated framework. A detailed understanding on the first-order and second-order convergence techniques using fixed-point iteration (FPI) method and Newton's method respectively is provided to solve the interface constraints equations developed at T&D PCC.
- Section 1.4 presents a detailed analysis of the test cases that were simulated to test the convergence of the developed T&D framework. Small-scale and large-scale test systems were simulated, and multiple test cases involving varying levels of load unbalance and PV variations in the distribution system are simulated and tested. A thorough comparison of convergence efficiency is done for FPI vs. Newton's method, co-simulation vs. standalone models, DC vs. LC vs. TC models, parallel vs. serial method of T&D interaction, and single-phase vs. three-sequence transmission model.
- Section 1.5 summarizes the findings and provides future research directions.

## 1.2 Transmission and Distribution System Modeling

The transmission systems model in MATLAB includes a detailed three-phase model with a 5-min ahead economic dispatch formulation solved using alternating current optimal power flow (ACOPF) model. Economic dispatch is implemented to achieve power balance. A sequence component-based three-phase power flow module is developed for transmission system power flow analysis. OpenDSS, a commonly used distribution system modeling, and analysis software is used to simulate the three-phase unbalanced distribution systems.

### 1.2.1 ACOPF Economic Dispatch

ACOPF is a static, non-linear programming problem with a non-linear objective function and linear and non-linear operational constraints. In this study, economic dispatch is done to optimally schedule the generator outputs of the IEEE 9-bus systems based on the generator cost functions with physical limits on real and reactive power generation and voltages. The objective function and the constraints are given below.

Minimize $\sum_{i=1}^{n}(a_i + b_i\, P_{gi} + c_i\, {P_{gi}}^2)$ *Objective function*

Subject to:

$$h(x) \quad \begin{cases} P_k = 0 \\ Q_k = 0 \end{cases}$$ *Equality constraints*

$$g(x) \quad \begin{cases} P_{gi} - P_{gimax} \leq 0 \\ P_{gimin} - P_{gi} \leq 0 \\ V_i - V_{imax} \leq 0 \\ V_{imin} - V_i \leq 0 \end{cases}$$ *Inequality constraints*

where, a, b and c are the fuel cost coefficients of each generator *i*. $P_{gi}$ is the power output of each generator, and *n* is the total number of generators in the system. The equality constraints of the power system are given by power flow equations that require the net injection of real and reactive power at each bus sum to zero along with the line losses. The inequality constraints reflect the operational limits. The cost functions of the generators in the IEEE 9-bus system are given as the following.

$$F(P_{g1}) = 150+5P_{g1}+0.11{P_{g1}}^2$$
$$F(P_{g2}) = 600+1.2P_{g2}+0.085{P_{g2}}^2$$
$$F(P_{g3}) = 150+1.0P_{g3}+0.1225{P_{g3}}^2$$

The algorithm begins with the implementation of a basic economic load dispatch formulation. The MATLAB function, equationsToMatrix, and linsolve are used to get the values of $P_{g1}$, $P_{g2}$, $P_{g3}$, and $\lambda$ as a result of economic load dispatch. The primary drawback with equal incremental cost scheduling is that it neglects all losses in the system. The only enforced equality constraint is the sum of the generation must equal the total load and demand. The sum of generation must equal the load demand plus any system losses. This is the reason for performing the ACOPF problem instead of the basic economic dispatch function. The ACOPF runs for a given load profile of the IEEE-9 bus system, and the optimal scheduling of the generators is obtained. The obtained generator scheduling for IEEE 9-bus system on a 5-minute interval for 24 hours is presented in Figure 1.6.

### 1.2.2 Transmission Systems Modeling and Analysis

The transmission system is predominantly modeled as a three-phase balanced power system and solved using a positive-sequence load flow analysis. This is acceptable when the physical components of the transmission system are three-phase balanced. But the positive-sequence results are inaccurate in cases where the system is supplying for unbalanced loads. For instance, with the proliferation of DERs in a largely unbalanced distribution system supplying many single-phase customers, the positive-sequence analysis on the transmission end is no longer adequate.

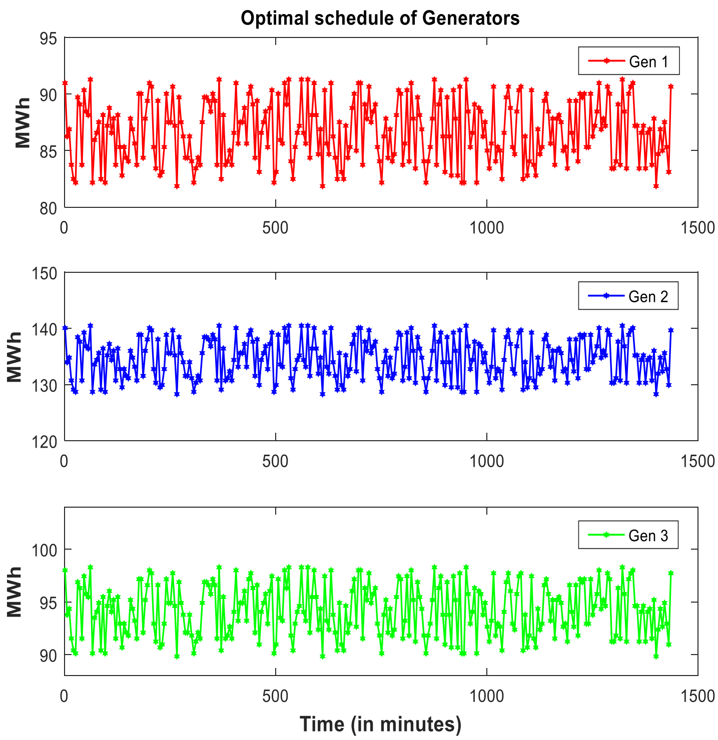


Figure 1.5 ACOPF generation schedule in every 5 minutes for 24 hours

The unbalanced power flow problem of the transmission system can either be formulated in phase frame or sequence frame. The three-phase transmission power flow model has once been an extensive field of research with Newton-Raphson and bus admittance techniques [18-21]. The Newton-Raphson technique has excellent convergence characteristics but requires recalculating $6N \times 6N$ Jacobian matrix at each iteration that may be computationally intensive. Several other methods were also proposed including the Z-bus Gauss method, complex formulations of Newton's method, fast decoupled method; however, they pose computational challenges.

The adoption of three-sequence modeling for the transmission systems unbalanced power flow analysis is a relatively recent field of interest [22-24]. The first paper in this domain used a Gauss-Seidel iteration scheme based on bus impedance matrix as a sequence model for three-phase unbalanced circuit analysis [22]. Later, a decomposed three-phase power flow solution using sequence components was presented in [23]. In this work, the three sequences were decoupled for analysis. However, it still required the calculation of $3N \times 3N$ admittance matrix. This paper introduced calculating the admittance matrices separately for each sequence component by introducing a decoupled line model [23]. Later, the reference in [24] came up with a simpler formulation that requires the calculation of $3N \times 3N$ admittance only for solving positive sequence components based on conventional power flows such as Newton-Raphson or fast-decoupled methods. The negative and zero sequences followed a simple linear solution with two $N \times N$ admittance matrices. This paper also included decoupled line model, sequence generator model, and sequence transformer phase shifts. This simplified the problem statement of solving the three-phase unbalanced power flow in the transmission system. The transmission system model for unbalanced analysis is developed using the sequence components model shown in Figure 1.7.

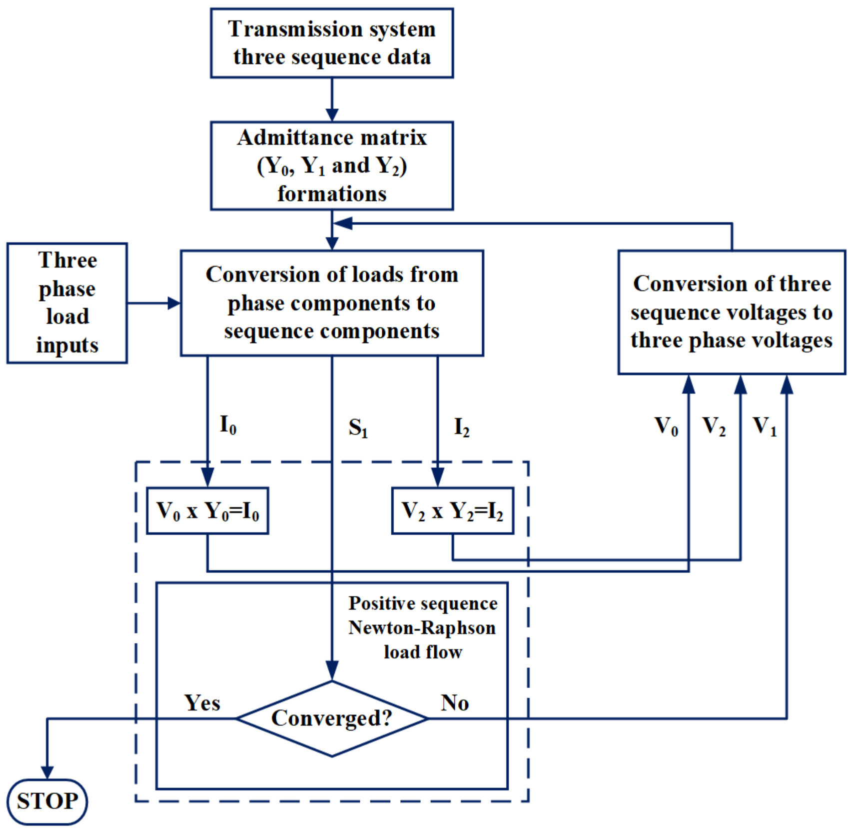


Figure 1.6 Three-sequence transmission system load flow

Note that the three-sequence approach to solving the transmission system is chosen over the three-phase modeling for the following reasons:

[1]. The Jacobian matrix calculation and storage is one of the most important concerns in solving a power flow problem for large networks. Using the sequence component method reduces the size of the Jacobian matrix from $6N \times 6N$ in a three-phase power flow model to $2N \times 2N$ for a positive-sequence model and two $N \times N$ for negative and zero sequence components [24].

[2]. The positive, negative, and zero sequence components in the sequence component analysis can be solved in parallel.

[3]. The computational time of the load flow problem is significantly reduced by solving only the positive sequence component using non-linear equations and linearizing the negative

and zero sequence components. This is desirable when solving T&D co-simulation with multiple integrated distribution system models.

The transmission systems power flow is modeled using the three-sequence power flow approach detailed in [24]. The system components (generators, transformers, and transmission lines) adopt a decoupled sequence component model. For the untransposed transmission lines, the sequence admittance matrix is full, unsymmetrical, and coupled. Since the mutual coupling in sequence line model is weak, it is decoupled into three independent sequence circuits by replacing the off-diagonal elements with the respective compensation current injections [24]. The decoupled three-sequence models are solved separately. With the specified generation fixed at the beginning of the iteration for the positive sequence model, it is solved using the Newton-Raphson technique. The negative and zero sequence components of the system model are solved using linear equations as,

$$Y_2 \,.\, V_2 = I_2$$
$$Y_0 \,.\, V_0 = I_0$$

where, the suffix 0 and 2 represent zero and negative sequence components, respectively. The positive-sequence power mismatch is used as the convergence criterion. Other convergence criteria, such as positive sequence voltage mismatch or phase voltage mismatch, can also be used. There are several advantages of using this sequence component method, and the major ones include the significant reduction in time and memory requirements to solve the three-sequence transmission load flow. In this method, the Jacobian matrix, negative and zero sequence admittance matrix for N buses and M branches result in solving a $6(N + 2M)$ non-zero elements instead of the $36(N + 2M)$ matrices that need to be solved in a three-phase power flow routine. Since the algorithm execution time depends on the size of the problem, this method reduces the CPU execution time by 83% [24]. In addition to this, the solution process can include transformer shifts introduced with special transformer connections. This formulation also includes injected currents and powers from loads and untransposed transmission lines that can be called as routines while solving the positive sequence model.

IEEE 9-bus [25] and 39-bus test systems [26] are used in this work for transmission system analysis and are shown in Figures 1.8a and 1.8b, respectively. IEEE 9-bus system consists of three generators, three loads totaling to 315 MW ad 115 MVAr and three two winding transformers. The base MVA here is 100, and the system operating frequency is 60Hz. The static and dynamic data for this system can be found in [25]. The total length of the transmission system is 40 miles. All 6 lines in the system are considered to have the same model. The typical 230 kV untransposed tower model is given in [25] is used to model the transmission lines in this test system and hence are used in the calculation of sequence admittance matrices for the decoupled transmission lines. IEEE 39-bus system with 10 generation sources and 18 load points is used in this study as our bigger transmission system model. The three-sequence data for the IEEE 39-bus system was obtained from PSS/E software [27], and three-sequence power flow solver is developed in MATLAB based on the three-sequence power flow method.

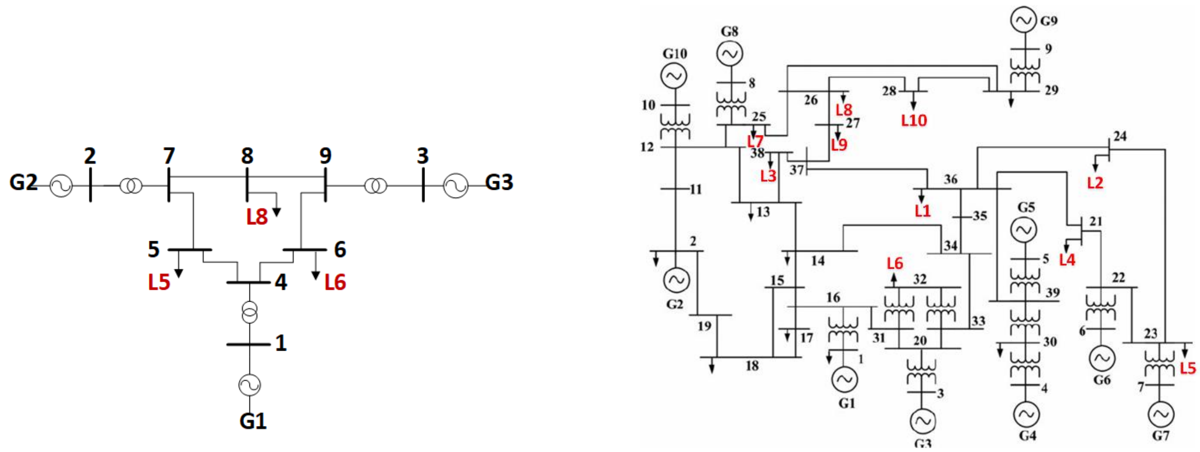

(a) (b)

Figure 1.7 Transmission test systems a) IEEE 9-bus system b) IEEE 39-bus system

### 1.2.3 Distribution System Modeling and Analysis

The distribution system three-phase modeling and analysis is done using OpenDSS, an open-source platform designed for distribution system analysis [28]. OpenDSS supports all frequency domain analysis performed for utility distribution system planning and analysis. There are multiple functionalities in OpenDSS along with its extraordinary capability to support planning and analysis of distributed generation (DG) technologies. OpenDSS allows to specify DERs' incremental capacity along with associated controls and help visualize their impacts on the distribution system. In addition to this, OpenDSS has explicit models of many real-world distribution feeders.

Three models of actual electric power distribution circuits are made public in OpenDSS. This thesis uses one of those feeders (Electric Power Research Institutes (EPRI) Ckt24 test system) for the distribution system model [29]. The sub-transmission level voltage is 230 kV, and the Ckt-24 operates at 34.5 kV system voltage. The system has 2 substation feeders with 3885 customers, of which 87% are residential loads. EPRI ckt-24 network is presented in Figure 1.9. OpenDSS is designed to solve both radial distribution circuits, and network (meshed) distribution system power flows. It can be also be used to solve transmission-style power flow for small to medium-sized systems. The circuit model designed can either be multi-phase or positive sequence model of a given distribution system. The power flow executes in various solution modes, including the standard single snapshot mode, daily mode, duty cycle mode, and others. It can also perform time-series simulation of a circuit as the load varies as a function of time. The time period can be hourly, daily, or yearly.

OpenDSS uses the following two simulation modes: Iterative power flow, and Direct solution. Loads and distributed generators are treated as injection sources for the Iterative power flow solution. In Direct solution mode, they are included as admittances in the system admittance matrix and solved directly. The two iterative power flow algorithms used by OpenDSS are Current injection method and the Newton's method. The voltages, power flows, currents, and losses for each component or the total system can be viewed from OpenDSS output terminals after the power flow operation. OpenDSS can be implemented either as a stand-alone executable program or as an in-process Component Object Model (COM) server DLL designed to be driven by a variety of existing software platforms like MATLAB, Python, R, and others. The executable version has a text-based user interface on the solution engine to assist users in developing scripts and viewing solutions. The COM interface is implemented on the in-process server DLL version of the program that allows users to perform new types of studies through existing program features. In this project, OpenDSS is executed using a MATLAB program.

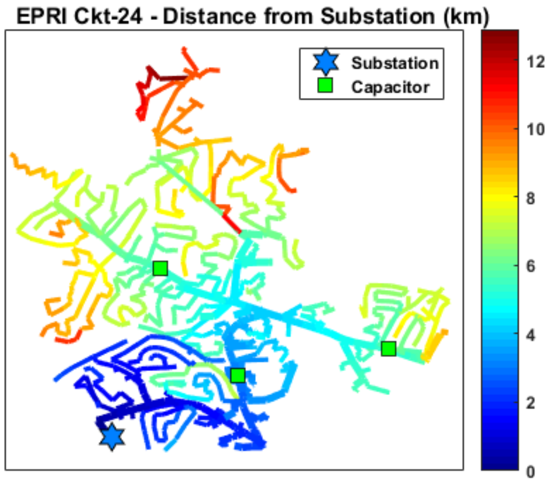


Figure 1.8 EPRI Ckt-24 OpenDSS distribution system model

### 1.2.4 PV Integration Models

The high-levels of distribution-connected PV penetration may result in multiple operational challenges for the integrated T&D systems including but not limited to overvoltages, excessive reverse power flow, increased power losses, severe phase unbalances, and power quality issues. This study specifically focuses on analyzing the impacts of distribution-connected PVs on transmission system voltages. In this section, we detail the method used to generate random PV deployment scenarios for a given distribution feeder. Following the related literature concerning PV hosting analysis for distribution feeders, similar stochastic analysis framework is adapted to generate numerous PV deployment scenarios. Multiple scenarios are simulated to fully capture the randomness associated with PV sizes and deployment locations for increasing customer penetration levels.

The method to simulate stochastic PV deployment scenarios is briefly detailed here. For each customer penetration level, multiple unique PV deployment scenarios are simulated using the Monte Carlo approach by associating a uniform random distribution to the PVs location and size. 100 different scenarios are created for each level of customer penetration that varies from 10%-100% in the steps of 10%. First, 10% of the customers in Ckt-24 feeder are selected at random using a uniform distribution and PVs are deployed at those load locations. The individual PV sizes connected to each customer is obtained based on the customer's peak load demand and customer type (residential or commercial). 100 such cases are generated for 10% customer penetration by randomly selecting PV locations and sizes. Customer penetration is then increased in steps of 10%. For each penetration level, 100 unique PV deployment scenarios are generated. So, in total, 1000 cases are simulated to study the voltage impacts of PVs on integrated T&D systems. For each scenario, co-simulation is solved, and the bus voltages at the substation bus are recorded after the co-simulation model converges. These voltages are reported in the results section for further analysis and discussions. For time-series simulations, a specific time window for three different days with different irradiance variability have been simulated. In that time window, the load in the distribution system is assumed constant. Three different days with different variabilities (low, medium, and high) of irradiance has been created. The low, medium, and high irradiance variability with a variability index of 1.33, 6.29, and 15.58, respectively, and the PV profile for each variability is presented in Figure 1.10 [30].

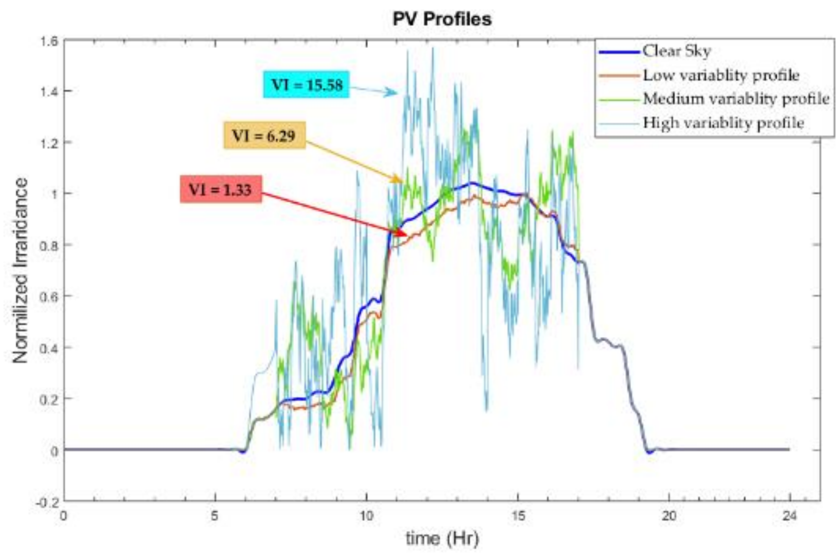


Figure 1.9 PV generation profile with low, medium, and high variabilities

## 1.3 T&D Co-Simulation Coupling Methods

A co-simulator is a tool that works on different set of simulators based on the time synchronization and execution coordination provided by a master algorithm. Each simulator is equipped with its own model and a solver that performs desired operations on the model. The simulators are then coupled by dynamically exchanging their input and output variables with each other. A simulator in co-simulation approach is a software module that is developed to perform modeling and analysis of a subsystem. The two major components of a simulator are the model and the solver. The model is a system designed with its specific details, and the solver carries out dedicated operations on the model based on the inputs provided. In this work, the simulators are three-sequence transmission and three-phase distribution systems developed in their respective platforms, MATLAB and OpenDSS, respectively.

The co-simulation master algorithm developed in MATLAB leads the simulation setup (framework). It leads all the simulators in the system by setting up the communication links between each of the simulators and the master algorithm. Once the communication is established, the master algorithm initializes each of the simulators by providing compatible starting conditions. It synchronizes the simulation by exchanging the events and variables between the simulators. The important tasks of the master algorithm in this framework are:

1) Set up communication links and initialize the simulators with specific inputs
2) Exchange and converge the boundary variables between the simulators and
3) Synchronize the time component throughout the simulation.

Due to the intermittent nature of the DERs, the strength of integration of T&D systems plays a vital role in the accuracy of studies when evaluating the impacts DER integration on transmission and distribution systems. As introduced before, there are three different coupling models: decoupled (DC), loosely coupled (LC), and tightly coupled (TC) models. In this section, we include detailed information on each of these coupling methods.

### 1.3.1 Decoupled Models

As mentioned before, the earlier power system analysis tools use models that are decoupled. In the DC model, the distribution network is represented as an equivalent load, and the upstream transmission network is modeled as an equivalent voltage source. The transmission system is first solved using aggregated load (including DERs), and the voltage at PCC is obtained. Then using that balanced voltage at PCC and assuming an ideal voltage source, the distribution system is solved. The transmission system models are solved in positive-sequence domain and assume the distribution system loads to be balanced. The DC model, therefore, cannot capture the impacts of high-levels of DER penetrations, single-phase loads and DERs, variable DER generation on the integrated transmission and distribution systems.

In a time-series power flow analysis, at each time-step, the transmission system is solved for the forecasted aggregated load at distribution substations. The obtained transmission bus voltage is used as the source bus voltage for the distribution system. The simulation moves to the next time-step, and the process repeats. Here, the total aggregated load is assumed balanced. Thus, in this method, the solutions obtained from solving the transmission and distribution system can be erroneous, especially for the cases with unbalanced loading conditions. The block diagram of the DC method and the workflow diagram for time-sequence analysis is shown in Figure 1.11.

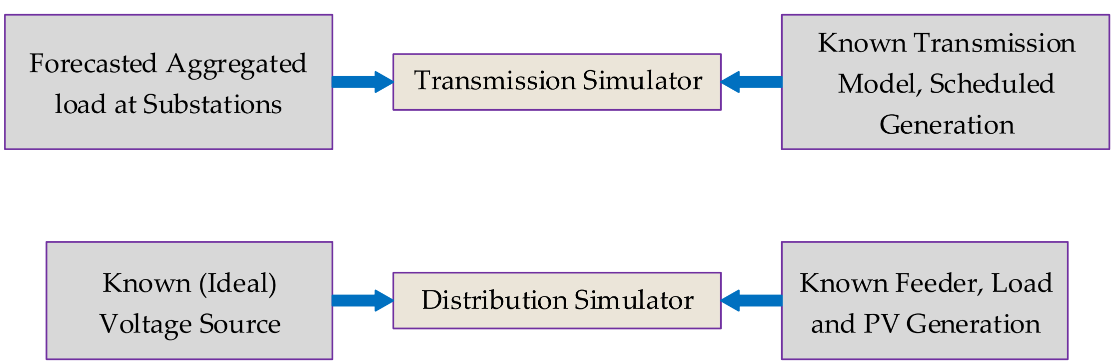


(a)

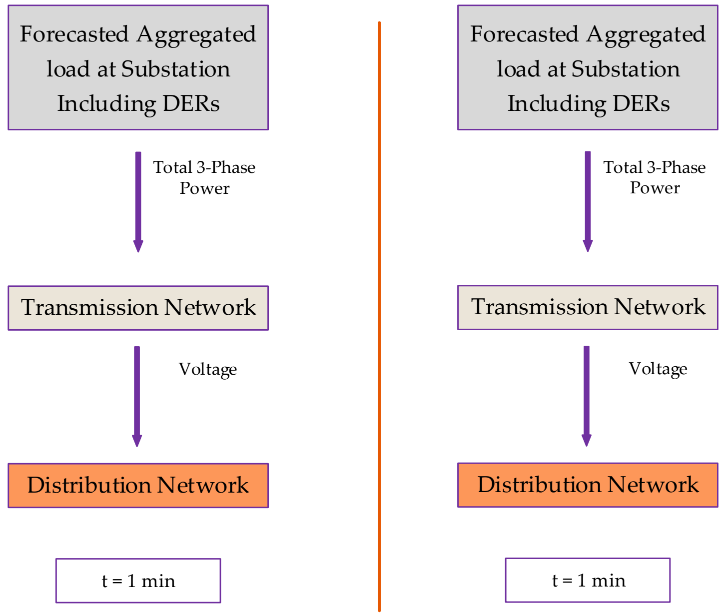


(b)

Figure 1.10 a) Decoupled T&D co-simulation model b) Time-series framework for DC model

### 1.3.2 Loosely Coupled Models

In loosely coupled (LC) model, unlike the decoupled (DC) model, the transmission and distribution system solutions are exchanged at the PCC, to capture the interactions between the two systems. Specifically, the real and reactive power demand at PCC, obtained by solving the distribution system is provided to the transmission system solver. The transmission system solves for voltages at PCC using the updated value of demand obtained from the distribution system solver. The time moves one step forward, and the PCC voltages (obtained from transmission solver) are provided to the distribution system solver. Distribution system solves for load demand at PCC and the process repeats. For time-series analysis, at a given time step (*t*), based on the aggregated load demand of the distribution system, the transmission system is solved for its voltages. This voltage is given to the distribution system as the source voltage, and the distribution system is solved to obtain the substation power demand. The substation power demand obtained from this time step (*t*) is given to the transmission system solver in the next time step (*t+1*). For slow changes in load, the LC coupled model provides accurate results. With frequent load changes, this method might be inaccurate because of not converging to common solutions in every time step. Although the LC model gives a lower error than the DC method, it is still not accurate enough. Note that unlike the DC model, the boundary parameters (voltages and load demand) are exchanged once between the two systems. However, the time-step is advanced without making the boundary values converge at the current time-step. Thus, the strength of T&D coupling in the LC model is weaker than stand-alone T&D models but stronger than DC model. The block diagram of the LC method and workflow diagram for time-sequence analysis is shown in Figure 1.12.

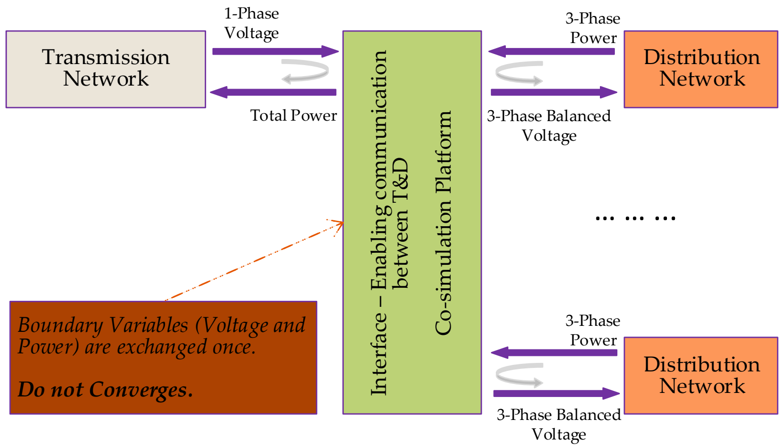


(a)

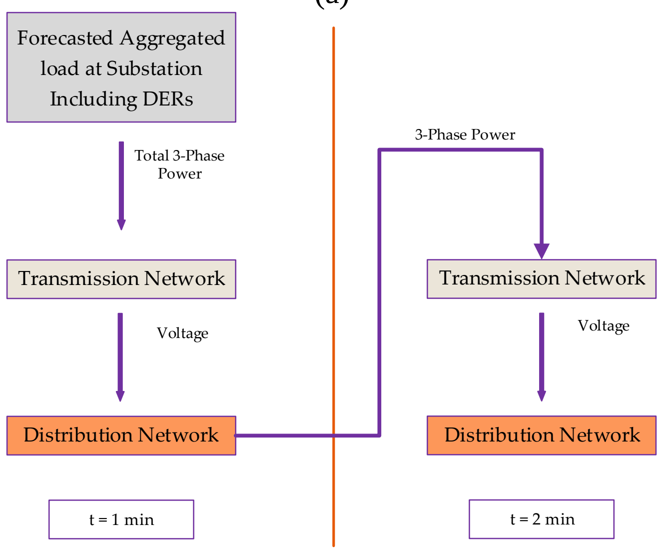


(b)

Figure 1.11 a) Loosely coupled (LC) model b) Time-series framework for LC model

### 1.3.3 Tightly Coupled Models

The proposed tightly coupled (TC) model provides strong coupling between the T&D systems thus bringing it closer to a standalone model. Instead of exchanging the boundary parameters only once at PCC, in this model, the variables are exchanged iteratively through the co-simulation platform until both solvers agree on the same voltage and load demand at the substation. The difference between LC and TC model is that the iteration in the TC model continues until the convergence is achieved. However, in LC, the convergence is not the goal and is a non-iterative approach.

Also, in the proposed TC model, 3-sequence transmission system solver is used, which helps with unbalance case studies. Similarly, in time-series analysis for the TC method, the convergence of boundary variables is ensured at each time-step, and only after convergence is achieved, simulation moves forward to the next timestamp. Note that the converged solution is the most accurate among all three methods due to the tight coupling of T&D in this method. The block diagram of the TC method and workflow diagram for time-sequence analysis is shown in Figure 1.13.

All components of the co-simulation framework are coordinated using a master algorithm written in MATLAB. The timing components and the convergence criteria are specified in the master algorithm. Since this co-simulation approach assists in comprehending both the subsystem level operations and the convergence at the point of common coupling (PCC), it leads to a co-simulation model that closely approximates a stand-alone unified model for the two systems.

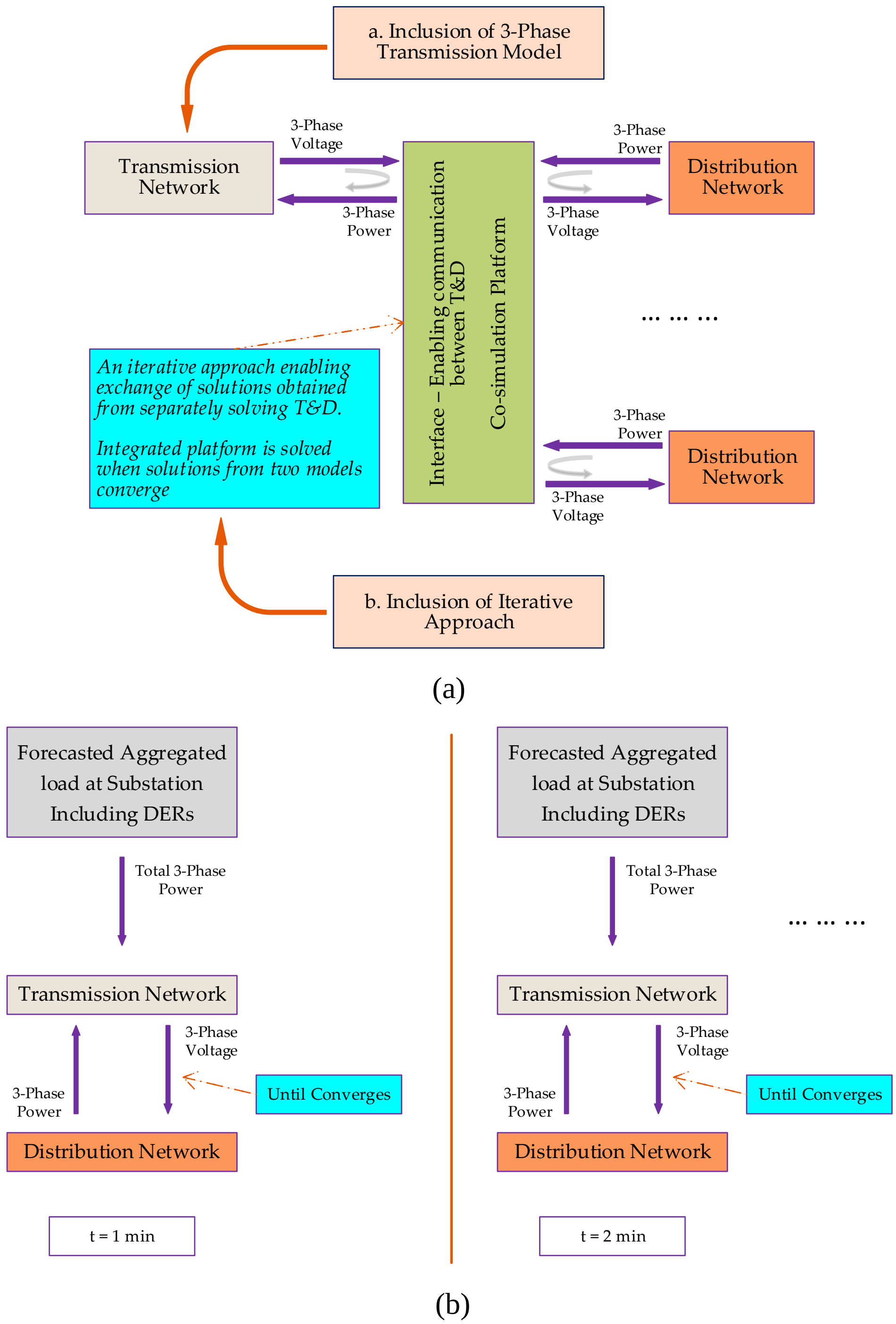


Figure 1.12 a) Tightly coupled (TC) model b) Time-series framework for TC model

## 1.4 Proposed Tightly Coupled T&D Co-simulation Framework

The co-simulation approach to exchanging boundary variables in an iterative framework is detailed in this section for snapshot solution and time-series framework. The basic framework is one where the system solves for one specific loading condition at any given time. This is the snapshot solution mode. The time component is then included where the system converges to varying load profiles of transmission and distribution systems in a time-series simulation. Both frameworks are explained in detail in this section with the emphasis on the performance of the master algorithm developed in MATLAB.

### 1.4.1 T&D Interaction Framework for Snapshot Solution:

In the proposed co-simulation framework, T&D systems are solved independently, and the interactions are captured by interchanging the solutions obtained from the two simulators. The key idea here is to simulate existing and/or potential interactions between the T&D networks. In this framework, the T&D systems are decoupled at the operational level and solved using their legacy software. Once the master algorithm initiates the simulation with specific starting conditions, the transmission and distribution simulators are solved in parallel. The solutions obtained from independently solving the two networks are interchanged between the two simulators by master algorithm synchronization after the iteration, as presented in Figure 1.14. The integrated model is solved when the solutions from the decoupled models converge.

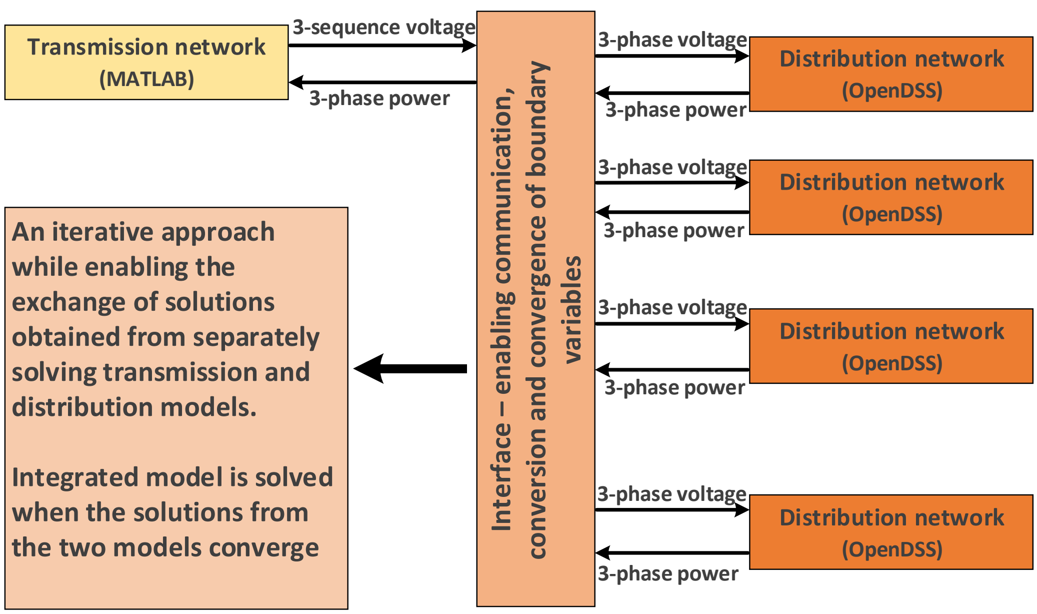


Figure 1.13 T&D Iterative framework for the co-simulation approach at PCC

The sequence components transmission system modeling and operations are carried out in MATLAB, and the modeling of the three-phase distribution system is done using OpenDSS. The sequence components bus voltages and angles obtained from transmission network solver and active and reactive power flow obtained from distribution network solver are interchanged at the PCC. The solutions obtained from independently solving the models are then exchanged between the two networks by making the output of the transmission system input to the distribution system and vice-versa. Exchanging the solutions follows an iterative framework, as shown in Figure 1.14. The simulation ends after the integrated model is solved, i.e. the solutions from the individual models have converged. This approach overcomes the limitations of the explicit co-simulation tools where the system advances to the next time step without converging the models in that interval. Also, this co-simulation approach assists in comprehending both the subsystem level operations and the convergence at the point of common coupling (PCC). This leads to a co-simulation model that closely approximates a stand-alone unified model for the two systems.

### 1.4.2 T&D Interaction Framework with Time Coordination

The time coordination provided by the master algorithm is exploited to account for DER based variations in the integrated T&D system analysis. The master algorithm synchronizing the integrated simulation is enabled to advance with time step in this section. As mentioned previously, the simulators exchange variables before moving to the next iteration or time step. These are called communication points. There are two separate time frames defined in this study for the master algorithm. i.e. macro and micro timestamps.

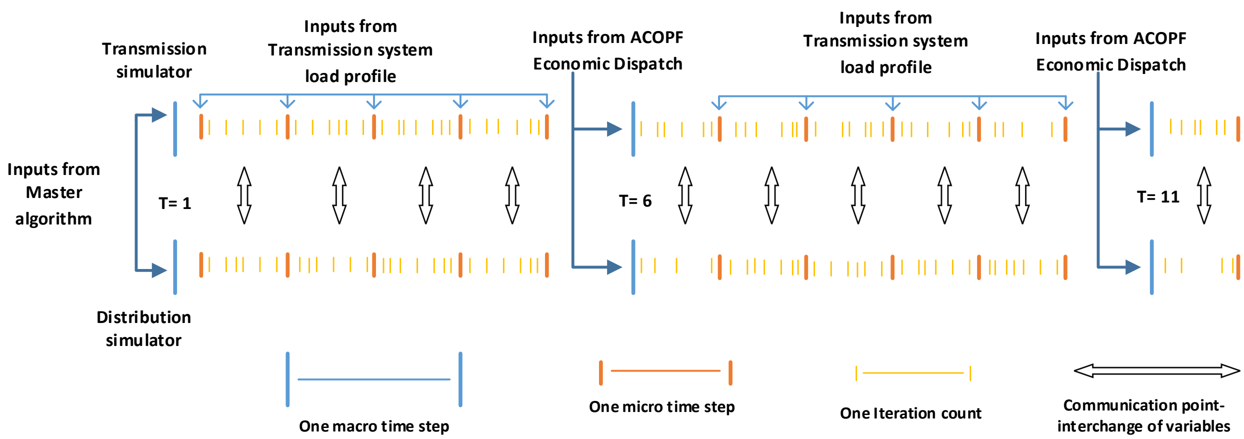


Figure 1.14 Time frames followed by the master algorithm to interchange boundary variables

The macro time steps are defined for every 5-minute interval in which the simulation restarts by initializing with a new set of inputs from the ACOPF formulation. The micro time stamps here define the time frame for convergence of transmission and distribution systems at the PCC. Within every micro time stamp, the system exchanges variables between the T&D simulators and is expected to converge before the start of the next micro time stamp. The micro timestamp has a 1-minute interval and is fixed in this study. The iterations inside the micro timestamps are the only communication points for the master algorithm in this study. The variables of exchange at the PCC are the three-sequence node voltages and angles obtained from the transmission system solver and the three-phase active and reactive power obtained at the PCC from the distribution system solver. The number of iterations within every micro time stamp varies depending on the T&D system conditions used for the simulation. Figure 1.15 presents communication points and time frames used by the master algorithm.

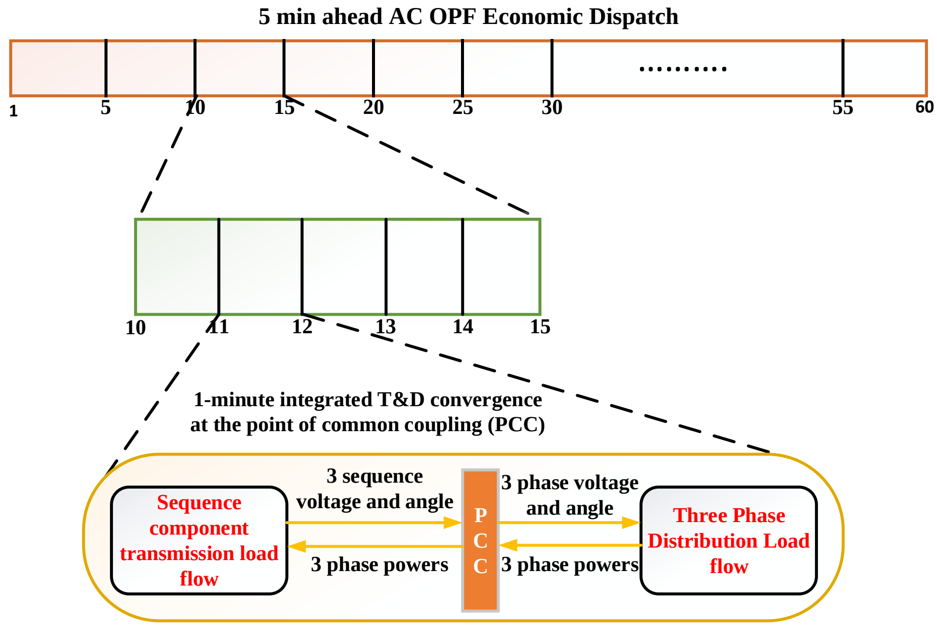


Figure 1.15 Time-series simulation algorithm of the integrated T&D system

The time-series simulation of the integrated T&D system can be visualized using Figure 1.16. The algorithm used for the real-time simulation of the integrated T&D system for 24 hours is detailed below:

1) At time stamp $t = 1$ of the master algorithm, ACOPF runs to give generator outputs based on its loading conditions at $t = 1$ .
2) At time stamp $t = 1$ (beginning of the first macro and micro timestamp) and iteration count=0:
    a) Master algorithm initiates the transmission system solver with the results from ED and distribution system solver with substation voltage and angle.
    b) The three-sequence transmission load flow and three-phase distribution load flow are solved in parallel for one micro time step.
    c) At the end of one micro time stamp, the three-sequence voltage at the PCC is converted to three-phase voltages and are provided as an input to the distribution system source node. The three-phase active and reactive power output at the distribution substation is provided as input to the transmission sequence load flow (i.e., the variables are exchanged at the PCC).
    d) The iteration count is incremented for every PCC variable exchange advanced.
    e) Steps a-d are repeated within one micro timestamp until the system converges.

3) Once convergence is achieved at the end of the first micro time stamp, the master algorithm created in MATLAB issues a timing signal to move to the next macro time stamp ($t = 2$) with inputs from transmission and distribution load shapes.
4) Steps 1-3 are repeated until the start of the next macro time stamp ($t = 6$) where the inputs are fetched from ACOPF formulation.
5) Steps 1-4 repeat for 24 hours of the simulation.

## 1.5 Mathematical Models for the Proposed TC T&D Co-simulation Framework

In this section, we present analytical formulations for the boundary variable update rules for iterative T&D coupling, also termed as co-iteration rules that are obtained by solving the nonlinear models for T&D co-simulation interface. The proposed mathematical models help characterize the convergence of the iterative co-simulation framework as a function of T&D system parameters. To this regard, we obtain models for T&D co-simulation interface and propose first-order and second-order convergent techniques based on Fixed-point iteration (FPI) and Newton's method to solve the associated nonlinear T&D interface equations. The proposed iterative coupling technique can be easily incorporated into any existing co-simulation platform capable of co-iteration such as HELICS. It should be noted that this work does not intend to replace the existing large-scale co-simulation platforms but aims to propose advances that will help refine the existing modeling and co-simulation techniques. The major focus is on developing improved methods with faster convergence for iterative coupling of accurately modeled T&D systems. First, a fixed-point iteration (FPI) method is used to solve the interface equations. Next, using Newton's method, a Jacobian-based update rule is developed for the T&D interface. The iterative coupling interface ensures convergence of boundary variables at each timestamp. Both first- and second-order methods proposed to solve iteratively coupled T&D system are validated for stressed system conditions. It should be noted that this work focuses on developing a T&D interface for quasi-static power system co-simulation. The proposed update rules can potentially be extended to iteratively coupled dynamic T&D co-simulation.

### 1.5.1 T&D Interface Coupling Equations

For coupled T&D system, the transmission system (Subsystem 1) is solved using three-sequence analysis while the distribution system (Subsystem 2) using a three-phase power flow, and the two subsystems are coupled at PCC. The input and output parameters for the subsystem representing transmission system are real and reactive power demand at the PCC ($P_T$, $Q_T$) and the voltage at PCC in sequence component ($V_T$) respectively. Similarly, the input and output parameters for the subsystem representing distribution system are phase voltages at PCC ($V_D$), and the real and reactive power demand at the PCC ($P_D$, $Q_D$) respectively. The transformation matrix $(\tau)$ converts the sequence to phase components. The mathematical equations governing the coupled system, solved using co-simulation are given below. The mathematical equations governing the coupled systems are given as,

$$V_T = f_1(S_T) \tag{1}$$
$$S_D = f_2(V_D) \tag{2}$$
$$S_T - S_D = 0 \tag{3}$$
$$\tau V_D - V_T = 0 \tag{4}$$

$f_1(x)$ - the non-linear equation defining three-sequence transmission power flow
$f_2(x)$ - the non-linear equation for three-phase distribution power flow

where $\tau = \begin{pmatrix} 1 & 1 & 1 \\ 1 & a^2 & a \\ 1 & a & a^2 \end{pmatrix}$ and $a = 1\angle 120°$.

Next, we present the mathematical model for the co-simulation interface. We define interface equations as a set of non-linear equations in (5) and (6).

$$I_T(S_T, V_D) \ : \ S_T - f_2(V_D) = 0 \tag{5}$$
$$I_D(S_T, V_D) \ : \ \tau V_D - f_1(S_T) = 0 \tag{6}$$

The residual components for each system at the interface corresponding to a given subsystem solution are then defined as the following:

$$R_T = S_T - f_2(V_D) = 0 \tag{7}$$
$$R_D = \tau V_D - f_1(S_T) = 0 \tag{8}$$

The co-simulation interface shown in Figure 1.17 solves non-linear equations defined in (5) and (6) subject to (1) and (2). The approach is detailed in Algorithm 1. First, subsystem equations, (1) and (2), are solved in parallel. The roots (output) of the subsystem equations are used for residual evaluation of the coupled system at the interface using (7) and (8). A global interface residual vector, $\mathscr{R}$ is defined to evaluate the condition for the convergence of the co-simulation framework, where $\varepsilon_1$and $\varepsilon_2$ are predefined tolerance parameters (9).

$$\mathcal{R} = \begin{bmatrix} R_T \\ R_D \end{bmatrix} \leq \begin{bmatrix} \varepsilon_1 \\ \varepsilon_2 \end{bmatrix} \tag{9}$$

The objective is to iteratively solve interface equations defined in (5) and (6) until the residual evaluated using (7) and (8) are within a permissible error tolerance. If the convergence criterion is not met, the boundary variables are updated. The update rules for boundary variables are derived in sections 3.2 and 3.3 for FPI and Newton's method, respectively. The process is repeated until the boundary variables converge.

### 1.5.2 FPI Method for T&D Convergence

The fixed-point iteration algorithm is one of the classic Jacobian-free solution techniques for solving nonlinear system of equations. The approach is to transform the root-finding problem to a fixed-point problem. For a set of non-linear equations defined as f(x) = 0, the FPI sequence is given as follows,

$$x_{n+1} = x_n \pm \alpha\, f(x_n) \tag{10}$$

The system is updated for the next iteration if the residual vector error convergence is not satisfied based on FPI iteration sequence as follows,

$$\begin{bmatrix} (P^T, Q^T)_{n+1} \\ (V^D, \delta^D)_{n+1} \end{bmatrix} = \begin{bmatrix} (P^T, Q^T)_n \\ (V^D, \delta^D)_n \end{bmatrix} + \begin{bmatrix} (P^D, Q^D)_n - (P^T, Q^T)n \\ T(V^T, \delta^T)n - (V^D, \delta^D)n \end{bmatrix} \tag{11}$$

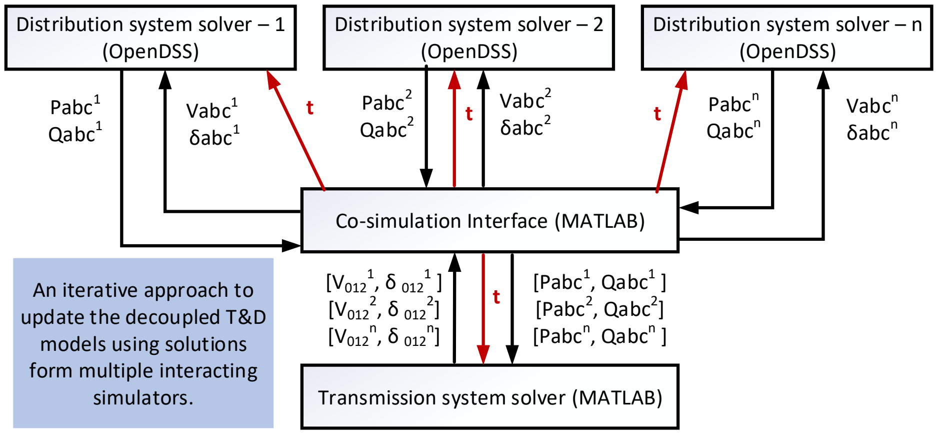

Figure 1.16 Proposed T&D co-simulation interface

Once the residual components are within a permissible error, the system is converged and moves to the next solution with inputs from transmission load profiles given as a new set of starting conditions provided by the co-simulation master algorithm. The algorithm for implementing the FPI method for the coupled T&D system is detailed in Algorithm 1. The co-simulation interface only focuses on solving interface equations and updating input to the two subsystems. The nonlinear equations for individual subsystems are solved using subsystem solvers. Until the convergence criterion is met, the input to the individual subsystems is updated using the FPI co-iteration sequence defined in (11). This method, therefore, iteratively exchanges the subsystem solutions until the boundary variables converge.

### 1.5.3 Newton's Method for T&D Convergence

The second-order convergence technique is referred to as Newton's method in this work. Newton's method to solve the non-linear system of equations, $f(x) = 0$ requires the first derivative of the function, i.e., $J(f(x))$. The iterative sequence for solving the $f(x) = 0$ using Newton's method is given as,

$$x_{n+1} = x_n - \Delta x \tag{12}$$

$$\Delta x = J\big(f(x_n)\big)^{-1} f(x_n) \tag{13}$$

where, $J$ is the Jacobian operator.

For the T&D co-simulation problem, the system of non-linear equations to be solved are the interface equations $I_T$ ($S_T$, $V_D$) and $I_D$ ($S_T$, $V_D$) as defined in (2) and (3). Same as FPI method, the interface equations are solved iteratively until the residuals defined are within a permissible error tolerance. Until the convergence criteria are met, the input to the individual subsystems, i.e., $S_T$ and $V_D$, are updated using Jacobian-based update rule. The Jacobian-based update rule for solving the interface equations is defined below. First, the Jacobian operator is obtained by differentiating the interface equations wrt. variables $S_T$ and $V_D$.

$$J = \begin{bmatrix} \frac{\partial I_T}{\partial S_T} & \frac{\partial I_T}{\partial V_D} \\ \frac{\partial I_D}{\partial S_T} & \frac{\partial I_D}{\partial V_D} \end{bmatrix} = \begin{bmatrix} \frac{\partial S_T}{\partial S_T} & -\frac{\partial f_2(V_D)}{\partial V_D} \\ -\frac{\partial f_1(S_T)}{\partial S_T} & \frac{\partial \tau V_D}{\partial V_D} \end{bmatrix} \tag{14}$$

where,

$$\frac{\partial f_1(S_T)}{\partial S_T} = \begin{bmatrix} \frac{\partial V_0}{\partial S_a} & \frac{\partial V_0}{\partial S_b} & \frac{\partial V_0}{\partial S_c} \\ \frac{\partial V_1}{\partial S_a} & \frac{\partial V_1}{\partial S_b} & \frac{\partial V_1}{\partial S_c} \\ \frac{\partial V_2}{\partial S_a} & \frac{\partial V_2}{\partial S_b} & \frac{\partial V_2}{\partial S_c} \end{bmatrix} \tag{15}$$

$$\frac{\partial f_2(V_D)}{\partial V_D} = \begin{bmatrix} \frac{\partial P_a}{\partial |V_a|} & \frac{\partial P_a}{\partial |V_b|} & \frac{\partial P_a}{\partial |V_c|} & 0 & 0 & 0 \\ \frac{\partial P_b}{\partial |V_a|} & \frac{\partial P_b}{\partial |V_b|} & \frac{\partial P_b}{\partial |V_b|} & 0 & 0 & 0 \\ \frac{\partial P_c}{\partial |V_a|} & \frac{\partial P_c}{\partial |V_b|} & \frac{\partial P_c}{\partial |V_c|} & 0 & 0 & 0 \\ 0 & 0 & 0 & \frac{\partial Q_a}{\partial |V_a|} & \frac{\partial Q_a}{\partial |V_b|} & \frac{\partial Q_a}{\partial |V_c|} \\ 0 & 0 & 0 & \frac{\partial Q_b}{\partial |V_a|} & \frac{\partial Q_b}{\partial |V_b|} & \frac{\partial Q_b}{\partial |V_b|} \\ 0 & 0 & 0 & \frac{\partial Q_c}{\partial |V_a|} & \frac{\partial Q_c}{\partial |V_b|} & \frac{\partial Q_c}{\partial |V_c|} \end{bmatrix} \tag{16}$$

Note that the terms corresponding to the interface equation (2) in $J$ are real and defined in terms of real and reactive power demand ($P_T$, $Q_T$), and absolute values of phase voltages ($|V_D|$). On the other hand, the terms corresponding to (3) in $J$ are defined in terms of complex quantities, i.e., complex power demand $S_T$ and complex sequence voltages $V_T$. Due to the different modalities of terms in $J$, (2) and (3) cannot be solved simply using the update rule specified in (13). To solve this problem first, we write the update equations for solving (2) and (3) using J separately in (17). Next, we develop an update rule by iteratively solving (17) using $J$ defined in (14).

$$\begin{gathered} \begin{bmatrix} \Delta P_T \\ \Delta Q_T \end{bmatrix} - \frac{\partial f_2\big(V_D(n)\big)}{\partial V_D(n)} \begin{bmatrix} |\Delta V_D| \\ |\Delta V_D| \end{bmatrix} = \begin{bmatrix} P_T(n) - P_D(n) \\ Q_T(n) - Q_D(n) \end{bmatrix} \\ -\frac{\partial f_1(S_T)}{\partial S_T} \Delta S_T + \tau \Delta V_D = \tau\big(V_D(n)\big) - V_T(n) \end{gathered} \tag{17}$$

Since the updates are defined in separate modalities; an iterative method is employed to solve for $S_T$ and $V_D$. The process is repeated until the changes in updates are not significant. Note that the proposed Newton-based method employs exactly the Jacobian operator, $J$, that is approximated over multiple iterations in (18)-(20).

$$\Delta V_D = \tau^{-1}(\tau\big(V_D(n)\big) - V_T(n) + \frac{\partial f_1(S_T(n)}{\partial S_T(n)} \Delta S_T \tag{18}$$

$$\begin{bmatrix} \Delta P_T \\ \Delta Q_T \end{bmatrix} = \begin{bmatrix} P_T(n) - P_D(n) \\ Q_T(n) - Q_D(n) \end{bmatrix} + - \frac{\partial f_2(V_D(n))}{\partial V_D(n)} \begin{bmatrix} |\Delta V_D| \\ |\Delta V_D| \end{bmatrix} \tag{19}$$

$$\Delta S_T = \Delta P_T + jQ_T \tag{20}$$

For a given iteration of co-simulation, the boundary variables obtained from the subsystem solvers are available. The current values of boundary variables are used to calculate $J$. Next, $J$ is used to obtain the Newton-based updates defined in (18)-(20). Although updates require iteratively solving (18)-(20), in practice, not more than two iterations are required to achieve sufficient accuracy. Using the current values of updates, the inputs to the subsystem solvers are modified, and subsystems are solved again in parallel. The second iteration of co-simulation begins, and $J$ is recalculated for the new value of boundary variables obtained from the subsystem solvers. This process is repeated until the residuals defined in (7)-(8) are within permissible error tolerance (see Algorithm 1).

*Algorithm 1: Solving Coupled System: FPI and Newton's method*

Initialize time index for the time-series simulation, t = 1.

**for** $t$=$1$:$t_{step}$:$T$ **do**

  Initialize Input Variables: ${}_tS_T$, ${}_tV_D$

  Initialize iteration count, n = 1

  Solve subsystems in parallel

  ${}_tV_T(n) = f_1({}_tS_T(n))$

  ${}_tS_D(n) = f_2({}_tV_D(n))$

  Check residual at the interface

$${}_t\mathcal{R}(n) = \begin{bmatrix} {}_tS_T(n) - {}_tS_D(n) \\ {}_tV_D(n) - \mathcal{T}^{-1}({}_tV_T(n)) \end{bmatrix}$$

  // Iteration loop

  **while** $|{}_t\mathcal{R}(n)| \geq \epsilon$ **do**

    Update boundary variables for next iteration

    Update rule for FPI method

$$\begin{bmatrix} {}_tS_T(n+1) \\ {}_tV_D(n+1) \end{bmatrix} = \begin{bmatrix} {}_tS_D(n) \\ \mathcal{T}^{-1}({}_tV_T(n)) \end{bmatrix}$$

    Update rule for Newton's Method

$$\begin{bmatrix} {}_tS_T(n+1) \\ {}_tV_D(n+1) \end{bmatrix} = \begin{bmatrix} {}_tS_T(n) \\ {}_tV_D(n) \end{bmatrix} - \begin{bmatrix} \Delta S_T \\ \Delta V_D \end{bmatrix}$$

    Increment iteration count

    n = n+1

    Solve subsystems in parallel

    ${}_tV_T(n) = f_1({}_tS_T(n))$

    ${}_tS_D(n) = f_2({}_tV_D(n))$

    Check residual at the interface

$${}_t\mathcal{R}(n) = \begin{bmatrix} {}_tS_T(n) - {}_tS_D(n) \\ {}_tV_D(n) - \mathcal{T}^{-1}({}_tV_T(n)) \end{bmatrix}$$

  **end**

**end**

Notice that $J$ needs to be updated at each iteration of the co-simulation. Although we have derived the update rules using only two subsystems, the proposed approach is general and applicable to a transmission system connected to multiple distribution feeders as demonstrated in the results section. This concludes the approach for Newton-based update rule to solve the T&D co-simulation interface equations and method to obtain the Jacobian operator, $J$.

## 1.6 Analysis and Results

For a detailed analysis of the developed quasi-static T&D co-simulation framework, two integrated T&D test systems are developed: TSm-1 and TSm-2. TSm-1 simulates a small transmission system (TS) model with three interconnected distribution system (DS) model; TS is modeled using IEEE 9-bus system that includes 3 load buses and 3 generators, and to model DS, we employ EPRI Ckt-24 that is available in OpenDSS. TSm-2 simulates a large integrated T&D system model where the TS is modeled using IEEE 39-bus system that includes 18 load buses and 10 generators, and the DS remains the same. For an integrated T&D modeling multiple load buses of the IEEE 39-bus system are replaced with EPRI Ckt-24 (DS system model). Note that EPRI Ckt-24 is a large 6000-bus test system that models a real-world distribution feeder with 3885 customers and 87% residential loads. The primary side has a voltage level of 13.2kV. At the secondary side, the voltage level is 480V and 240V for 3-phase and 1-phase feeder respectively. PV systems, representing DERs in this study, are deployed in EPRI Ckt-24 distribution feeder as described in Section 2.4 to introduce generation variability.

This section details the analysis performed on the quasi-static co-simulation framework using two different test systems. The platform is compared for convergence with increasing DER penetrations and load unbalances between two interface models (i.e., FPI vs. Newton's), parallel vs. serial method of T&D interactions and three-sequence vs. single-phase TS models. The results are validated using a stand-alone integrated T&D model developed in OpenDSS. In addition to this, multiple test cases are developed to demonstrate the impacts of PV variability, PV penetrations, and load unbalances on the integrated model is compared for decoupled, loosely coupled and tightly coupled models.

The cases for PV variability are simulated for three different scenarios with low, medium, and high variations in PV generation profiles, as shown in Figure 1.10. The simulated cases for low, medium and high PV variability incur a variability index (VI) of 1.33, 6.29, and 15.58, respectively [30]. One PV deployment scenario with random size and location of PVs is simulated using Monte-Carlo simulations as discussed previously. Here, two cases with different PV power factors (pf) of values pf = 1 and pf = 0.98 are simulated. A specific 1-hour (12.00-1.00pm) time window of the day is selected for simulations while the loads in DS are assumed to be constant during the specified 1-hour time window. Next, cases with 10 different PV penetration levels are simulated by varying customer penetrations levels from 10% to 100%. In addition, for each simulation, load unbalance is varied from 10% to 50% in the steps of 10% by varying the customer load distribution in each of the phases of the DS. Here, the PV deployment cases are also unintentionally unbalanced as the PV systems are randomly deployed on the different phases.

The small-scale test system is used to evaluate the trend in simulation errors as the DER/PV penetrations, load unbalance, and PV variability are increased for the interconnected DS. Despite the simulation errors being less, the test case demonstrates the variations in T&D simulation errors for different coupling methods and convergence models. The simulation errors are observed to be more pronounced for the larger T&D system model with a similar trend as observed for the small test system. The development of the two test systems is detailed next.

### 1.6.1 Test System Development

**Test System-1**

For the small-scale test system-1 (TSm-1), IEEE 9-bus system is used. Load points, L5, L6, and L8 of the IEEE 9-bus TS are replaced by modified EPRI Ckt-24 DS, as shown in Figure 1.18. EPRI Ckt-24 distribution feeder is presented in Figure 1.19. The IEEE 9-bus transmission test system includes three generators at buses 1, 2 and 3 and three loads at buses 5, 6 and 8 [25]. Note that the load buses are the potential locations for integrating the distribution feeders. EPRI Ckt-24 is based on a real-world feeder and supplies for a total of 3885 customers at 34.5 kV voltage level using two equally loaded feeders [29]. The peak demand recorded at the substation is 52.1 MW, and 11.7 MVAR and the feeder is comprised of 87% single-phase/two-phase residential loads. A substation transformer is used to connect the 34.5 kV distribution system to the 230 kV transmission bus.

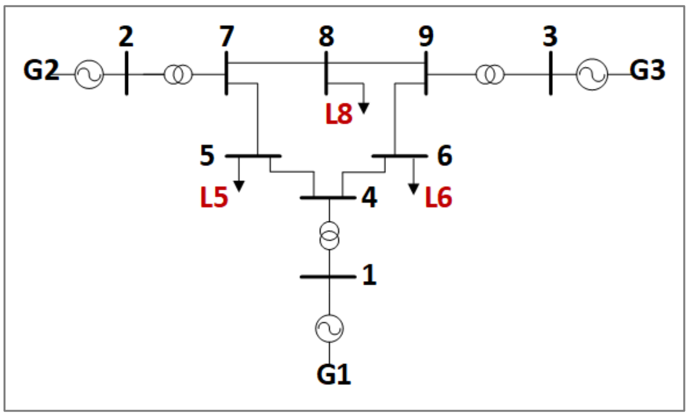


Figure 1.17 IEEE 9-bus transmission test system

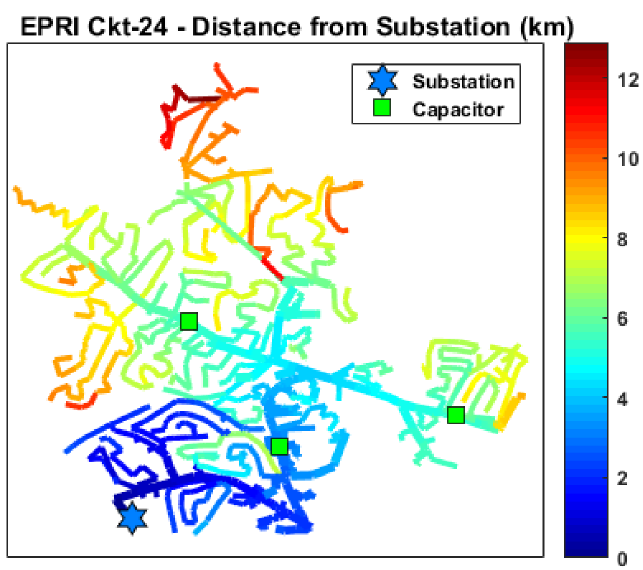


Figure 1.18 EPRI Ckt-24 distribution system

**Test System-2**

Test system-2 (TSm-2) simulates a larger integrated T&D system. We employ IEEE 39-bus test system as the TS model, as shown in Figure 1.20. For an extensive simulation, we simulate three different integrated T&D test systems by varying the number of T&D coupling points. Note that IEEE 39-bus test system includes 18 load buses that can serve as a potential connection point for the DS. A substation transformer is used to connect the 34.5 kV distribution system to the 345-kV transmission bus. Larger test system is obtained by replacing the ten aggregated load points L1-L10 of the IEEE 39-bus transmission system each with EPRI Ckt-24 distribution test feeder. In this work, unless otherwise stated, % PV penetration refers to the percentage of DS customers with PV.

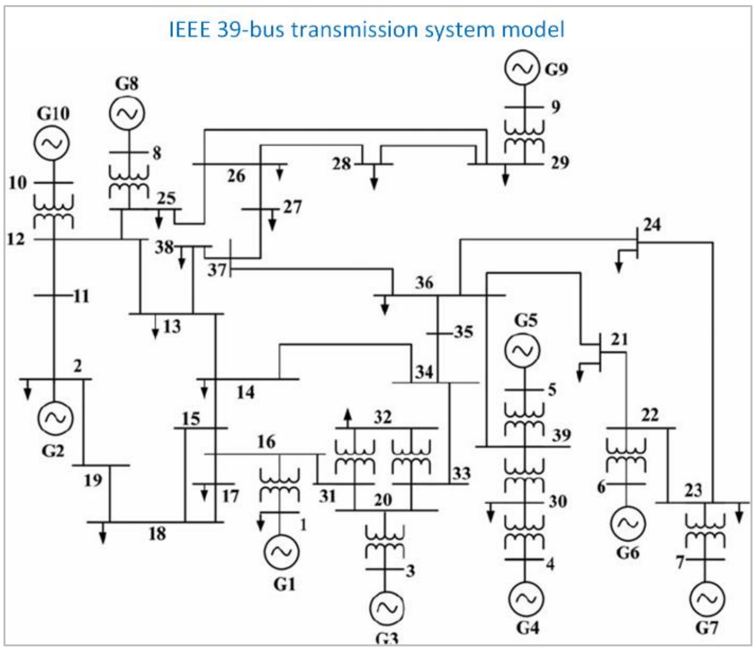


Figure 1.19 IEEE 39-bus transmission test system

### 1.6.2 Convergence using FPI vs. Newton's Method

**Test System 1 - Small Test System Results**

For TSm-1, two integrated T&D are developed in this section. Test System-1 (TS1) is obtained by replacing the aggregated load at bus 6 of the 9-bus transmission system with EPRI Ckt-24. Test System-2 (TS2) is obtained by replacing all the load points, L5, L6, and L8, of the IEEE 9-bus system with Ckt-24.

***A. Convergence of Base case and Increased system loading:***

The base-case loading scenario simulates the loading condition with no intentional unbalances in the distribution feeder. The base case is relatively balanced with approximate per-phase complex power demand equal to 17.8 MW +5.1j MVAr. The co-simulation approach is implemented for the base-case load scenario for both test systems and, the load demand and bus voltages at PCC for each iteration are shown in Table 1.1. Table 1.1 also compares the number of iterations required by the FPI method and Newton's method to solve the interface equations. It can be seen from the table that phase voltages both from distribution and transmission system solvers converge for both co-simulation methods in four iterations. In the base case, the converged positive sequence voltage from using the proposed three-sequence transmission model is 1.0442 p.u. while the positive sequence only converged value is 1.0441 p.u. The difference in converged values between the two models is more pronounced as the system unbalance increases along with load variations.

Table 1.1 Test system-1 voltage convergence at bus 6 PCC

Voltage Convergence using FPI Method

| System | Phase | Iter. 1 | Iter. 2 | Iter. 3 | Iter. 4 |
|---|---|---|---|---|---|
| Transmission | Phase A | 1.0437 | 1.0435 | 1.0437 | 1.0437 |
| | Phase B | 1.0453 | 1.0451 | 1.0454 | 1.0454 |
| | Phase C | 1.0432 | 1.0430 | 1.0433 | 1.0433 |
| Distribution | Phase A | 1.05 | 1.0437 | 1.0435 | 1.0437 |
| | Phase B | 1.05 | 1.0453 | 1.0451 | 1.0454 |
| | Phase C | 1.05 | 1.0432 | 1.0430 | 1.0433 |

Voltage Convergence using Newton's method

| System | Phase | Iter. 1 | Iter. 2 | Iter. 3 | Iter. 4 |
|---|---|---|---|---|---|
| Transmission | Phase A | 1.0437 | 1.0441 | 1.0437 | 1.0437 |
| | Phase B | 1.0453 | 1.0457 | 1.0454 | 1.0454 |
| | Phase C | 1.0432 | 1.0437 | 1.0433 | 1.0433 |
| Distribution | Phase A | 1.05 | 1.0440 | 1.0438 | 1.0437 |
| | Phase B | 1.05 | 1.0455 | 1.0455 | 1.0454 |
| | Phase C | 1.05 | 1.0437 | 1.0434 | 1.0433 |

Both test systems are also compared for varying loading conditions. The load multiplier for the distribution feeder is adjusted to increase the demand in all phases. This results in an increased loading without causing any additional unbalance. Both co-simulation methods are compared again for the new loading conditions, and the results are shown in Table 1.2. In general, as the system loading is increased, both FPI and Newton's method take a longer time to converge with a proportional increase in the number of iterations required. However, Newton's method converges faster with lesser number of iterations. The improvement in the performance of Newton's is more pronounced during increased loading conditions.

Table 1.2 Number of iterations and time required for convergence at PCC for TSm-1

NUMBER OF ITERATIONS(N) AND TIME(T) REQUIRED FOR CONVERGENCE

| | FPI Method | | | | Newton's Method | | | |
|---|---|---|---|---|---|---|---|---|
| Load multiplier | TS-1 | | TS-2 | | TS-1 | | TS-2 | |
| | N | T (s) | N | T (s) | N | T (s) | N | T (s) |
| 1 | 4 | 1.83 | 4 | 2.71 | 4 | 3.18 | 6 | 4.71 |
| 1.5 | 6 | 2.34 | 7 | 5.42 | 5 | 4.77 | 7 | 7.15 |
| 2 | 8 | 5.84 | 9 | 8.17 | 6 | 5.12 | 7 | 6.51 |
| 2.5 | 10 | 6.18 | 10 | 9.14 | 7 | 5.74 | 7 | 7.42 |

### *B. Model Convergence for Load Unbalance:*

The proposed co-simulation methods are compared for multiple load unbalance scenarios for both test systems, TS1 and TS2, where unbalance is defined using ANSI C84.1. The load unbalance scenarios are simulated by modifying load allocation factors for the loads connected to one of the phases. We select Phase A to simulate low loading conditions by modifying the load allocation factor. To this regard, both current and voltage unbalance are of interest.

Table 1.3 shows eight unbalance loading scenarios simulated for both test systems. The unbalance is characterized by the percentage of current and voltage unbalance. For Cases 1-4, current unbalance seen at the PCC is varied from 20%-60%. It is noted that percentage voltage unbalance increases with the increase in the percentage of current unbalance. Similar to Cases 1-4, Cases 5-8 also simulate a current unbalance of 20%-60% with an increased level of voltage unbalance. Cases 5-8 are obtained by increasing the loading of the distribution system by 1.5 times while keeping the level of current unbalance same as in Cases 1-4. An increased level of voltage unbalances recorded due to the increased system loading. The converged total apparent power for each unbalance case is also shown in Table 1.3.

Table 1.3 Simulated cases for unbalanced load conditions

SIMULATED CASES FOR UNBALANCED LOAD CONDITIONS

| Unbalance | Cases | | | | | | | |
|---|---|---|---|---|---|---|---|---|
| | 1 | 2 | 3 | 4 | 5 | 6 | 7 | 8 |
| Current(%) | 20 | 40 | 50 | 60 | 20 | 40 | 50 | 60 |
| Voltage(%) | 0.22 | 0.80 | 1.43 | 2.00 | 0.39 | 1.35 | 2.37 | 3.00 |
| $S_T$(MVA) | 45 | 60 | 80 | 95 | 67.5 | 90 | 120 | 142.5 |

The maximum number of iterations and time taken for interface equations to converge for both test systems, TS1 and TS2, are detailed in Table 1.4. Both the unbalance in currents and voltages, affect the system convergence characteristics. For Cases 1-8, as current unbalance is increased, the time and the number of iterations taken to converge by FPI and Newton's method increases. However, Newton's method takes fewer iterations to converge with significantly lesser time. The degree of voltage unbalances also affects the time taken for the system to converge. For instance, both Case 4 and Case 8, resulting in 60% current unbalance, but due to increased loading in Case 8, the voltage unbalance is higher. Due to this, the FPI method takes 42 iterations to converge in 26.98 sec for Case 8 as compared to 16 iterations in 17.23 sec for Case 4 when solving Test System-2 (TS2). The performance of Newton's method is significantly better than the FPI method, and the improvements are more pronounced for higher levels of system unbalance. In fact, for Case 8, Newton's method takes 13 iterations in 15.53 sec as compared to 42 iterations in 26.98 sec taken by FPI method for TS2. Even at the maximum stressed condition (Case 8) for the system, the computational time for the Jacobian operator in Newton's method is only 5.14 sec. This demonstrates the efficiency and scalability of Newton's method in highly stressed environments.

Another key observation is that the FPI method takes a higher number of iterations for single vs. multiple feeder cases. The performance of Newton's method, however, is approximately the same for both single and multi-feeder cases. This would be of significant advantage for the analysis of a large-scale integrated T&D system with multiple interconnected distribution feeders.

Table 1.4  Number of iterations and time required for convergence for simulated cases in Table 1.3

NUMBER OF ITERATIONS(N) AND TIME(T) REQUIRED FOR CONVERGENCE FOR UNBALANCED LOAD CONDITIONS

| Unbalance cases | FPI Method | | | | Newton's Method | | | |
|---|---|---|---|---|---|---|---|---|
| | TS-1 | | TS-2 | | TS-1 | | TS-2 | |
| | N | T (s) | N | T (s) | N | T (s) | N | T (s) |
| Case 1 | 6 | 4.61 | 6 | 6.91 | 5 | 5.83 | 5 | 6.32 |
| Case 2 | 9 | 6.47 | 10 | 10.71 | 7 | 6.14 | 7 | 7.14 |
| Case 3 | 11 | 7.73 | 12 | 13.28 | 7 | 6.72 | 8 | 7.51 |
| Case 4 | 14 | 10.46 | 16 | 17.23 | 9 | 7.51 | 9 | 9.03 |
| Case 5 | 8 | 8.14 | 9 | 11.81 | 6 | 5.74 | 7 | 6.95 |
| Case 6 | 12 | 12.06 | 13 | 15.07 | 7 | 8.12 | 8 | 9.71 |
| Case 7 | 20 | 18.89 | 30 | 21.34 | 9 | 10.56 | 11 | 14.04 |
| Case 8 | 28 | 22.18 | 42 | 26.98 | 10 | 12.84 | 13 | 15.33 |

To further describe the solution methodology for FPI and Newton's method, the solution for interface equations for each iteration corresponding to Case 8 for TS2 are analyzed. The plot for total apparent power at PCC obtained at each iteration using the distribution system and transmission system solvers for the two methods are shown in Figure 1.21. Similarly, plots for voltage at Phase A of the PCC obtained using distribution and transmission system solvers using two methods are also shown. Note that while solutions and errors for FPI method oscillate before converging, the error for Newton's method decreases at each iteration, thus allowing for faster convergence.

Next, the results for co-simulation obtained using a three-sequence transmission model vs. a positive-sequence transmission model are compared. The results for the converged positive sequence voltages at Bus-6 for the two cases are shown in Table 1.5 for varying levels of system unbalance. As the unbalance increases, the difference in the converged positive sequence voltages obtained using the two models increases significantly. This indicates that during unbalanced load conditions, using a positive-sequence transmission system model may lead to significant errors in T&D co-simulation.

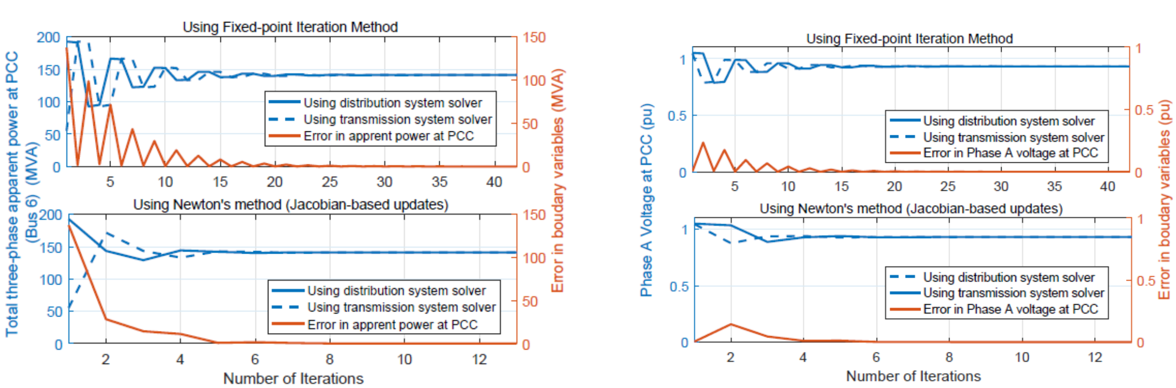


Figure 1.20  Convergence of total three-phase apparent power demand and phase-A voltage magnitude at bus 6 for TS-2 with unbalanced load condition corresponding to case 8

Table 1.5 Comparison of converged positive sequence voltage at PCC for simulated cases in Table 1.3

| Unbalance cases | With three-sequence transmission model | With positive sequence transmission model |
|---|---|---|
| | V (p.u.) | V (p.u.) |
| Case 1 | 1.0382 | 1.0319 |
| Case 2 | 1.0208 | 1.0164 |
| Case 3 | 0.9913 | 0.9767 |
| Case 4 | 0.9719 | 0.9489 |
| Case 5 | 1.0067 | 1.0003 |
| Case 6 | 0.9721 | 0.9635 |
| Case 7 | 0.9371 | 0.9129 |
| Case 8 | 0.9247 | 0.9018 |

**Test System 2 - Large Test System Results**

***A. The convergence of the Base case and Increased system loading:***

The base case loading scenario simulates the loading condition with no intentional unbalances in the distribution feeder. The base case is relatively balanced with approximate per-phase complex power demand equal to 17.8 MW +5.1j MVar. The co-simulation approach is implemented for the base-case load scenario using the two convergence methods and the load demand, and bus voltages at PCC for each iteration are shown in Tables 1.6 and 1.7. Tables 1.6 and 1.7 also compares the number of iterations required by the FPI method and Newton's method to solve the interface equations, respectively. It can be seen from the table that phase voltages both from distribution and transmission system solvers converge for both co-simulation methods in three iterations. The significance of convergence in Newton's method is more pronounced under highly unbalanced loading conditions.

Table 1.6 TSm-2 voltage convergence at the PCC's using FPI method

| | **Iter. 1** | | | **Iter. 2** | | | **Iter. 3** | | |
|---|---|---|---|---|---|---|---|---|---|
| **PCC** | Phase A | Phase B | Phase C | Phase A | Phase B | Phase C | Phase A | Phase B | Phase C |
| **L1** | 0.9849 | 0.9848 | 0.9849 | 0.985 | 0.9849 | 0.985 | 0.9847 | 0.9847 | 0.9847 |
| **L2** | 1.0089 | 1.0088 | 1.0088 | 1.0089 | 1.0089 | 1.0089 | 1.0087 | 1.0087 | 1.0087 |
| **L3** | 0.9982 | 0.9982 | 0.9982 | 0.9983 | 0.9983 | 0.9983 | 0.9981 | 0.9981 | 0.9981 |
| **L4** | 1.0419 | 1.0418 | 1.0418 | 1.0419 | 1.0418 | 1.0419 | 1.0418 | 1.0417 | 1.0418 |
| **L5** | 1.04 | 1.0399 | 1.04 | 1.04 | 1.04 | 1.04 | 1.0399 | 1.0399 | 1.0399 |
| **L6** | 1.0119 | 1.0119 | 1.0119 | 1.012 | 1.012 | 1.012 | 1.0118 | 1.0118 | 1.0118 |
| **L7** | 1.0573 | 1.0572 | 1.0573 | 1.0573 | 1.0573 | 1.0573 | 1.0573 | 1.0572 | 1.0572 |
| **L8** | 1.0484 | 1.0483 | 1.0483 | 1.0484 | 1.0484 | 1.0484 | 1.0483 | 1.0483 | 1.0483 |
| **L9** | 1.0304 | 1.0304 | 1.0304 | 1.0305 | 1.0305 | 1.0305 | 1.0303 | 1.0303 | 1.0303 |
| **L10** | 1.052 | 1.052 | 1.052 | 1.0521 | 1.052 | 1.0521 | 1.052 | 1.0519 | 1.052 |

Table 1.7 TSm-2 voltage convergence at the PCC's using Newton's method

| PCC | Iter. 1 | | | Iter. 2 | | | Iter. 3 | | |
|---|---|---|---|---|---|---|---|---|---|
| | Phase A | Phase B | Phase C | Phase A | Phase B | Phase C | Phase A | Phase B | Phase C |
| **L1** | 0.985 | 0.985 | 0.9849 | 0.9847 | 0.9847 | 0.9847 | 0.9847 | 0.9847 | 0.9847 |
| **L2** | 1.0089 | 1.0086 | 1.0086 | 1.0087 | 1.0087 | 1.0087 | 1.0087 | 1.0087 | 1.0087 |
| **L3** | 0.9982 | 0.9982 | 0.9982 | 0.9981 | 0.9981 | 0.9981 | 0.9981 | 0.9981 | 0.9981 |
| **L4** | 1.042 | 1.042 | 1.042 | 1.0418 | 1.0417 | 1.0417 | 1.0418 | 1.0417 | 1.0418 |
| **L5** | 1.041 | 1.04 | 1.041 | 1.0399 | 1.0399 | 1.0399 | 1.0399 | 1.0399 | 1.0399 |
| **L6** | 1.0121 | 1.0122 | 1.0122 | 1.0118 | 1.0118 | 1.0118 | 1.0118 | 1.0118 | 1.0118 |
| **L7** | 1.0574 | 1.0572 | 1.0573 | 1.0573 | 1.0572 | 1.0572 | 1.0573 | 1.0572 | 1.0572 |
| **L8** | 1.0483 | 1.0481 | 1.0482 | 1.0483 | 1.0483 | 1.0483 | 1.0483 | 1.0483 | 1.0483 |
| **L9** | 1.0304 | 1.0305 | 1.0304 | 1.0303 | 1.0303 | 1.0303 | 1.0303 | 1.0303 | 1.0303 |
| **L10** | 1.0518 | 1.0518 | 1.0519 | 1.052 | 1.052 | 1.052 | 1.052 | 1.0519 | 1.052 |

This TS is also compared for varying load conditions on the distribution end. The load multiplier for the distribution feeder is adjusted to increase the demand in all phases. This results in an increased loading without causing any additional unbalance. Both co-simulation methods are compared again for the new loading conditions, and the results are shown in Table 1.8. In general, as the system loading is increased, both FPI and Newton's method take a longer time to converge with a proportional increase in the number of iterations required. However, Newton's method converges faster with lesser number of iterations. From the previous report, even with the significant increase in the size of the T&D system simulated, the tightly coupled co-simulation method converges, and the Newton's method shows improvement in convergence time for both the smaller and larger simulation models.

Table 1.8 Number of iterations and time required for convergence at PCC for TSm-2

| Load Multiplier | FPI Method | | Newton's method | |
|---|---|---|---|---|
| | No. of Iter | Time (s) | No. of Iter | Time (s) |
| 1 | 3 | 13.3708 | 3 | 9.4412 |
| 1.5 | 4 | 18.6556 | 3 | 14.0888 |
| 2 | 6 | 23.2759 | 4 | 19.1615 |
| 2.5 | 9 | 42.4352 | 6 | 34.3105 |

### *B. Model Convergence for Load Unbalance:*

The proposed co-simulation methods are compared for multiple load unbalance scenarios using both convergence methods where unbalance is defined using ANSI C84.1. The load unbalances are simulated by modifying load allocation factors for the loads connected to one of the phases. We select Phase A to simulate low loading conditions by modifying the load allocation factor. To this regard, only current unbalance is of interest. Table 1.9 shows four unbalance loading scenarios simulated. The unbalance is characterized by the percentage of current unbalance. In these cases, current unbalance seen at the PCC is varied from 20%-50%. It is noted that percentage voltage unbalance increases with the increase in the percentage of current unbalance. The maximum number of iterations and time taken to convergence using both methods are presented in Table 1.9.

The unbalance in current, and hence, the unbalance in voltage affect the system convergence characteristics. For these cases, as current unbalance is increased, the time and the number of iterations taken to converge by FPI and Newton's method increases. However, Newton's method takes fewer iterations to converge with significantly lesser time. For instance, with 50% current unbalance, FPI method takes 9 iterations to converge in 32.9886 sec as compared to 6 iterations in 21.8377 sec. The performance of Newton's method is significantly better than the FPI method, and the improvements are more pronounced for higher levels of system unbalance. By comparison with the previous report, this demonstrates the efficiency and scalability of Newton's method for highly stressed environments.

Table 1.9 Number of iterations and time required for convergence with increasing loading conditions for TSm-2

| **% Current Unbalance** | **FPI Method** | | **Newton's method** | |
|---|---|---|---|---|
| | **No. of Iter** | **Time (s)** | **No. of Iter** | **Time (s)** |
| 20 | 5 | 19.1654 | 4 | 14.9815 |
| 30 | 5 | 22.4416 | 4 | 15.1547 |
| 40 | 6 | 29.9332 | 5 | 19.4632 |
| 50 | 9 | 32.9886 | 6 | 21.8377 |

To further describe the solution methodology for FPI and Newton's method, the solution for interface equations for each iteration corresponding to 50% current unbalance case are analyzed. The plot for Phase A voltage converge at the L1 PCC obtained at each iteration using the distribution system and transmission system solvers for the two methods are compared in Figure 1.22a and 1.22b. Similarly, plots for residual vector at the L1 PCC obtained using distribution and transmission system solvers using two methods are also shown. Note that while solutions and errors for FPI method oscillate before converging, the error for Newton's method decreases at each iteration, thus allowing for faster convergence.

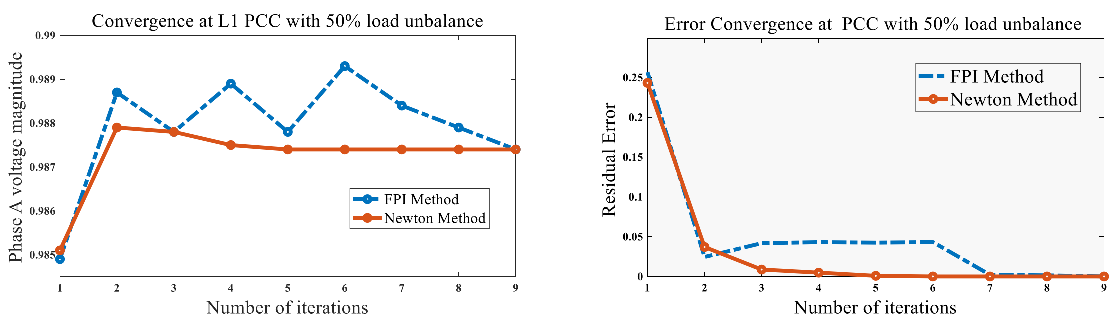


(a) (b)

Figure 1.21 Convergence at L1 PCC with unbalanced load condition of a) phase-A voltage magnitude and b) residual vector

### 1.6.3 Three-Sequence vs. Positive- sequence Transmission Model

#### *A. Test System-1:*

This section compares the results for co-simulation obtained using a three-sequence transmission model vs. a positive-sequence transmission model. The results for the converged positive sequence voltages at Bus-6 PCC for the two cases are shown in Table 1.10 for different levels of system unbalance. As the unbalance increases, the difference in the converged positive sequence voltages obtained using the two models increases significantly. This indicates that during unbalanced load conditions, using a positive-sequence transmission system model may lead to significant errors in T&D co-simulation.

Table 1.10 Comparison of converged positive sequence voltages at bus-6 PCC

| Unbalance cases | With three-sequence transmission model | With positive sequence transmission model |
|---|---|---|
| | V (p.u.) | V (p.u.) |
| Case 1 | 1.0382 | 1.0319 |
| Case 2 | 1.0208 | 1.0164 |
| Case 3 | 0.9913 | 0.9767 |
| Case 4 | 0.9719 | 0.9489 |
| Case 5 | 1.0067 | 1.0003 |
| Case 6 | 0.9721 | 0.9635 |
| Case 7 | 0.9371 | 0.9129 |
| Case 8 | 0.9247 | 0.9018 |

***B. Test System-2:***

In this case, the single-phase LC model (SPLC) is compared with the 3-phase LC model (TPLC) and the error is presented in Table 1.11 for several test cases with 3 different irradiance variabilities as shown in Figure 1.8 using the larger test system model. Both the voltage magnitude error and power demand (load) error at the PCC is compared in the table. Here, L** represents load unbalances and P** represents PV penetrations, i.e., Case L50P80 means load unbalance is 50%, and customer PV penetration is 80%. It can be seen that for the case L50P40 with high variability when 1-phase transmission model is used, the error in the LC model is 10 times higher than that of the 3-phase transmission model. This is true for both voltage magnitude error and load demand error at the PCC. Thus, it can be observed that the single-phase TS model leads to inaccurate results when used for DER integration impact studies.

### 1.6.4 Co-Simulation Vs. Stand-Alone Models

The objective of this section is to validate the TC co-simulation model results with an equivalent standalone T&D system model. In this section, the TSm-1 is modified to include EPRI Ckt-24 distribution feeders at all three load points of the IEEE 9-bus TS. The standalone equivalent T&D model for modified TSm-1 is developed and solved using OpenDSS. OpenDSS is a real-world distribution feeder simulator that can also handle small transmission system simulations. The power flow equations for the simulated stand-alone T\&D model are solved using OpenDSS. The results obtained at the PCC using the standalone model are analyzed and compared with those obtained using TC co-simulation model, and the results are resented in Table 1.12. This study validates the TC co-simulation approach using larger integrated standalone T&D system model. Here, the standalone model is simulated with varying PV deployment scenarios on all ckt-24 feeders connected to the TS. The voltages at the PCC obtained using TC co-simulation, and standalone models are compared for the same simulation conditions.

Table 1.11 Comparison of error for single-phase loosely coupled (SPLC) vs. three-phase loosely coupled (TPLC) models

| Case 1 (pf = 1.00) | | | | | | |
|---|---|---|---|---|---|---|
| | Voltage Magnitude Error % | | | | | |
| | Low Var | | Med Var | | High Var | |
| Case | 3-Phase | 1-Phase | 3-Phase | 1-Phase | 3-Phase | 1-Phase |
| L10P20 | 0.0496 | 0.4680 | 0.0532 | 0.4709 | 0.0536 | 0.4553 |
| L50P10 | 0.2255 | 1.9003 | 0.2348 | 1.9118 | 0.2311 | 1.9109 |
| L10P40 | 0.0460 | 0.4642 | 0.0568 | 0.4707 | 0.0694 | 0.4698 |
| L50P40 | 0.2007 | 2.0535 | 0.2038 | 1.9885 | 0.2124 | 2.0112 |
| L10P60 | 0.0310 | 0.4484 | 0.0601 | 0.4656 | 0.0781 | 0.4605 |
| L50P80 | 0.1846 | 2.1677 | 0.2334 | 2.1863 | 0.2601 | 2.1948 |
| | Power Demand Error % | | | | | |
| L10P20 | 0.0914 | 0.7972 | 0.0958 | 0.7993 | 0.0900 | 0.7900 |
| L50P10 | 0.6364 | 6.0384 | 0.6503 | 6.0950 | 0.6537 | 6.0955 |
| L10P40 | 0.0662 | 0.7875 | 0.0902 | 0.7980 | 0.1097 | 0.7972 |
| L50P40 | 0.5054 | 5.4822 | 0.5130 | 5.8882 | 0.5400 | 5.7837 |
| L10P60 | 0.1308 | 0.7271 | 0.1157 | 0.7824 | 0.1348 | 0.7916 |
| L50P80 | 0.5153 | 4.7496 | 0.6286 | 4.7850 | 0.7114 | 4.7617 |

For the validation, scenario 25 of the 100 different PV deployment scenarios is selected. Here, the co-simulation framework is referred to as Model-1, and the standalone T&D model is referred to as Model-2. The voltages at PCC are compared in Table 1.12 for varying PV penetration levels. As can be observed from this table, the difference in voltages at the three PCC points obtained by solving the standalone model (Model-2) and using TC co-simulation (Model-1) is less than 0.0001 pu.

Table 1.12 Comparison of converged positive sequence voltage at T&D PCC using TC co-simulation model and stand-alone T&D model

| | Model-1 Voltages (p.u.) | | | Model-2 Voltages (p.u.) | | |
|---|---|---|---|---|---|---|
| % PV | Bus 5 | Bus 6 | Bus 8 | Bus 5 | Bus 6 | Bus 8 |
| 10% | 1.0444 | 1.0511 | 1.0558 | 1.0444 | 1.051 | 1.0557 |
| 20% | 1.0447 | 1.0516 | 1.0576 | 1.0446 | 1.0514 | 1.0574 |
| 30% | 1.0449 | 1.0519 | 1.0588 | 1.0449 | 1.0518 | 1.0585 |
| 40% | 1.0449 | 1.0521 | 1.0598 | 1.0449 | 1.0521 | 1.0595 |
| 50% | 1.0448 | 1.0523 | 1.0608 | 1.0448 | 1.0522 | 1.0606 |
| 60% | 1.0446 | 1.0522 | 1.0617 | 1.0446 | 1.0522 | 1.0616 |
| 70% | 1.0442 | 1.0521 | 1.0625 | 1.0441 | 1.052 | 1.0627 |
| 80% | 1.0438 | 1.0518 | 1.0633 | 1.0437 | 1.0517 | 1.0635 |
| 90% | 1.0433 | 1.0514 | 1.0639 | 1.043 | 1.0513 | 1.0640 |
| 100% | 1.0426 | 1.0509 | 1.0644 | 1.0424 | 1.0508 | 1.0646 |

Initially, in this work, the three distribution systems connected to individual transmission load points were solved by a series implementation (SI) technique. This means that following each solution of the transmission system, the three distribution systems are solved independently but is a sequence (one after the other). Typically, all three distribution systems can be solved together and in parallel by distributing the individual distribution systems to different computer cores. We call this approach the parallel implementation (PI) of the co-simulation method. To test the PI co-simulation method for added computational advantage, we have implemented both FPI and

Newton-based co-simulation approach using the MATLAB Parallel Computing Toolbox. In this implementation, the three distribution systems connected to IEEE 9-bus system are solved simultaneously, i.e. in parallel.

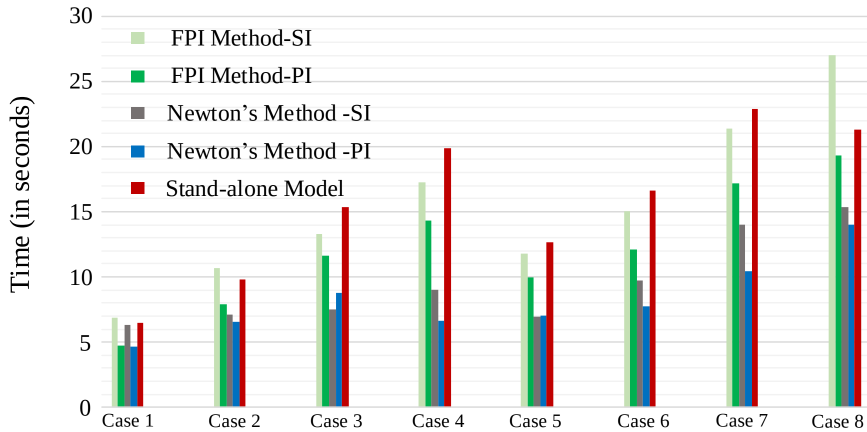


Figure 1.22 Comparison of time taken for convergence in TSm-1 using co-simulation model and stand-alone model

The time taken for solving the eight test cases described in Table 1.3 by co-simulation methods (both SI and PI implementation) are compared against the stand-alone solver. The results are shown in Figure 1.23. Newton's method with parallel implementation converges the fastest for all test cases. Generally, all co-simulation methods converge relatively faster than the stand-alone model except in Case 8 when FPI method in SI mode takes longer time to converge. However, for the same case (case 8), the convergence time improves significantly on implementing the FPI method in PI mode, i.e., when the three distribution systems are solved in parallel. Overall, the co-simulation models converge faster than the stand-alone model for the selected test system, especially with parallel implementation.

### 1.6.5 Comparison of T&D Coupling Methods

For the comparison between DC, LC, and TC method, time-sequence analysis has been done. The IEEE 9-bus transmission system with one load point replaced by EPRI Ckt-24 is used as one of the tests systems in this simulation. The larger test system model developed in this report is also used to demonstrate the need for TC models. A specific time window for three different days with different PV generation variability scenarios is simulated. In that time window, the loads in the distribution systems are assumed to be constant. Three days of PV profiles with different variabilities (low, medium, and high) in PV irradiance are simulated. The low, medium, and high PV variability have a variability index (VI) of 1.33, 6.29, and 15.58, respectively, where VI is defined using [30]. One PV deployment scenario from the previous report has been used for this analysis. A one-hour time -window (12.00-1.00pm) is selected. In this analysis, PV penetration is varied from 10% to 100% where penetration is defined as the percentage of customers with PVs. For each simulation study, the load unbalance is varied from 10% to 50% in the steps of 10% by changing the customer load distribution in each of the three phases. Nonetheless, the PVs are mostly unintentionally unbalanced. For time-series analysis, DC, LC, and TC models are compared for their accuracy in modeling T&D interactions. The comparison is made for different levels of PV variability, multiple PV penetration scenarios, different number of T&D coupled points, and multiple load unbalance cases. For consistency, every coupling model includes a 3-phase transmission model solver. The single-phase model and three-phase transmission models are separately compared for a few specific cases. Note for the IEEE 9-bus system the errors due to the LC model in estimating interface voltages are small as this is a very small test system. In later simulations with larger test system (IEEE 39-bus interfaced with 10 EPRI Ckt 24), we will see higher levels of error due to the LC model.

## A. Impact of PV Variability

The impact of PV generation variability accuracy of the T&D co-simulation for different coupling models is evaluated. Three different days with different levels of PV irradiance variability are selected for time-series analysis to show the impact of PV variability on interface error for both LC and DC models. The PV penetration (% of MW) with respect to PV irradiance variability has been shown in Table 1.13.

In Table 1.13, U** represents load unbalance, and P** represents PV penetrations. It is clear that with the increment of variability, the error in voltage magnitude for the LC model and DC model increases. Also, the error in DC is higher than LC model, which reflects that the strength in the coupling of T&D plays a vital role in the percentage of error. The stronger the coupling of T&D, the less error it will generate in estimating voltage magnitude. For low variability (VI- 1.33), medium variability (VI- 6.29) and high variability (VI- 15.88), the voltage magnitude at PCC from LC and TC model and error for LC model has been shown in Figure 1.24. In this case, the load unbalance is 40%, and PV penetration is 80%. Also, the pf for these PVs are 1. With variability, error in LC also increases.

Table 1.13 % Mean error comparing the converged voltages in DC, LC and TC models

| | **Mean % error TC vs. LC (Voltage)** | | | | | |
|---|---|---|---|---|---|---|
| ***Cases*** | **Case 1 (pf = 1.00)** | | | **Case 2 (pf = 0.98)** | | |
| | **Low** | **Med** | **High** | **Low** | **Med** | **High** |
| ***U10P20*** | 0.0496 | 0.0532 | 0.0536 | 0.0471 | 0.0523 | 0.0583 |
| ***U50P10*** | 0.2255 | 0.2348 | 0.2311 | 0.1881 | 0.2282 | 0.1922 |
| ***U10P40*** | 0.0460 | 0.0568 | 0.0694 | 0.0365 | 0.0576 | 0.0732 |
| ***U50P40*** | 0.2007 | 0.2038 | 0.2124 | 0.1928 | 0.2271 | 0.2622 |
| ***U10P60*** | 0.0310 | 0.0601 | 0.0781 | 0.0293 | 0.0621 | 0.0868 |
| ***U50P80*** | 0.1846 | 0.2334 | 0.2601 | 0.1767 | 0.2312 | 0.2766 |
| ***L10P100*** | 0.0294 | 0.0679 | 0.1044 | 0.0228 | 0.0846 | 0.1272 |
| | **Mean error TC vs. DC (Voltage)** | | | | | |
| ***Cases*** | **Case 1 (pf = 1.00)** | | | **Case 2 (pf = 0.98)** | | |
| | **Low** | **Med** | **High** | **Low** | **Med** | **High** |
| ***U10P20*** | 1.8202 | 1.9134 | 1.9799 | 1.7396 | 1.8496 | 1.8911 |
| ***U50P10*** | 8.7808 | 8.7979 | 8.8337 | 8.7346 | 8.7709 | 8.8022 |
| ***U10P40*** | 1.7135 | 1.8822 | 1.9603 | 1.4396 | 1.6675 | 1.7311 |
| ***U50P40*** | 8.5821 | 8.8098 | 8.8743 | 8.1355 | 8.4648 | 8.5266 |
| ***U10P60*** | 1.5643 | 1.7997 | 1.8933 | 1.2733 | 1.5874 | 1.6598 |
| ***U50P80*** | 8.1002 | 8.5097 | 8.5678 | 7.6411 | 8.1229 | 8.1743 |
| ***U50P100*** | 7.9033 | 8.3504 | 8.4257 | 7.3589 | 7.8884 | 7.9224 |

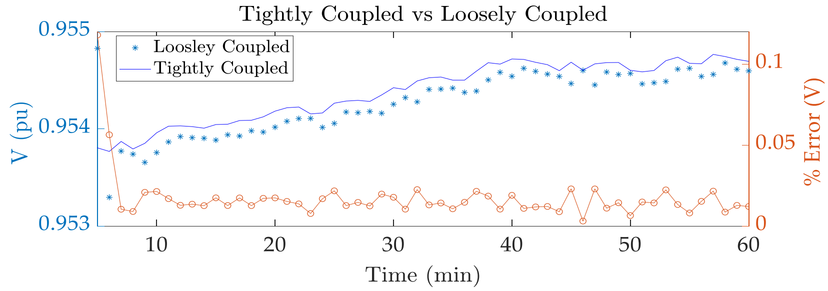


(a)

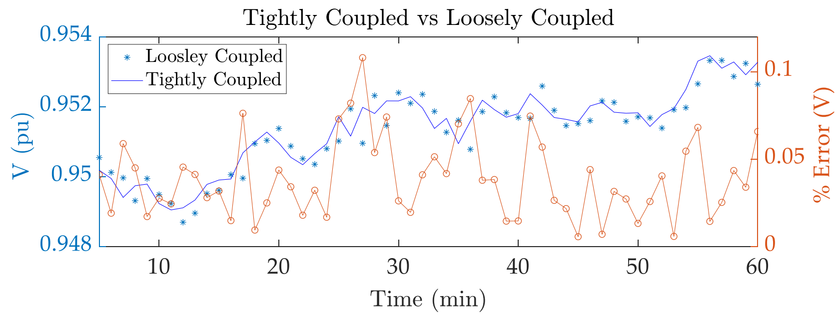


(b)

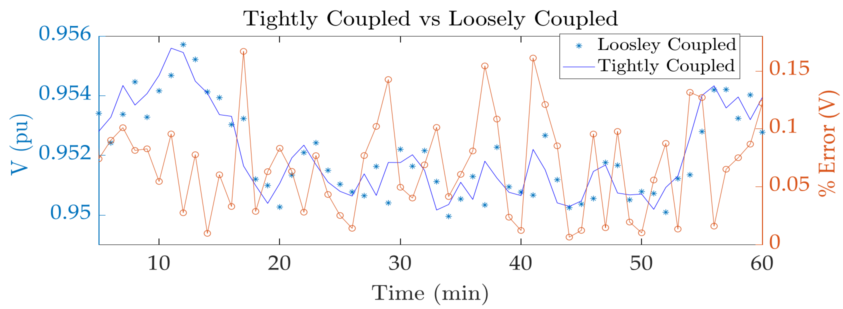


(c)

Figure 1.23 Voltage magnitude and error % at PCC for a) low variability b) medium variability c) high variability

## B. Impact of Load Unbalance

Next, the impact of load unbalance on the LC and DC model is evaluated. In Figure 1.25, the voltage magnitude for 1 hour at the PCC for 40% load unbalance has been shown. Figure 1.25a is for medium variability, and Figure 1.25b is for the high variability of irradiance cases at 20% customer PV penetration. For 20, 40, and 80% of customer PV penetration, 10, 20, and 40% load unbalance scenarios have been evaluated and compared.

The mean percentage error in voltage magnitude at PCC for LC and DC model for cases 1 and 2 (pf 1 and pf 0.98) is shown in Table 1.14. Also, the error for the medium and high variability of PV irradiances is compared for different levels of load unbalances for a specific PV penetration scenario. From the table, as load unbalance increases, the error in voltage magnitude for the LC model and DC model also increases. For the DC model, the error can go as high as 10%. Thus, with more load unbalance in the distribution system, the DC and LC co-simulation platform are less accurate and start to deviate more and more from the actual state of the system.

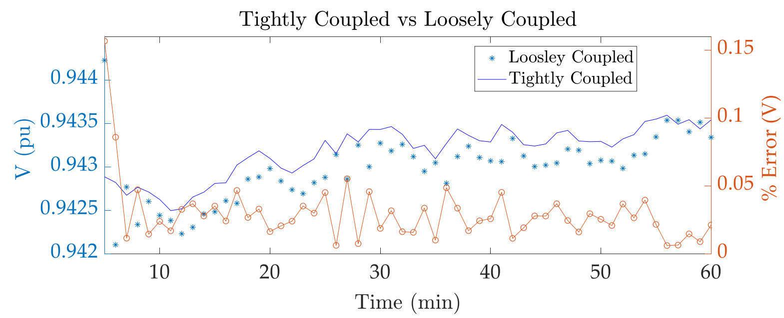


(a)

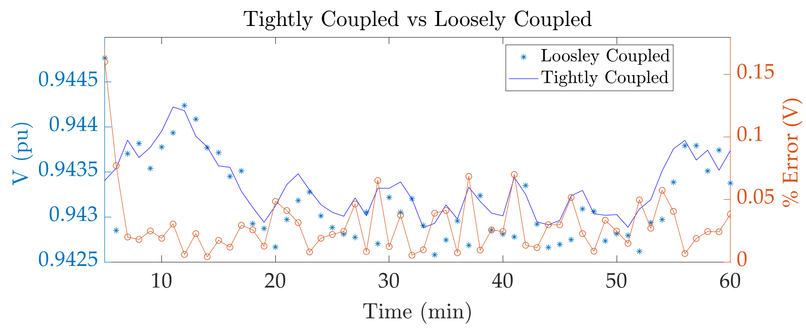


(b)

Figure 1.24 Voltage magnitude and % error at 40% load unbalance a) medium variability b) high variability

Table 1.14 Impact of load unbalance

| ***Cases*** | **Mean % error TC vs LC (Voltage)** | | | | **Mean % error TC vs DC (Voltage)** | | | |
|---|---|---|---|---|---|---|---|---|
| ***PV 20%*** | **Case 1 (pf = 1.00)** | | **Case 2 (pf = 0.98)** | | **Case 1 (pf = 1.00)** | | **Case 2 (pf = 0.98)** | |
| ***LU %*** | ***Medium*** | ***High*** | ***Medium*** | ***High*** | ***Medium*** | ***High*** | ***Medium*** | ***High*** |
| ***10*** | 0.0532 | 0.0536 | 0.0523 | 0.0583 | 1.9134 | 1.9799 | 1.8496 | 1.8911 |
| ***20*** | 0.1223 | 0.1305 | 0.1228 | 0.1317 | 5.3513 | 5.3950 | 5.3136 | 5.3540 |
| ***40*** | 0.3076 | 0.3087 | 0.2999 | 0.3080 | 10.5985 | 10.6586 | 10.5871 | 10.6374 |
| ***PV 40%*** | **Case 1 (pf = 1.00)** | | **Case 2 (pf = 0.98)** | | **Case 1 (pf = 1.00)** | | **Case 2 (pf = 0.98)** | |
| ***LU %*** | ***Medium*** | ***High*** | ***Medium*** | ***High*** | ***Medium*** | ***High*** | ***Medium*** | ***High*** |
| ***10*** | 0.0568 | 0.0694 | 0.0576 | 0.0732 | 1.8822 | 1.9603 | 1.6675 | 1.7311 |
| ***20*** | 0.1294 | 0.1459 | 0.1309 | 0.1508 | 5.2604 | 5.3325 | 5.0563 | 5.1125 |
| ***40*** | 0.3035 | 0.3157 | 0.3038 | 0.2334 | 10.6254 | 10.7200 | 10.4909 | 10.5702 |
| ***PV 80%*** | **Case 1 (pf = 1.00)** | | **Case 2 (pf = 0.98)** | | **Case 1 (pf = 1.00)** | | **Case 2 (pf = 0.98)** | |
| ***LU %*** | ***Medium*** | ***High*** | ***Medium*** | ***High*** | ***Medium*** | ***High*** | ***Medium*** | ***High*** |
| ***10*** | 0.0620 | 0.0882 | 0.0686 | 0.1040 | 1.7571 | 1.8486 | 1.4745 | 1.5198 |
| ***20*** | 0.1410 | 0.1697 | 0.1442 | 0.1812 | 4.9877 | 5.0668 | 4.7656 | 4.8224 |
| ***40*** | 0.2296 | 0.3188 | 0.3063 | 0.3138 | 10.5479 | 10.6539 | 10.3938 | 10.4856 |

### C. Impact of PV Penetration

In this simulation case study, the impact of PV penetration on the strength of coupling of T&D is evaluated. For the same load unbalance and same irradiance variability, the PV penetration is increased, and the results from TC, LC, and DC co-simulation platform are compared. In Figures 1.26 and 1.27, the voltage magnitudes at PCC for 10% and 80% PV penetration is presented for 2 different load unbalance (10% and 50%) cases. In Table 1.15, the mean error percentage for substation voltage magnitude obtained using LC and DC models is shown. Five different levels of PV penetration (20, 40, 60, 80 and 100%) with 10, 20 and 50% load unbalance scenarios are compared. With the increment in load unbalance in the distribution system, the error in voltage magnitude for loosely coupled (LC) model increases.

With more PVs in the distribution system, the aggregated PV variability increases, which causes higher errors in the LC model as can be seen from Figure 1.28. However, unlike LC co-simulation model, DC models' error decreases with increased PV penetrations because the voltage unbalance at substation decreases (load decreases). As DC solves distribution system as an aggregated load and does not account for any load unbalances, this decreased unbalance causes reduced error. But still, the error is as high as 9% in voltage magnitude.

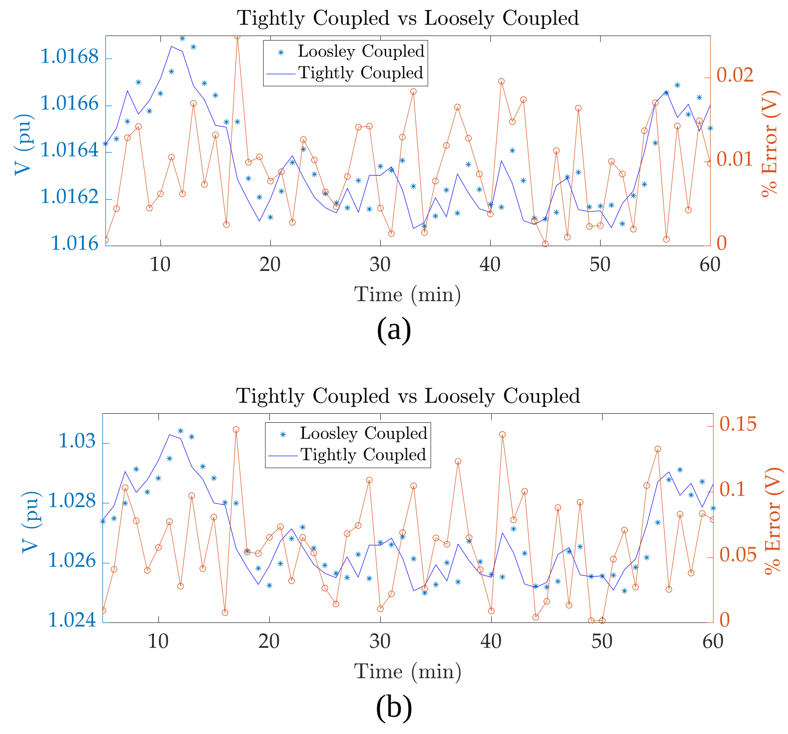


Figure 1.25 Voltage magnitude and % error with 10%load unbalance at a) 10% PV penetration b) 80% PV penetration

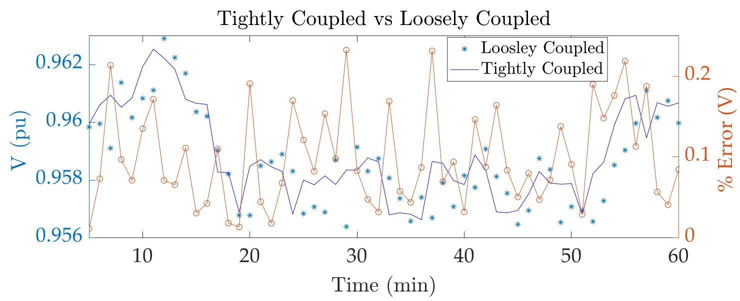


(a)

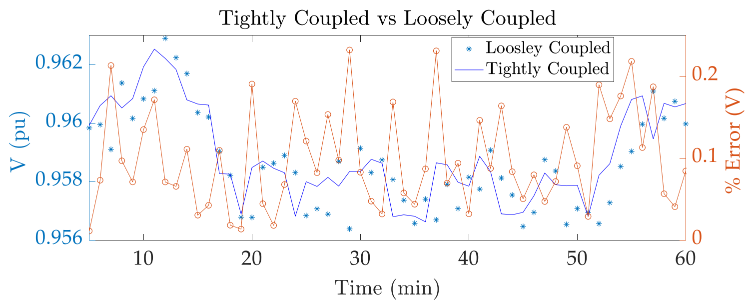


(b)

Figure 1.26 Voltage magnitude and % error with 50%load unbalance at a) 10% PV penetration b) 80% PV penetration

Table 1.15 Impact of PV penetration

| ***Cases*** | **Mean % error TC vs LC (Voltage)** | | | | **Mean % error TC vs DC (Voltage)** | | | |
|---|---|---|---|---|---|---|---|---|
| ***LU 10%*** | **Case 1 (pf = 1.00)** | | **Case 2 (pf = 0.98)** | | **Case 1 (pf = 1.00)** | | **Case 2 (pf = 0.98)** | |
| ***PV %*** | ***Medium*** | ***High*** | ***Medium*** | ***High*** | ***Medium*** | ***High*** | ***Medium*** | ***High*** |
| ***20*** | 0.0532 | 0.0536 | 0.0523 | 0.0583 | 1.9134 | 1.9799 | 1.8496 | 1.8911 |
| ***40*** | 0.0568 | 0.0694 | 0.0576 | 0.0732 | 1.8822 | 1.9603 | 1.6675 | 1.7311 |
| ***60*** | 0.0601 | 0.0781 | 0.0621 | 0.0868 | 1.7997 | 1.8933 | 1.5874 | 1.6598 |
| ***80*** | 0.0620 | 0.0882 | 0.0686 | 0.1040 | 1.7571 | 1.8486 | 1.4745 | 1.5198 |
| ***100*** | 0.0679 | 0.1044 | 0.0846 | 0.1272 | 1.6693 | 1.7324 | 1.2343 | 1.2417 |
| ***LU 20%*** | **Case 1 (pf = 1.00)** | | **Case 2 (pf = 0.98)** | | **Case 1 (pf = 1.00)** | | **Case 2 (pf = 0.98)** | |
| ***PV %*** | ***Medium*** | ***High*** | ***Medium*** | ***High*** | ***Medium*** | ***High*** | ***Medium*** | ***High*** |
| ***20*** | 0.1223 | 0.1305 | 0.1228 | 0.1317 | 5.3513 | 5.3950 | 5.3136 | 5.3540 |
| ***40*** | 0.1294 | 0.1459 | 0.1309 | 0.1508 | 5.2604 | 5.3325 | 5.0563 | 5.1125 |
| ***60*** | 0.1358 | 0.1595 | 0.1375 | 0.1649 | 5.1005 | 5.1817 | 4.9157 | 4.9822 |
| ***80*** | 0.1410 | 0.1697 | 0.1442 | 0.1812 | 4.9877 | 5.0668 | 4.7656 | 4.8224 |
| ***100*** | 0.1453 | 0.1794 | 0.1541 | 0.1977 | 4.8441 | 4.9041 | 4.5429 | 4.5729 |
| ***LU 50%*** | **Case 1 (pf = 1.00)** | | **Case 2 (pf = 0.98)** | | **Case 1 (pf = 1.00)** | | **Case 2 (pf = 0.98)** | |
| ***PV %*** | ***Medium*** | ***High*** | ***Medium*** | ***High*** | ***Medium*** | ***High*** | ***Medium*** | ***High*** |
| ***20*** | 0.1918 | 0.1957 | 0.1926 | 0.2056 | 5.3513 | 5.3950 | 5.3136 | 5.3540 |
| ***40*** | 0.2038 | 0.2124 | 0.2271 | 0.2622 | 5.2604 | 5.3325 | 5.0563 | 5.1125 |
| ***60*** | 0.2208 | 0.2491 | 0.2261 | 0.2726 | 5.1005 | 5.1817 | 4.9157 | 4.9822 |
| ***80*** | 0.2334 | 0.2601 | 0.2312 | 0.2766 | 4.9877 | 5.0668 | 4.7656 | 4.8224 |
| ***100*** | 0.2425 | 0.2843 | 0.2176 | 0.2566 | 4.8441 | 4.9041 | 4.5429 | 4.5729 |

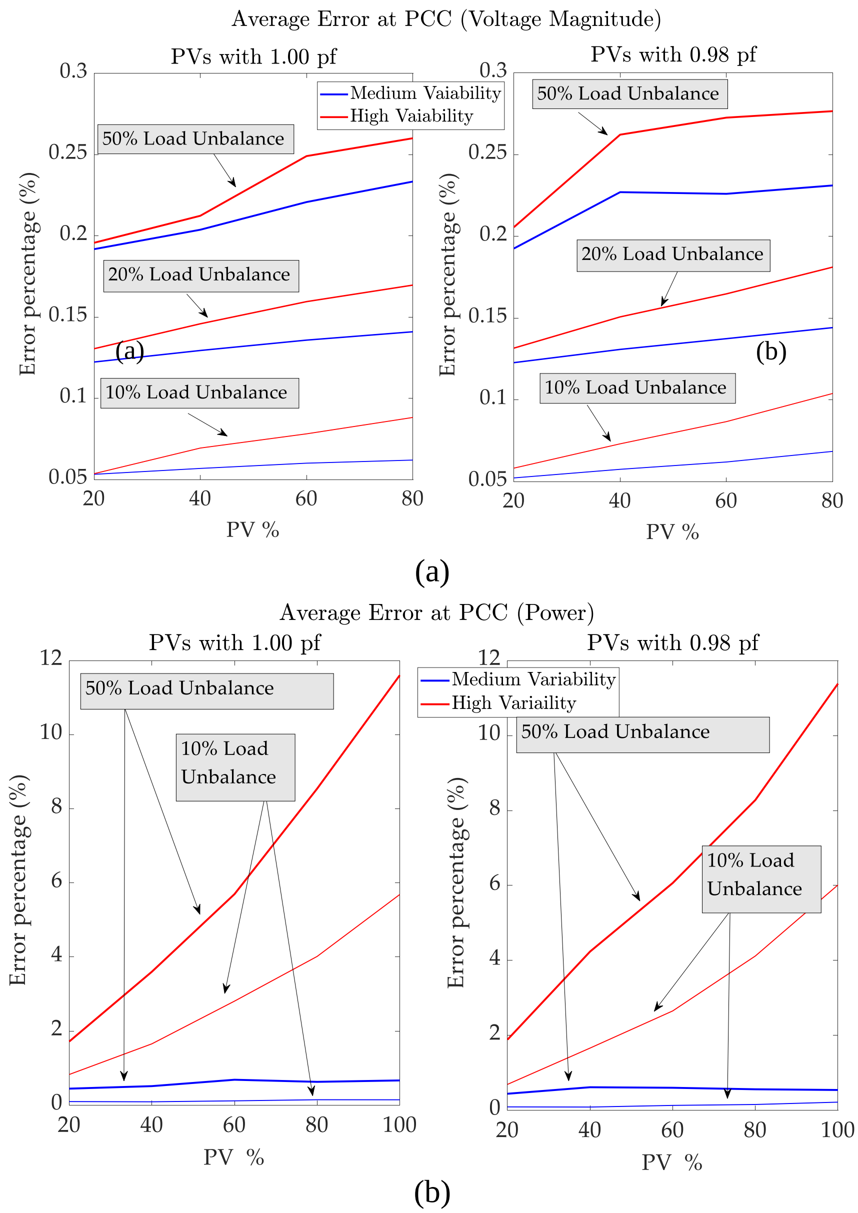


Figure 1.27 LC Method - Impact of different variables on error in a) Voltage magnitude b) Power flow at T&D PCC

From the previous discussions, it is clear the accuracy of LC and DC models are affected by the PV variability, degree of load unbalance, and PV penetration levels. In Figure 1.28, the error of the LC model with respect to these variables is shown. It is evident that with increased PV penetration, the error in the LC model increases. The error in the LC model also increases with the increase in load unbalance and the PV generation variability. In addition, the power factor of PVs also instigates additional errors in the LC model. With the reactive-power generation capabilities, i.e., lower pf PVs cause a higher error in loosely coupled T&D models. Note that unlike PCC voltages, the error in substation power demand is significantly high even for LC models and can go as high as 12% at 50% load unbalance and 100% PV penetration level.

## D. Impacts on the Distribution System

The errors introduced in co-simulation due to LC and DC models are not only limited to the transmission systems but also have significant impacts on the distribution system solutions. In Figure 1.29, the mean error for the maximum voltage at the distribution system (both at primary and secondary feeder level) is compared for the LC model.

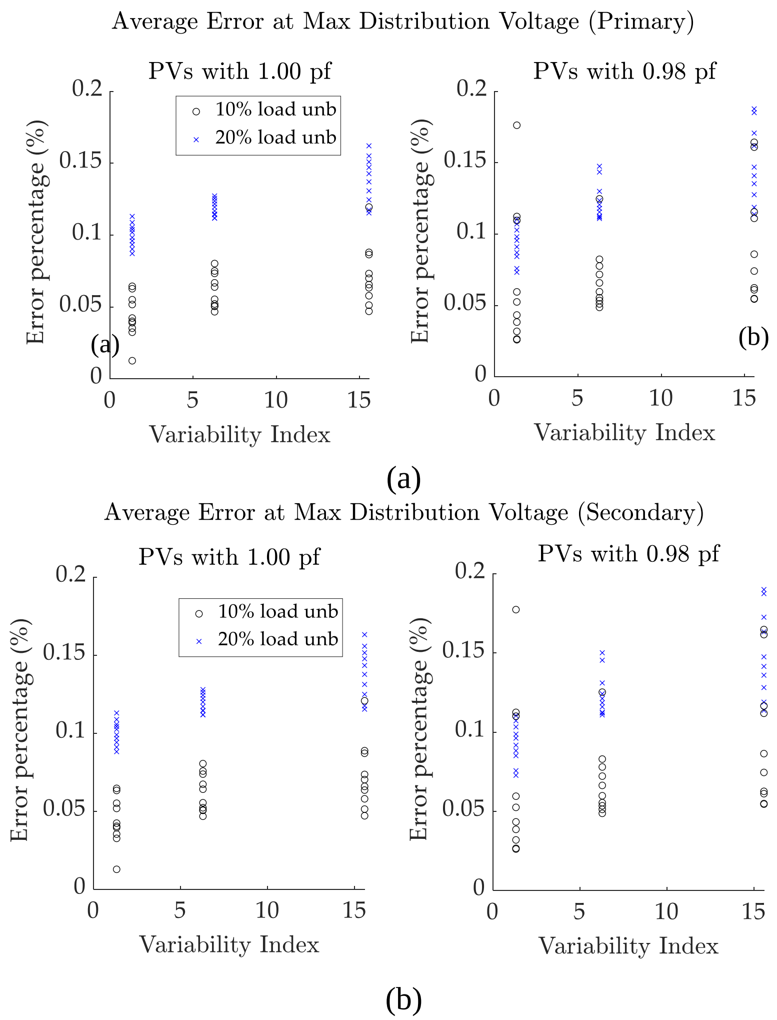


Figure 1.28 LC Method - Impact of different variables on error in distribution side
a) primary b) secondary

With increased variability, error at both primary and secondary feeder level increases for DC and LC models. Also, increased load unbalance contributed to additional errors in simulation results. The error for the DC model is very high, and it can go as high as 5% for only 20% load unbalances. Clearly, both the LC and DC co-simulation model is not accurate enough for estimating the distribution systems' real scenario. In addition to that, the decoupled model causes a very high error, which makes the model obsolete for such cases.

### E. Impact of system size on T&D Co-Simulation Error

Further simulation studies are conducted to evaluate the errors in LC and DC models using IEEE 39-bus transmission system interfaced with multiple large distribution test system. The voltage magnitude of the substation connected at bus 33 of the IEEE 39-bus transmission system is compared for co-simulation error due to the loosely coupled model against the iteratively/tightly coupled model. In this study, 40% load unbalance and 80% PV penetration with medium variability of irradiance scenario is simulated.

It can be seen from Figure 1.30 that when simulating more interconnection points with distribution feeder, the LC model introduces higher co-simulation error. On interfacing IEEE 39-bus system with only two distribution systems (modeling the rest of load points as aggregated loads), the error for the loosely coupled model is around 0.9% which is higher than previous smaller test case (IEEE 9 bus system interfaced with 1 distribution system). If five load points for the transmission systems are co-simulated using detailed distribution feeder models, the error in co-simulation due to LC model increase to 1.7%. When 10 distinct transmission load buses are interfaced with distribution feeders, the error can go as high as 2.2% in voltage magnitude. We conclude that for larger co-simulation cases with several T&D coupling points, the LC model is expected to lead to higher errors in co-simulation. This is due to the fact that every loosely coupled T&D point in the integrated system contributes to the modeling error that is accumulated for the whole system. Thus, in all practical scenarios, a tightly coupled approach is needed when high variability is expected from distribution connected DERs. Higher levels of system unbalance, and DER penetration scenarios also call for an iterative coupling.

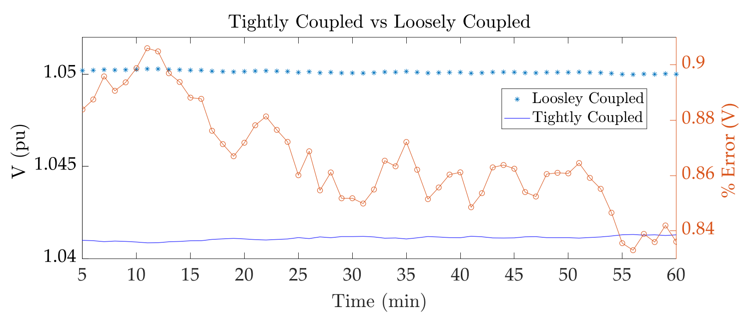


(a)

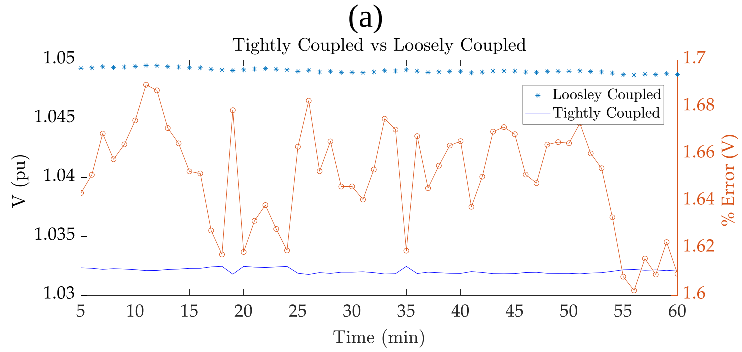


(b)

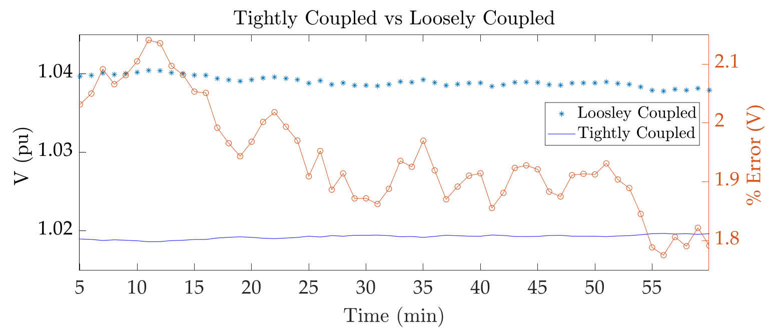

(c)

Figure 1.29 Impact of number of T&D coupling on error for medium variability case with a) 2 distribution systems b) 5 distribution systems c) 10 distribution systems

## 1.7 Conclusion

This work presents an iteratively coupled co-simulation framework for unbalanced integrated T&D system analysis. The primary objective is to bring co-simulation approach close to standalone T&D system model that can accurately model unbalanced load conditions and increased demand variability that are likely to be realized in feeders with an increased level of DER penetrations. The proposed integrated T&D framework is a valuable resource for evaluating the impacts of DERs on transmission system operations and understanding the power quality issues that would be difficult to study on a decoupled T&D model. The proposed framework is comprised of a 5-min ahead ACOPF economic dispatch formulation, a three-sequence AC power flow for the transmission system, a three-phase AC power flow for the distribution system, and an iterative coupling approach for T&D interface. The inherent complexity of modeling the integrated T&D systems in a single platform is addressed by iteratively coupling the models designed in their legacy software. This makes the framework proposed comparable to stand-alone unified models. The idea of integrating multiple distribution systems to transmission system load points is proposed and tested.

Furthermore, an analytical framework is developed to mathematically represent the T&D co-simulation interface and first-order and second-order convergent methods, using FPI and Newton's method, respectively, are proposed to solve the nonlinear interface equations. The results conclude that the proposed framework converges for different levels of system loading and unbalance conditions. Newton's method requires less time to converge as compared to FPI method and the stand-alone model. The improvements in the number of iterations and the time taken to converge are more pronounced for stressed system conditions.

In addition to this, the effect of coupling nature of T&D has been assessed for DC, LC, and TC co-simulation models in a quasi-static time-series simulation environment. Specifically, the effects of T&D coupling strength on the accuracy of T&D co-simulation are evaluated. Several cases with PV variability, DER penetration, and load unbalance is simulated, and integrated T&D test systems are solved using DC, LC, and TC co-simulation methods. It is shown that both DC and LC T&D co-simulation models incur errors when modeling integrated T&D systems with unbalanced load conditions due to single-phase customers and/or high PV/DER penetrations; as expected DC model leads to significantly high errors compared LC and TC models and are not suitable for DER impact analysis. Multiple PV deployment scenarios by varying the locations and sizes of PVs are simulated, and their impacts on transmission and distribution system voltages are also studied.

The following are the major observations based on different test studies: (1) DC model is significantly more inaccurate compared to the LC model (2) the percentage error in power demand is higher than the voltage magnitude at the T&D PCC (3) error in the LC model are higher during stressed system conditions such as high PV variability, high levels of load unbalance, high percentages of PV penetrations; the LC model leads to higher error when PVs incur a higher generation variability; (4) errors in the LC model increase as the number of coupled T&D points in the integrated T&D system are increased; for the larger T&D test systems LC model leads to significantly higher errors; and (5) the strength of T&D coupling affects other nodes in the T&D systems as well, i.e. both LC and DC model introduces significant errors in estimating the states of other buses in both TS and DS.

Finally, it is concluded that with the increase in system size, a higher error in incurred by the LC model indicating that LC model is insufficient to conduct DER impact analysis on integrated T&D system, especially during stressed system conditions. Furthermore, it is also concluded that the single-phase transmission model is unable to represent actual system conditions and is inadequate for integrated T&D system analysis when DS introduces significant system unbalance. Thus, the currently used LC co-simulation methods that employ a single-phase TS model is not accurate for DER impact studies when DS introduces unbalanced system conditions due to single-phase loads and DERs. The simulated test cases clearly demonstrate the advantages of the TC co-simulation model over LC and DC methods. Finally, it is concluded that the proposed TC model can accurately represent integrated T&D systems during stressed system conditions and is expandable to conduct an accurate DER impact analysis and can replicate the standalone T&D system without any complexity in modeling.

# 2. Hybrid T&D Co-Simulation Framework and Integration of Distribution-Connected Battery Energy Storage Systems for Frequency Regulation

## 2.1 Introduction

### 2.1.1 Background

The increasing penetrations of distributed energy resources (DERs) and energy storage systems (ESS) is proving to be a promising solution in the movement towards a decarbonized grid [31]. Unfortunately, with these rapid transformations, and the uncertainties in supply and demand unbalances arising from the high variability in generation patterns due to renewable resources such as solar and wind resources, the grid is facing unprecedented operational challenges at both transmission and distribution levels [32, 33]. Frequency regulation provided by automatic generation control (AGC) plays a critical role in maintaining the supply-demand balance. Note that frequency regulation provided by AGC acts on a time-scale of minutes, after the generator governor control has responded, and before the hour by hour generation capacity is brought online.

With the integration of a significant amount of DERs, specifically, photovoltaic systems (PVs), the system operators are facing critical challenges with regard to maintaining supply and demand balance [34]. It is important to account for the intermittency in generation from these resources as they can adversely affect the grid frequency. Traditionally, a majority of frequency regulation capability is provided by specially equipped generators. As technologies evolve, the participation of new types of flexible energy resources such as battery storage systems and flywheels, with their significantly faster ramping capabilities, can reduce the need to procure additional regulation capacity on account of variable generation resources [35]. For example, following the FERC Orders 755 [36] and 784 [37], all independent system operators (ISO) and regional transmission organizations (RTO) in the U.S. have implemented pay-for-performance regulation markets to procure AGC services form distribution connected BESS while accounting for the state of charge (SoC) constraint of BESS in their regulation dispatch. To further utilize the fast-responsive capability of BESS beyond the traditional AGC framework, some system operators, such as Pennsylvania-New Jersey-Maryland Interconnection (PJM), have introduced fast regulation signals. Units participating in fast regulation follow a regulation signal (RegD) that changes much faster than the traditional AGC signal (RegA) for additional compensation. The system operators also benefit from improved regulation accuracy [38, 39].

Owing to these advances, recently, several studies have proposed bidding strategies for BESS participation in the ancillary services markets [40-44]. Traditionally, the regulation signals are dispatched at the transmission level, and the distribution system modeling and operational constraints are approximated at the transmission level. These studies assess the BESS regulation capacities using SoC constraints. However, the effects of dispatching the BESS regulation signals on distribution system operational constraints are not analyzed. Most of the existing studies evaluate the integration challenges of BESS in providing ancillary services to the grid either only at the distribution level or individually at transmission and distribution levels using a decoupled T&D system analysis [38-45]. That is, distribution-connected BESS is represented as an aggregated model at the transmission and distribution coupling point in the simulation studies. The rapid changes in the BESS operations due to fast regulation dispatch can potentially affect distribution-level operating constraints requiring an integrated T&D system modeling and analysis. In this chapter, we address these and associated challenges of evaluating the impacts of distribution-connected DERs on bulk grid frequency response and assessing the utility of distribution-connected BESS in providing frequency regulation services.

### 2.1.2 Problem Statement – Need for Hybrid T&D Co-Simulation

The ISOs are confronted with multiple challenges when attempting to incorporate distribution-connected BESS to provide frequency regulation services for the bulk grid. The challenges are listed below:

1. First, having uncertainties about the system disturbances and the frequency changes makes it difficult to schedule the BESS accurately [34].
2. Second, the contribution of BESS regulation services in the upcoming time slots depends on their utilization at the current time slot [40].
3. Third, the AGC scheduling at the ISO level is non-trivial because it depends on the power flow changes of the distribution network, which in turn affects the BESS charging levels and their capability to provide for frequency regulation [41].

In order to successfully integrate BESS technologies in the grid to enable their participation in providing secondary control services specifically, frequency regulation services, they must be included in the distribution system planning process, and their impacts should be evaluated for the integrated transmission and distribution systems. Note that while a fully dynamic T&D model can capture these scenarios, it is unnecessarily complicated. This is because, although the transmission system needs to be modeled in a dynamic mode to study the bulk grid AGC response, for frequency regulation concerns, the effects of distribution-connected DER generation variability can be captured using quasi-static simulations for distribution systems. This calls for a hybrid co-simulation platform that can appropriately model the bulk grid frequency response due to variable DERs.

In this chapter, an iteratively coupled T&D hybrid co-simulation framework is developed to study the effects of distribution-connected DERs/PVs on AGC response and the utility of BESS in maintaining supply-demand balance for scenarios with highly variable DER/PV generation profiles. The proposed hybrid co-simulation framework is demonstrated using IEEE 9-bus transmission system model coupled with multiple EPRI Ckt-24 distribution system models. The generator's dynamic model for the IEEE 9-bus transmission system is available in PSAT MATLAB toolbox. The quasi-static model for distribution system is developed using OpenDSS. The interactions between transmission and distribution systems at the point of common coupling (PCC) is captured using a tightly-coupled co-simulation interface developed in MATLAB. The developed hybrid T&D co-simulation platform is used to understand the PV integration impacts at both transmission and distribution levels, specifically, the effects of PV generation variability on the AGC dispatch signals. The utility of distribution-connected BESS on improving the AGC response by providing frequency regulation services is also detailed.

### 2.1.3 Specific Contributions

This work adds the following innovations to the existing literature:

1. *Hybrid T&D co-simulation platform:* Development of a hybrid T&D co-simulation platform with transmission system operating in dynamic mode (in msec) to accurately capture the frequency changes due to rapidly varying load demand at the T&D PCC by modeling distribution systems in a quasi-static mode (in sec.).
2. *Impacts of PV variability analysis:* The developed hybrid T&D co-simulation platform is used to understand the PV integration impacts at both transmission and distribution levels. The effects of PV generation variability are studied on the AGC dispatch signals.
3. *BESS to improve Frequency Regulation:* An approach is detailed to understand the applicability of distribution-connected BESS in augmenting transmission system operation by providing frequency regulation services. This is achieved by accurately capturing the interactions between transmission and distribution systems at the point of common coupling (PCC) while modeling both systems using a tightly-coupled hybrid co-simulation approach.

### 2.1.4 Chapter Organization

The rest of the chapter is organized as follows:

- Section 2.2 provides the modeling details of the hybrid T&D co-simulation framework. It includes a background on the existing transmission and distribution system modeling practices and the changes that are needed to simulate BESS frequency regulation studies. This section details the dynamic transmission system model developed in MATLAB PSAT toolbox. The use of OpenDSS in simulating quasi-static distribution system analysis using three-phase power flow method is also detailed. The simulated cases for PV deployment using a Monte-Carlo approach are summarized.
- Section 2.3 details the AGC distribution strategy employed in this work. An independent AGC strategy based on ACE signal distribution is developed in this report. A dynamic available AGC (DAA) index is used to obtain the BESS AGC availability.
- Section 2.4 presents a detailed analysis of the test cases that were simulated to demonstrate the advantages of using BESS in providing frequency regulation. Two systems, one where the BESS is aggregated at the transmission load point, and the other, with BESS distributed along the distribution feeder is developed to demonstrate the effectiveness of the proposed hybrid T&D co-simulation platform to perform AGC regulation studies. A comparison of AGC schedules with and without BESS is also presented.
- Section 2.5 summarizes the findings and provides future research directions along with the future scope for this part of the project.

## 2.2 Transmission and Distribution System Modeling

### 2.2.1 Transmission System Dynamic Modeling

To manage the frequent load changes, the governor control of the generators responds to balance the supply and demand using the primary frequency control within few seconds of the supply-demand imbalance. A secondary frequency control given by AGC is employed to correct the Area Control Errors (ACE), which acts in a time scale of minutes after the governor frequency control has responded. To track both the primary and secondary frequency control signals, the transmission system dynamics needs to be modeled. In this work, a dynamic model for the transmission system is simulated using power system analysis toolbox (PSAT) in MATLAB [16].

The transmission system dynamic model in PSAT can be solved using either the forward Euler Integration method or trapezoidal method. The forward Euler integration is a first-order method while the trapezoidal integration method is a workhorse solver for electromagnetic differential-algebraic equations (DAEs). The Euler's integration, being faster than other integration methods, is used in this work. PSAT solves time-domain simulations with specified fixed time steps. In this study, it is required to create a co-simulation model at the interface of transmission and distribution system. Hence an iterative model for the existing time-domain simulation is developed in PSAT, which is detailed further in Section 2.4.

The DAE for the transmission system analysis is given as,

$$\dot{x} = f(x, y) \tag{21}$$
$$0 = g(x, y) \tag{22}$$

where, x is the set of variables for generator dynamics and y is the network power flow solution variables. The mathematical model for Euler's integration method is given as,

$$\dot{x} = f(x), \tag{23}$$
$$x(t_0) = x_0 \tag{24}$$
$$x(t) = x(t_0) + \int_{t_0}^{t} f(x(u) \tag{25}$$
$$\frac{dx}{dt} = \frac{x(t_k+h) - x(t_k)}{h} \tag{26}$$
$$x(t_k + h) = x(t_k) + hf(x + t_k) \tag{27}$$

where, h is the fixed time step of integration and u is the intermediary control variable.

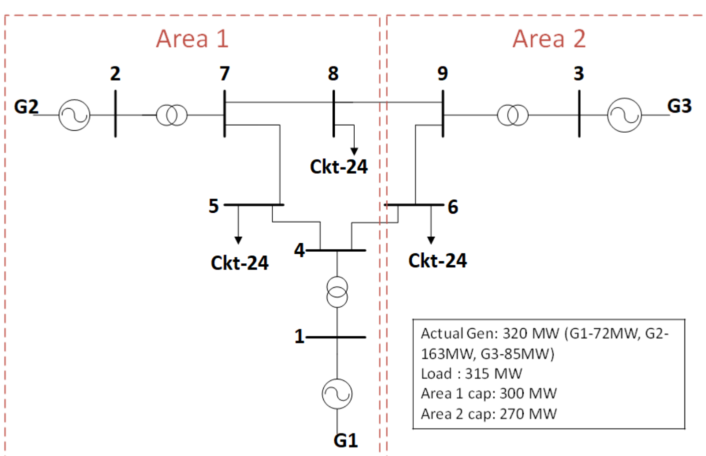


Figure 2.1 IEEE 9-bus transmission test system

IEEE 9-bus test system is used as the transmission system with three synchronous generators, six lines and three loads (see Figure 2.1). The IEEE 9-bus transmission system dynamic data is available in PSAT toolbox. Generators are modeled with governors (Type 2) and exciters (Type 2). Loads are represented as constant impedances. For more information on the system modeling, please refer to [47,48]. The IEEE 9-bus system area model is presented in Figure 2.1.

### 2.2.2 Distribution System Modeling:

The distribution system three-phase modeling and analysis is done using OpenDSS, an open-source platform designed for distribution system analysis [49]. OpenDSS supports all frequency domain analysis performed for utility distribution system planning and analysis. There are multiple functionalities in OpenDSS along with its extraordinary capability to support planning and analysis of distributed generation (DG) technologies. OpenDSS allows to specify DERs' incremental capacity along with associated controls and help visualize their impacts on the distribution system. In addition to this, OpenDSS has explicit models of many real-world distribution feeders.

Three models of actual electric power distribution circuits are made public in OpenDSS. This report uses one of those feeders -- Electric Power Research Institutes (EPRI) Ckt24 test system [50]. The sub-transmission level voltage is 230 kV and Ckt-24 operates at 34.5 kV system voltage. The system has 2 substation feeders with 3885 customers, of which 87% are residential loads. EPRI ckt-24 network is presented in Figure 2.2.

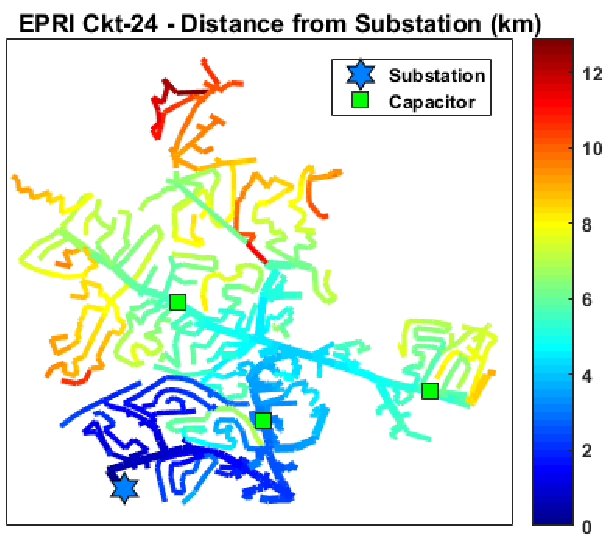


Figure 2.2 EPRI Ckt-24 OpenDSS distribution system model

To simulate the DER integration scenarios, PV systems are connected at the load buses in the distribution system. Following the related literature concerning PV hosting analysis for distribution feeders, a stochastic analysis framework is adapted to generate numerous PV deployment scenarios by varying PV sizes and locations. A random PV deployment scenario is chosen for real-time AGC simulations. Three different days with different variabilities (low, medium, and high) of irradiance are created. The low, medium, and high irradiance variability with a variability index of 1.33, 6.29, and 15.58, respectively, and the PV profile for each variability is presented in Figure 2.3.

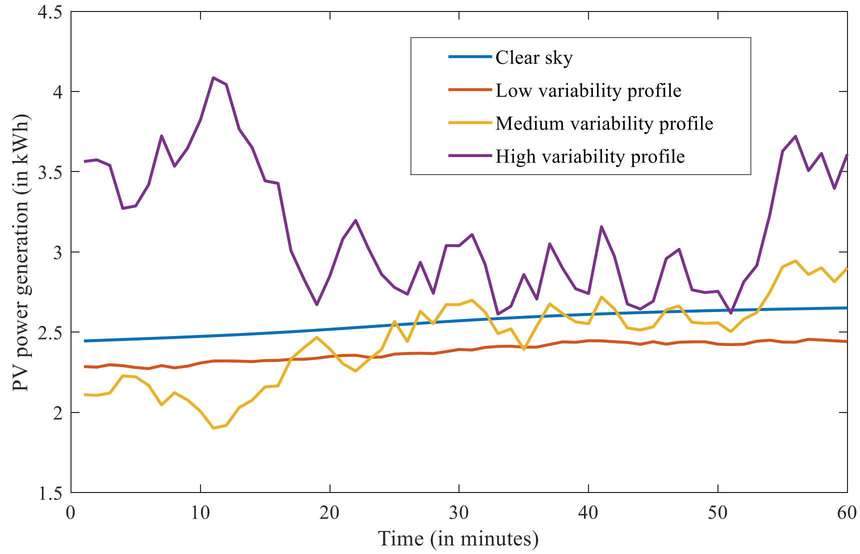


Figure 2.3. PV generation profile with low, medium, and high variabilities for an hour

### 2.2.3 Battery Modeling

The storage element in OpenDSS is used as the battery model in this work. The storage element is essentially a generator that can be dispatched to either produce power (discharge) or consume power (charge) within its power rating and its stored energy capacity. A storage element can either act independently or be controlled by a Storage Controller element. Note that there will only be power discharged if the present charge level (kWhStored) is greater than the specified reserve level. The Storage element will only take charge when the kWh stored value is less than kWhRated. The rate of charge and discharge values can be specified in OpenDSS. Daily, Yearly, and DutyCycle modes for time-varying simulation is supported by OpenDSS. The storage element can also produce or absorb reactive power (vars) within the kVA rating of the inverter. That is, a Storage Controller object requests a certain amount of kvar, and the storage element provides it if the inverter has any capacity left. The storage element can produce/absorb vars while idling. Losses are important when evaluating storage schemes. The model allows a separate specification of charging and discharging efficiencies. In charging or discharging mode, the Storage element is generally modeled as a simple constant (P+jQ) model (model=1, the default).

For the integrated T&D test system development, the three load nodes in the IEEE 9-bus transmission system is replaced with EPRI Ckt-24 distribution feeders each and is presented in Figure 2.4. 10 BESS are distributed along each of the connected EPRI Ckt-24 systems as presented in Figure 2.3. Each BESS has a rated power capacity of ±10 kW with 4.21 kWh energy rating. Each connected Ckt-24 feeders can thus replace 300 kW of conventional generation in providing frequency regulation services. The active power output and the SoC of the BESS are monitored through the OpenDSS simulation platform.

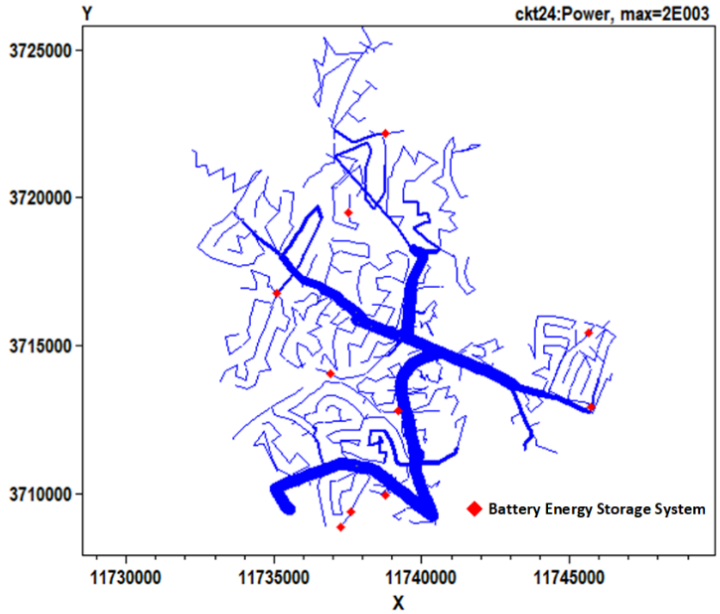


Figure 2.3  Battery distribution model in EPRI Ckt-24 DS

### 2.2.4 Hybrid T&D Co-Simulation Framework

As discussed in section 2.1, an iterative interface model is developed within the PSAT MATLAB toolbox. The transmission system dynamic model for this integrated T&D system is developed in PSAT and solved in msec while the distribution system modeling is done using OpenDSS. For more information on the coupling methods, refer to Section 2.5 in Part I of the report. IEEE 9-bus system where the load points L5, L6, and L8 replaced with EPRI Ckt-24 each is used as the test system for the simulation studies as shown in Figure 2.4.

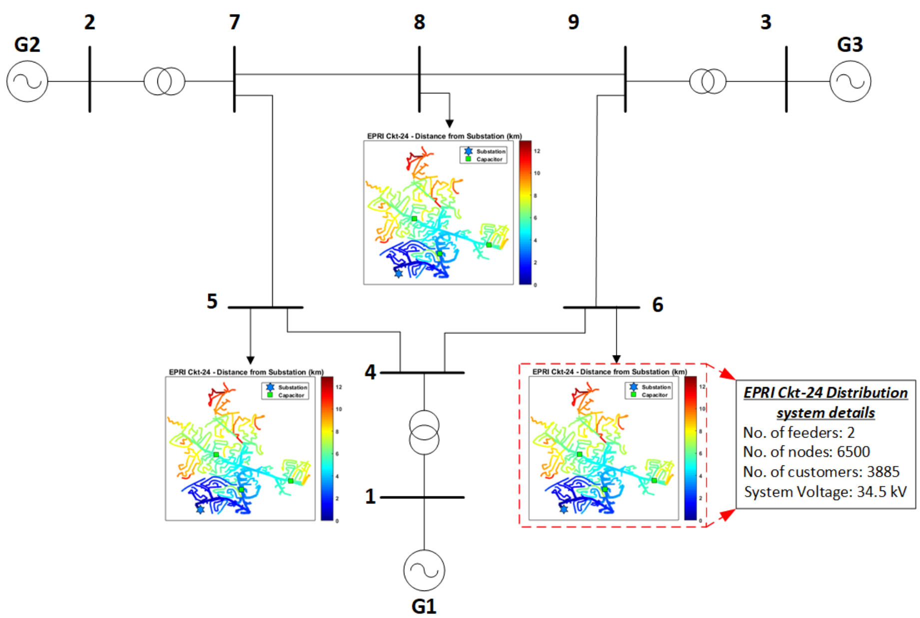


Figure 2.4  Integrated T&D test system model

The overall system model for the hybrid T&D co-simulation framework is presented in Figure 2.5. For the transmission system operations, an economic dispatch problem is formulated for the transmission network using forecasted load and DER data. The economic dispatch problem aims to achieve 5-min ahead of power balancing for frequency regulation. An AGC module that operates in the time scale of 4-6 sec is operated to minimize the system frequency deviations. The transmission system operated in dynamics mode (in msec) helps observe the frequency deviations, primary frequency response, and secondary frequency response of the system. The BESS distributed in the OpenDSS DS module is providing fast frequency regulation response to the system by following the RegD signal developed based on AGC availabilities provided by the ESS.

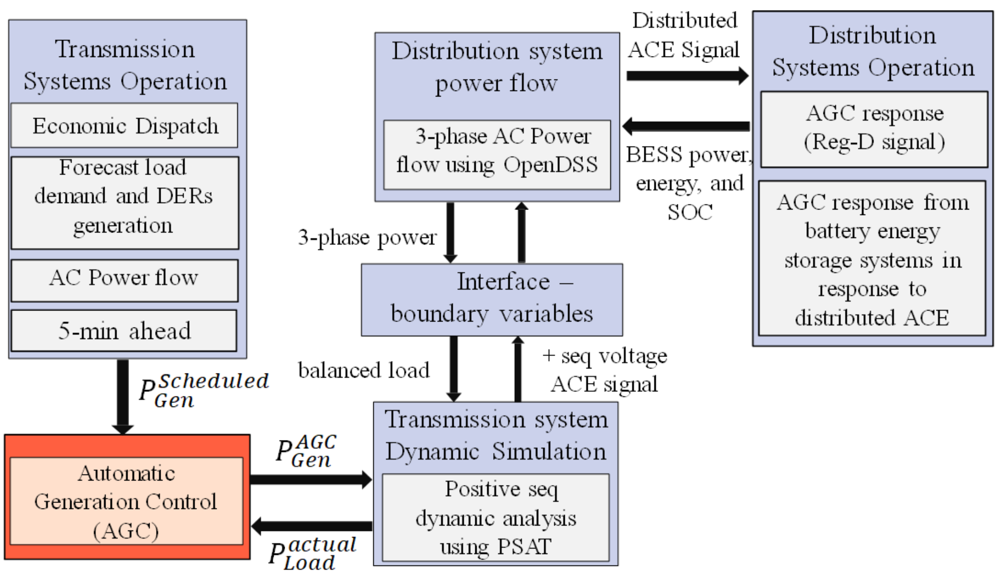


Figure 2.5 Hybrid T&D co-simulation framework

## 2.3 AGC Distribution Strategy

The frequency response of a power system network to any system disturbance is performed in two stages, namely the primary frequency response and secondary or AGC response. The primary frequency response of the power system grid serves to limit the maximum frequency deviation during and/or immediately after the disturbance owing to the inherent system inertia (present in the rotating masses connected to the system). This response restores the system frequency to a value as close to the target grid frequency as possible. However, even after the primary frequency response actions, a steady-state frequency deviation persists between the actual and desired system frequency. This is where the system AGC response serves as a secondary control action to regulate the system frequency to the target value and maintain the interchange power between system control areas at the scheduled values by adjusting the output of the selected generators.

### 2.3.1 Independent AGC Control Strategy

For the purposes of the AGC study, each control area of an interconnected power system network is represented by an equivalent model exhibiting its overall performance. Such equivalency is valid and does not compromise on the fidelity of the resulting AGC model since the AGC study is not intended to consider inter-machine oscillations within each area. A representative AGC model for the two areas in IEEE 9-bus system is presented in Figure 2.6. This equivalent model includes a generator equivalent, an equivalent for the load damping coefficient, an equivalent for the primary frequency regulation loop and a delay block representing mechanical components (turbines and governors) contained within the control area.

A control signal made up of inter-area power transfer deviation and weighted area frequency deviation fed into area AGC loop would accomplish the primary objective of AGC response. This control signal, which is known as Area Control Error (ACE) for the control area, is given by:

$$ACE = (\Delta P_{actual}{}^{tieline} - \Delta P_{contract}{}^{tieline}) + \beta\, \Delta f \qquad (28)$$

where,
$\Delta P_{actual}{}^{tieline}$ is the actual power exchange through the tie-line,
$\Delta\, P_{contract}{}^{tieline}$ is the scheduled power interchange at the tie-line,
$\beta$ is the bias factor, and
$\Delta f$ is the frequency deviation in that area.

Traditionally, the system AGC regulation is developed through a PI controller with a low-order filter to smooth the fast variations of the ACE signal which may cause wear and tear on governor motors and turbine valves of conventional AGC units. The low-order filter with a typically large time constant, i.e., 1 minute, can reduce the noise at the expense of speed of response which inhibits the inherent benefits of the fast response capability of BESS. Therefore, an independent AGC participation strategy based on ACE signal distribution from the literature is used in this work [53]. The independent AGC control strategy for an area is demonstrated in Figure 2.6. The ACE control shown in Figure 2.7 is implemented using the system equivalents developed in AGC control loop for the two-area transmission system model and presented in Figure 2.8.

### 2.3.2 AGC Availability Metrics

For conventional units, the available AGC capability can be determined purely based on the amount of reserve. However, in the case of BESS, since the amount of stored energy varies over time, the ACE signal is distributed based on the Dynamic Available AGC (DAA) index of the BESS and the assigned ACE signal is sent to the independent AGC PI controller associated with the BESS AGC control loop as shown in Figure 2.6. Figure 2.7 presents the ACE distribution strategy for the conventional units and the BESS model for one area of the test system. A similar control framework is implemented in other areas of the test system. Here, $\beta_1$ represents the droop factor for area 1. $\Delta f_1$ and $\Delta P_{12}$ represents the frequency deviation and tie-line deviation from the scheduled values in Area 1. The BESS AGC capability represents the DAA index of the BESS connected to Ckt-24 feeders in Area 1. The DAA is 1-minute sustainable charge/discharge capability of BESS considering SOC status and limits. The BESS is continuously calculated and reported at each AGC interval, typically 4-6 seconds.

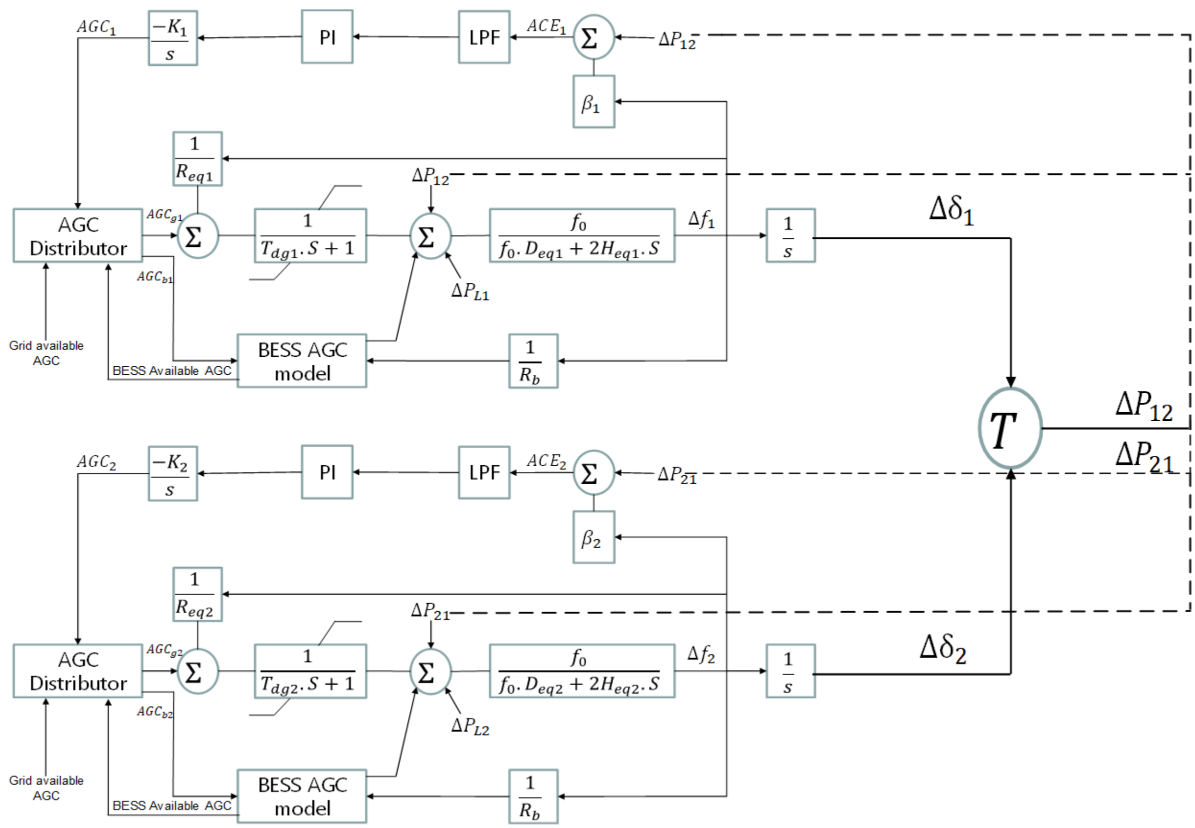


Figure 2.6 AGC control strategy for the two-area transmission system

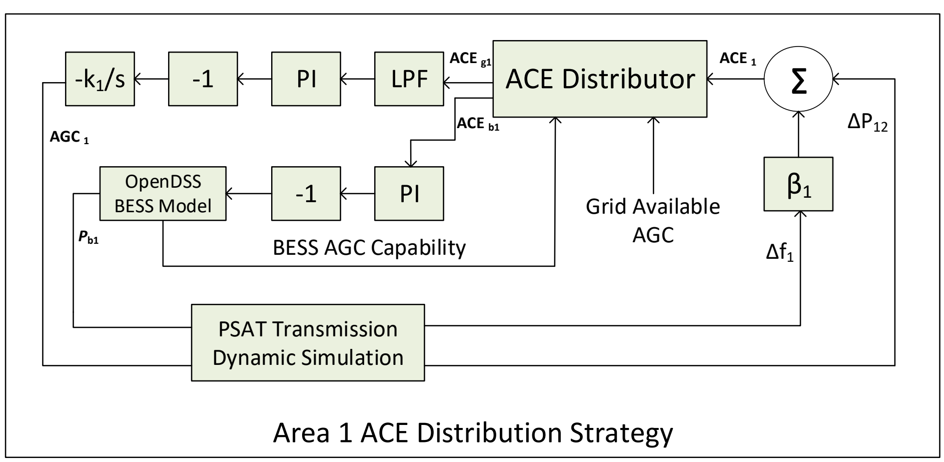


Figure 2.7 ACE distribution control strategy

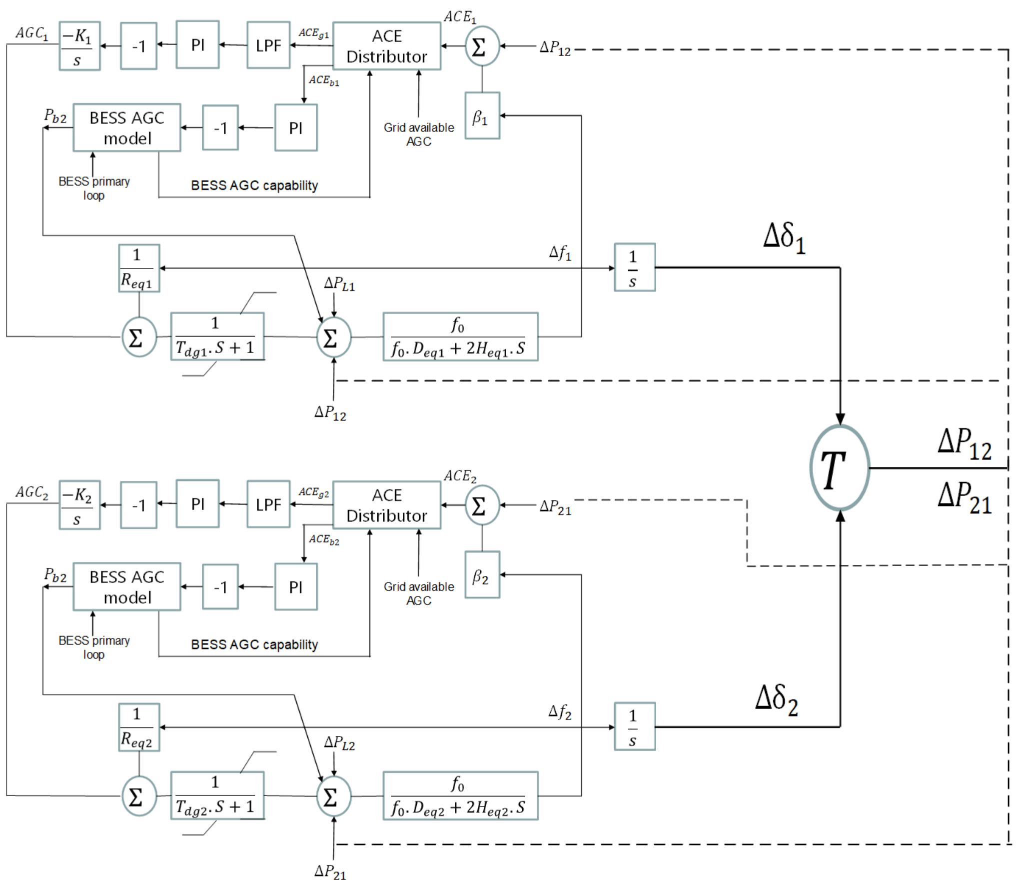

Figure 2.8  Independent ACE control strategy for the two-area transmission system

In order to prevent any compromise on the speed of response, the BESS AGC control loop is characterized using a filter with a very small time constant. This allows for fully leveraging the fast response capability of BESS. Figure 2.8 shows independent control loops for AGC for the conventional generators and BESS for two areas. The ACE index for battery and the other conventional units are calculated as,

$$ACE_{bi} = ACE_i \times \frac{DAA_{bi}}{DAA_{bi}+AA_{gi}} \quad (29)$$

$$ACE_{gi} = ACE_i - ACE_{bi} \quad (30)$$

where,
$ACE_{bi}$ is the ACE signal for BESS based on availabilities of BESS and conventional units,
$DAA_{bi}$ and $AA_{gi}$ are the BESS and conventional units' availabilities,
$ACE_{gi}$ is the ACE signal for conventional generation units, and
$ACE_i$ is the corresponding area ACE signal.

In this method, owing to the fast response of BESS units, they are given higher priority in comparison to conventional units. In other words, if the area regulation burden falls within the BESS dynamic capability as calculated for that AGC interval, it is completely assigned to BESS.

Otherwise, the BESS is assigned a regulation based on its highest capability for that interval with the remaining portion of the total area regulation burden being assigned to conventional units.

## 2.4 Analysis and Results

The real-time AGC simulation is performed using the developed hybrid T&D co-simulation platform with PVs having highly variable generation profiles. This section details the test system models and test cases developed in this work. Detailed simulation results of the secondary frequency control using the ACE distribution strategy is also discussed.

### 2.4.1 Test System

For the real-time AGC simulations using ACE distribution strategy with BESS, the following test system model is developed. The transmission and distribution systems used for hybrid co-simulation framework are IEEE 9-bus system [47] and EPRI Ckt-24 distribution feeder model [50], respectively. The generator dynamic model for the IEEE 9-bus transmission system is available in PSAT MATLAB toolbox. This system has two areas, three generator buses (including slack bus) and 3 loads, as shown in Figure 2.1. The overall system load is 315 MW with a 3MW tie-line flow from Area 2 to Area 1. EPRI Ckt-24 is a large 6000-bus distribution feeder with 3885 customers and 87% residential load and is shown in Figure 2.2. The primary side has a voltage level of 13.2kV, and the secondary side voltage level is 480V and 240V for 3-phase and 1-phase lines, respectively. PVs are deployed in EPRI Ckt-24 distribution feeder as described in Section 2.2 to introduce generation variability.

For the integrated T&D test system development, the three load buses in IEEE 9-bus transmission system model is replaced with EPRI Ckt-24 distribution feeder, see Figure 2.4. A total of ten BESS is distributed on each of the connected EPRI Ckt-24 systems. Each BESS has a rated power capacity of ± 10 kW with 4.21 kWh energy rating. Each connected Ckt-24 feeders can thus replace 300 kW of conventional generation in providing frequency regulation services. The active power output and the SoC of the BESS are monitored through the OpenDSS simulation platform. The standard deviation of the system ACE with and without BESS, with aggregated BESS and with distributed BESS, with LC and TC platforms are compared for performance in the real-time AGC simulations.

### 2.4.2 Results and Discussions

#### A. Transmission and Distribution System Parameters - with and without BESS

The following sections utilize BESS in providing frequency regulation services. To demonstrate the benefits of using a hybrid co-simulation platform to modeling the frequency regulation services provided by the conventional generation resources along with BESS, AGC simulation studies are performed using ACE distribution strategy discussed in Section 2.3. The simulation is carried out for 1 hour of the day (12pm-1pm) with high PV variability. The load profiles of the two areas in the test system during the specified hour is presented in Figures 2.9 and 2.10. The standard deviation of the system ACE is used for evaluating the performance with and without BESS.

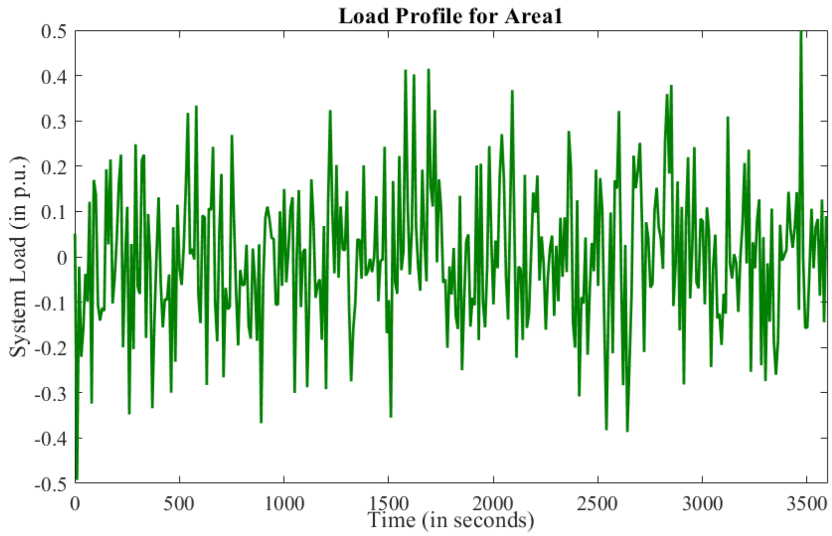


Figure 2.9 Load profile for Area 1 of the integrated test system

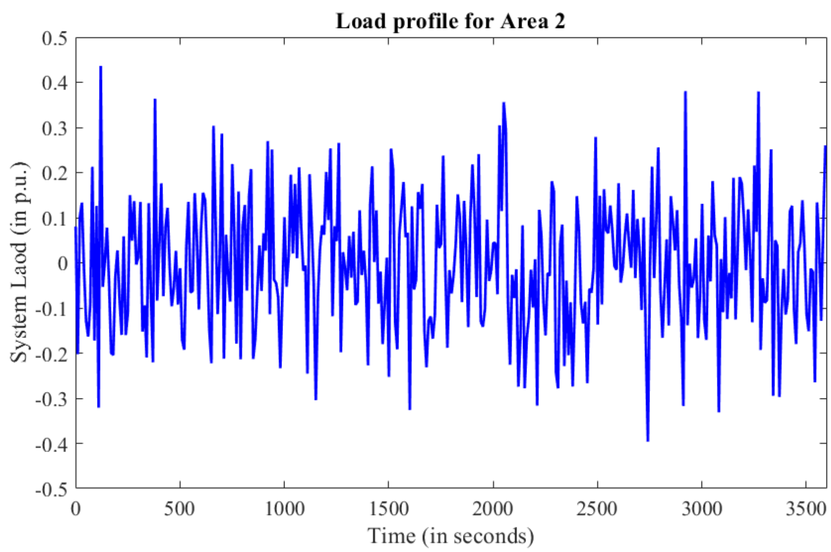


Figure 2.10 Load profile for Area 2 of the integrated test system

**A.1 Frequency Deviation and ACE Response - with and without BESS**

The simulation is performed initially without the presence of BESS in the system, i.e., the conventional generators in the IEEE 9-bus system (G2, G3) providing the frequency regulation services. The system ACE response is calculated for this initial simulation. Now, BESS are introduced in each of the Ckt-24 feeders connected in the test system and the ACE distribution strategy (presented in Section 2.3) to utilize the BESS services is simulated and the system ACE response is calculated again. The system frequency is also observed in both cases and compared in Figure 2.11. The standard deviation of the system ACE response observed in both simulation cases is compared in Figure 2.12.

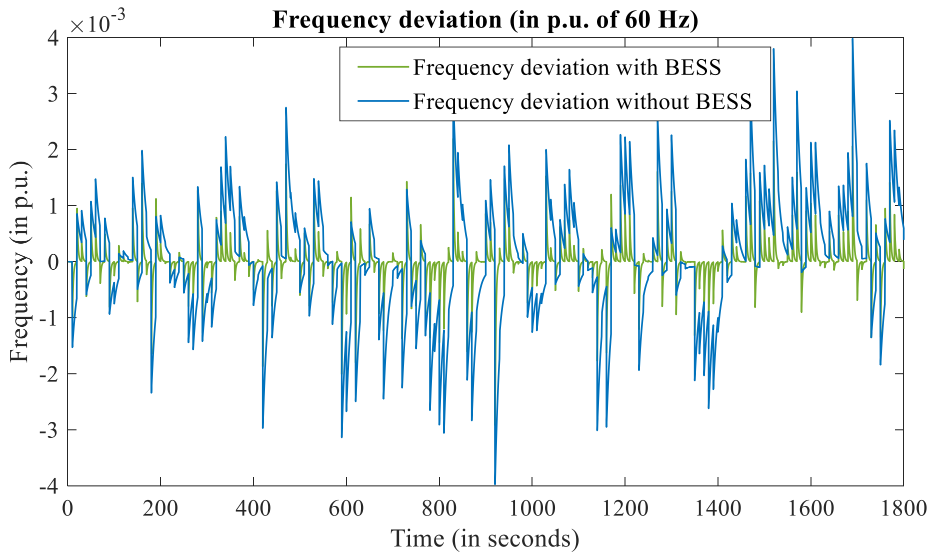


Figure 2.11 System frequency response with and without BESS regulation

As seen in Figures 2.11 and 2.12, the inclusion of BESS improves both the system frequency regulation and ACE response significantly. It can also be seen that the standard deviation of the system ACE is very low for the simulation case with BESS compared to the one without BESS. This is due to the fact that the independent AGC control loop for the BESS can better track the variations in demand. In the absence of an integrated T&D framework and with the aggregation of the battery capacity at the PCC not accounting for the SoC constraints, a similar ACE response of the system cannot be obtained.

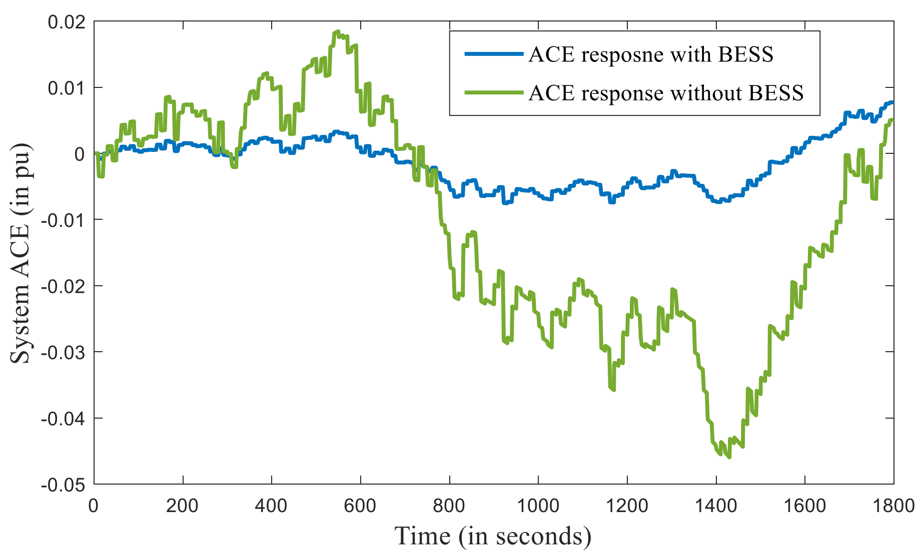


Figure 2.12 System ACE response with and without BESS regulation

### A.2 Impacts on Distribution Systems Voltages – with and without BESS

In this section, for the simulation case described in Section A.1, corresponding distribution system voltages are observed. The EPRI Ckt-24 distribution is populated with 10 batteries of equal capacity and SoC for the case with BESS response. The high variability profile for PVs is simulated. The comparison of primary voltage profiles along the distance of the feeder with and without BESS is presented in Figure 2.13.

As it can be observed from the figure, the voltage profiles are different. The results are shown for t=480s where the BESS dispatch has led to the violation of the system voltage constraints. This distribution system profile is unobservable to ISO when the AGC regulation is conducted by the ISO without complete details of the distribution system model. In this scenario, co-simulation plays an important role for DSO to observe the system voltages when the ISO dispatches distribution-connected BESS that may violate system operating constraints.

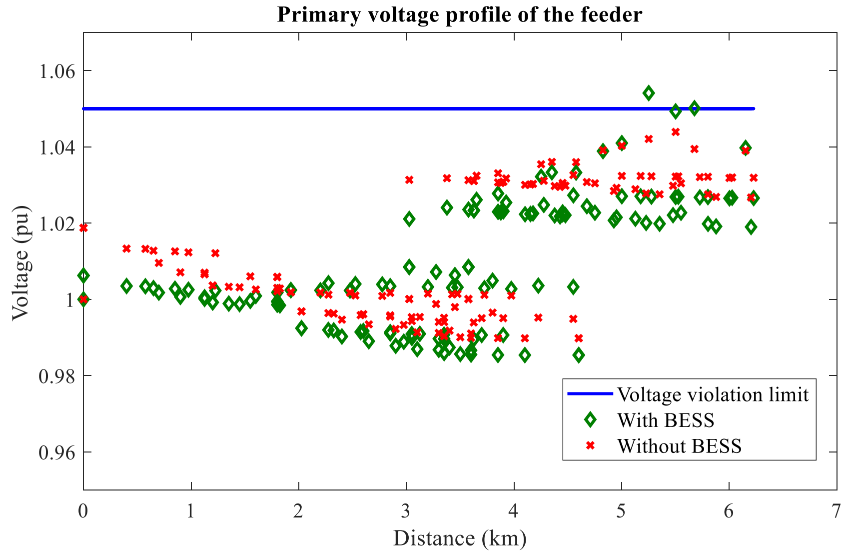


Figure 2.13 Distribution system voltage profile with and without BESS regulation

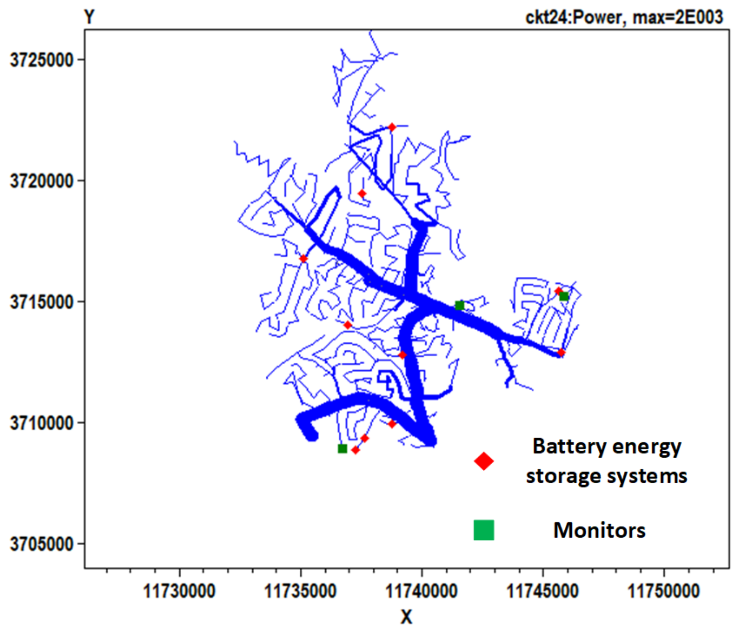


Figure 2.14 Ckt-24 BESS and monitor locations

In addition to this, the time-series voltage plots of nodes violating the voltage limit is presented in Figure 2.15. As it can be seen from the figure, with BESS dispatch the voltage plots looks different and violate allowed voltage limits, which cannot be observed by the operator without a complete distribution system model. The nodes monitored are presented in Figure 2.14.

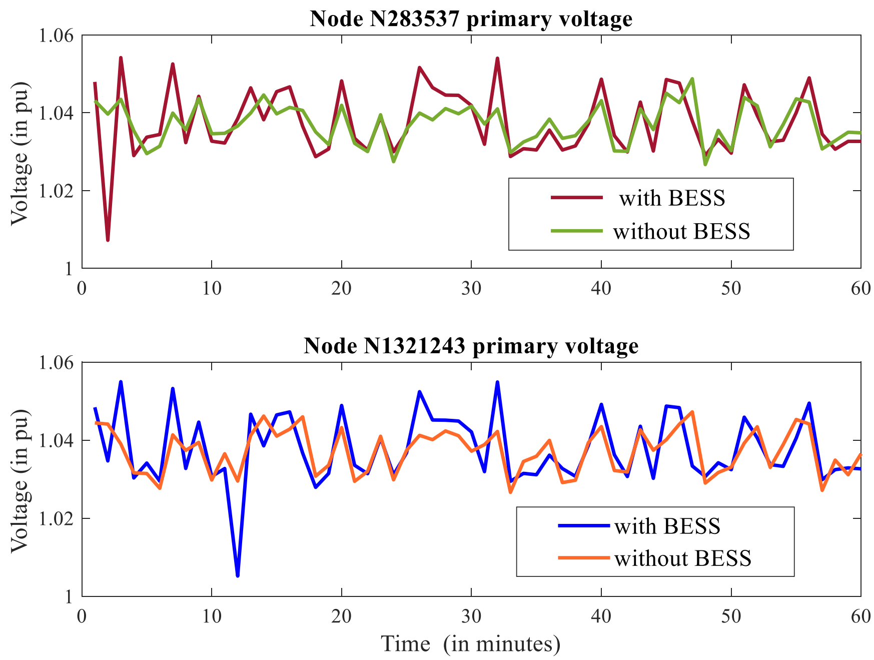


Figure 2.15 Time-series voltage profile of DS nodes with and without BESS regulation

### B. Aggregated vs. T&D Co-simulation Models - Impacts on ACE and Frequency Response

This section details the need for a co-simulation platform in performing frequency regulation studies. As discussed previously, the AGC scheduling at the independent system operator (ISO) level is non-trivial because it depends on the power flow changes of the distribution network, which is affected by the charging demand fluctuations to provide regulation services. This section demonstrates this issue at the ISO level by simulating the ACE response of the system without complete distribution system model and compares the same with ACE response for T&D co-simulation model, where the ISO has detailed information about the distribution system model.

#### B.1 Impacts of PV Variability on System ACE and Frequency Deviation – Aggregated vs. T&D Co-simulation Model

The simulation is carried out using IEEE 9-bus as the transmission system model and EPRI Ckt-24 as the distribution model. For the first case, the PV systems and loads are aggregated at the transmission load point (PCC), and for the second case, the complete distribution system model is simulated. The simulation is carried out for 1-hour of the day (12pm-1pm) with low, medium, and high PV variabilities as discussed in Section 1.6.5. The simulated case for low, medium and high PV variability incurs a variability index (VI) of 1.33, 6.29, and 15.58 [52], and the results are presented in Figure 2.16.

As seen from the figure, with the increase in PV variability, the ACE deviation is increasing in all three cases. Similarly, the aggregate model where the DS loads are approximated at the transmission load point, the ACE deviation is found to be increasing in all three cases. As mentioned previously, the distribution system model is required for studying ACE response in system frequency regulation with high DER penetrations.

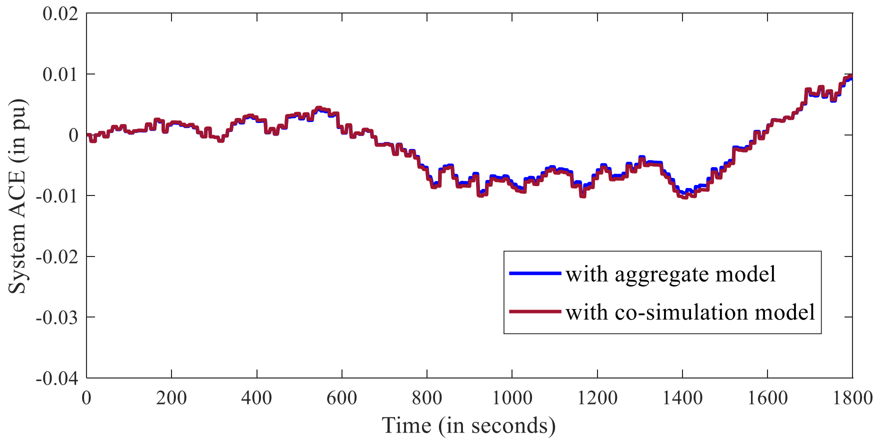


(a)

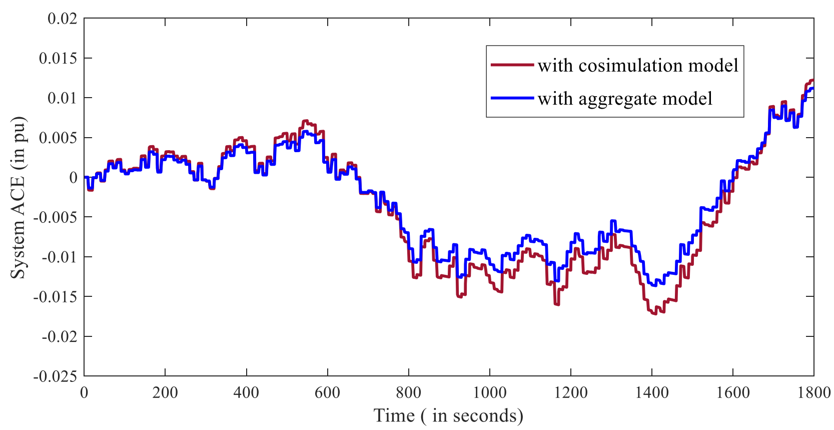


(b)

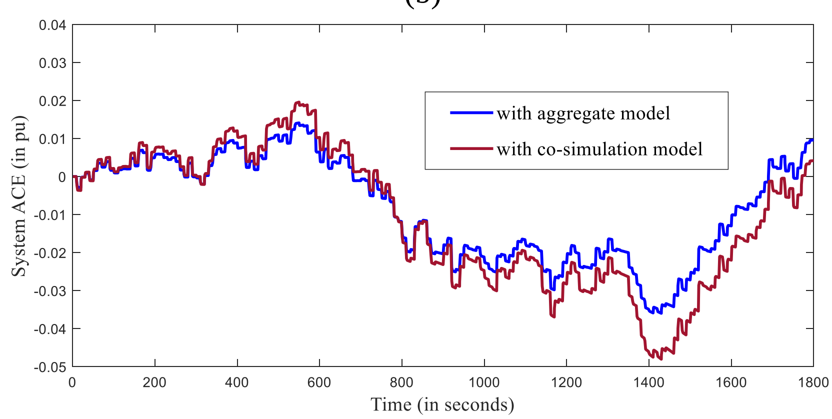


(c)

Figure 2.16 ACE response of the system with and without co-simulation platform for a) low PV variability b) medium PV variability c) high PV variability

**B.2 BESS to improve System ACE and Frequency Deviation – Aggregated vs. T&D Co-simulation Model (High Variability Case)**

In this section, two comparisons are made. One, where the 10 BESS distributed across the distribution system have equal capacity and SoC constraints while in the other, the overall BESS capacity is distributed to 10 batteries differently. Four different cases are run in this section. In cases 1 (aggregated model) and case 2 (co-simulation model), the BESS is dispatched equally. In case 3 (co-simulation model) and case 4 (aggregate model), the dispatch is different among the ten batteries. Also, for the aggregated model, the ACE schedule is obtained from availability of aggregated PV and BESS (i.e., without complete distribution system model) and the schedule is dispatched by simulating the entire distribution system model. The ACE response of the system for cases 3 and 4 is presented in Figure 2.15 and the frequency response for case 3 is presented in Figure 2.17.

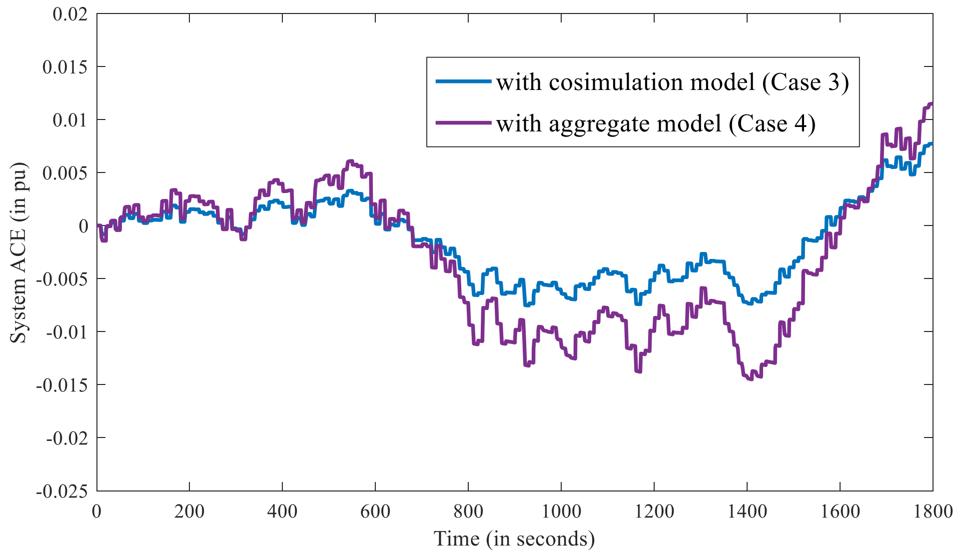


Figure 2.17 System ACE response with and without BESS regulation

As it can be seen from Figure 2.17, the ACE magnitude and deviation in co-simulation model is much better compared to the aggregate model. This is because the schedule of the resources obtained with aggregated model may be inaccurate while dispatching to a set of battery with different capacities. The frequency response of the co-simulation model with distributed battery is presented in Figure 2.18. The system frequency response in AGC regulation with independent ACE strategy using distributed BESS and co-simulation model can better model the AGC requirements of achieving zero frequency deviation.

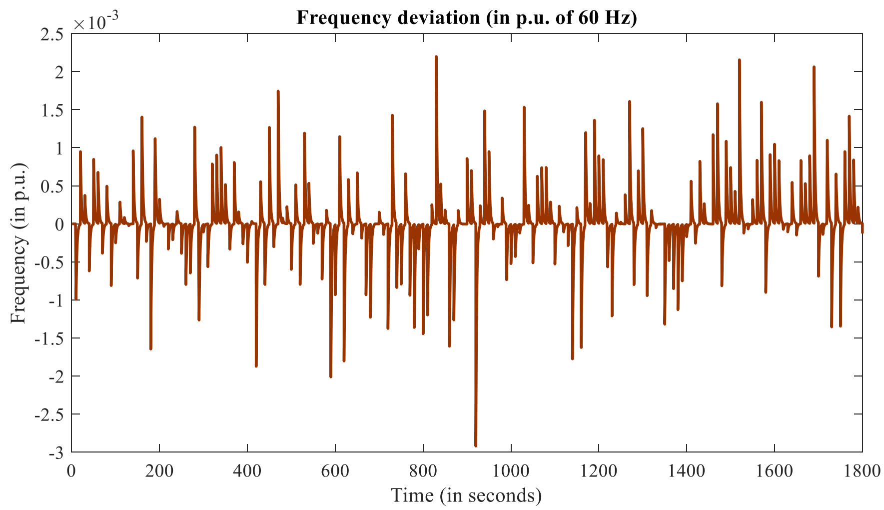

Figure 2.18 System frequency response with distributed battery using co-simulation (Case 3)

The battery power output for the four cases discussed above is presented in Figure 2.19. For the simulation with different BESS dispatch, the BESS is assigned a fixed AGC burden without considering the different AGC availabilities as seen in cases 3 and 4. Due to this, as seen in case 4, the battery output power is observed to suddenly drop to zero. For all other cases, the battery output is observed to be decreasing gradually as it approaches minimum SoC levels. This demonstrates the need of co-simulation platform (with complete distribution system) to dispatch batteries with different capacities and availabilities, which is a more realistic battery dispatch simulation test case.

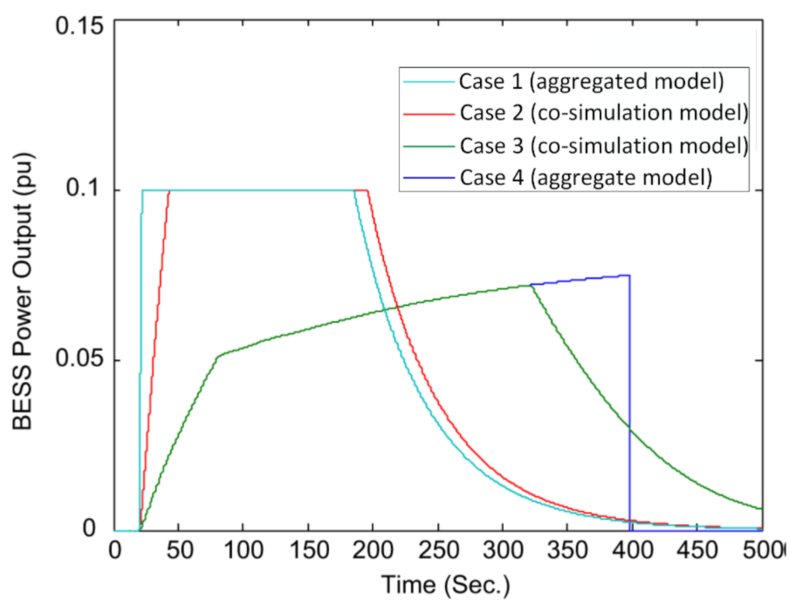

Figure 2.19 BESS Dispatch with and without co-simulation platform in four cases

### C. ACE Response with LC vs. TC Interaction Models

This simulation is carried out to evaluate the impact of T&D coupling strength towards the accuracy of frequency regulation simulations. Here, the same simulation conditions presented in section 2.4.2A are utilized to compare loosely coupled and tightly coupled T&D co-simulation models. In LC model, the interchange at the PCC happens only once, while in the TC model the interface variables converge before moving to the next time step. The comparison results are presented in Figure 2.20. From the observation, it is clear that the ACE response is better (less standard deviation) in the TC case study. This is because the TC model captures the interactions between transmission and distribution system accurately even in cases with high PV variabilities.

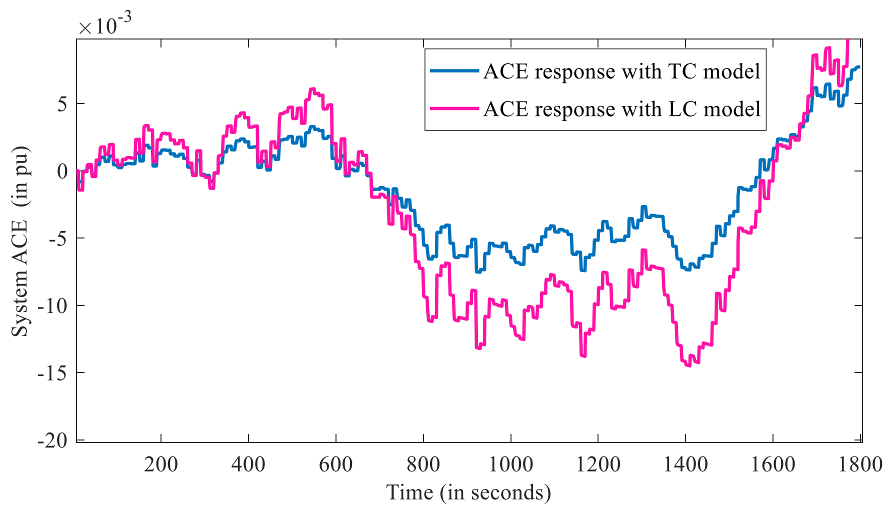


Figure 2.20 System ACE response from LC vs. TC integration models

## 2.5 Conclusion

This chapter is focused on the development of an integrated T&D platform to exploit the benefits of using the BESS to provide frequency regulation services for the bulk grid. This led to a hybrid T&D co-simulation platform where transmission system is operated in dynamic mode in 1-msec interval while the distribution system is operated in a quasi-static mode in 1-sec interval. The BESS is distributed among multiple locations in the distribution feeder. The frequency regulation operation also termed as secondary frequency control, performed using AGC is operated every 4 sec. It is observed that the transmission system dynamic operations help track both the primary and secondary frequency responses. The simulations are carried out for cases with high PV variability, and the results are compared with and without the presence of BESS, with aggregate and distributed BESS modeling, with LC and TC models, and the frequency regulation and system ACE responses are observed. It is shown that the hybrid T&D co-simulation platform helps better exploit the full potential of the distribution-connected BESS in providing the frequency regulation responses. This study can be further extended to observe and mitigate the problems faced by distribution systems operators due to BESS dispatch for AGC.

# 3. Dynamic T&D Co-Simulation Framework and Impacts of Faults

## 3.1 Introduction

### 3.1.1 Background

Increased penetration of renewable-based sources, especially solar photovoltaic (PV) systems (rooftop, community, and small industrial applications, from few kW to MW ranges) in distribution network has changed the way grid operates. High intermittent nature of DERs such as PVs may impact system response to disturbances and in turn the reliability of the Bulk Electric System[1] (BES) [54]. Fault Induced Delayed Voltage Recovery (FIDVR) and Rate of Change of Frequency (ROCOF) are some of the distribution system responses that need to be incorporated when studying transient events in the transmission systems. Interconnection standards IEEE 1547-2003, 1547a-2014 has incorporated the measures in the form of cessation when the voltage and frequency go below pre-defined value [55], [56]. Inverters were not allowed to participate in ride-through schemes, dynamic voltage, and frequency support. These measures did not aggravate the existing problem because of low PV penetrations. However, at high-levels of PV penetrations, tripping off the inverter-based generation may significantly increase the loads on the bulk power grid. As a matter of fact, the loss of a large amount of DERs during the transients is similar to system performance when losing a large generator. To address these and related emerging challenges, recently, the revised interconnection standard IEEE 1547-2018 incorporated the voltage and frequency ride-through requirements for DERs to minimize the potential impacts of such scenarios on the bulk grid operations [57].

For example, during a transmission systems fault, voltage is depressed over a wide area extending into distribution system during and post fault period. At high penetrations and without ride-through requirements per old interconnection standard, DERs could potentially trip and aggravate the stress on the grid. These situations would cause delayed voltage recovery phenomenon with the motor loads consuming more reactive power to magnetize further exacerbating the voltage stability problems for the bulk grid [58]. To address the DER tripping during suppressed voltages, revised interconnection standard allowed the ride through during voltage and frequency excursions based on the designation of different categories of DER by utilities [57]. As the distance from fault location increases, voltage depression is less severe in the distribution systems. DERs located closest to the fault would likely experience very low voltage, and the ones located far from the event location do not experience the same low voltage scenario. There is a need for dynamic voltage studies in the form of co-simulation during the fault events to identify the loss of the portion of DER that would cause stability issues on the bulk grid. Based on the outcome of the studies, reasonable expectation of DER ride-through profiles can be set. The duration of these ride-through profiles should be based on the minimum and delayed fault clearing times on transmission systems. For example, delayed clearing of fault on 115kV system can range from 0.3 to over a second based on protection coordination. Other applications for the co-simulation framework are the Under Frequency/Under Voltage Load Shedding schemes (UFLS/UVLS) and protection. Utilities need to review the load shedding scheme profiles designed without DERs in the distribution systems.

[1] Transmission systems operate at 100kV or higher with few exclusions

A co-simulation framework studies the mutual effect between systems while solving the T&D in the domain-specific tools. Fault dynamic studies using co-simulation approach will help the utility planners to identify the potential bottlenecks and take necessary actions to ensure reliable bulk-grid operation with high-levels of DER penetration. Several dynamic T&D co-simulation studies are proposed to assess the impacts of DERs on-bulk system [58] – [60]. Integrated T&D dynamics model is developed using positive-sequence for transmission systems and three-phase approach for distribution systems in [57]. In [58], T&D dynamic co-simulation is developed using PSAT & OpenDSS with MATLAB interface. Building upon the existing literature, the primary objective of this study is to develop a T&D dynamic co-simulation framework and simulate the effects of high DER penetrations during faults on the bulk system. Inverter controls in the DER are modeled based on IEEE 1547-2018. In this study, a positive sequence dynamic model for the transmission system is developed in PSAT [61]. OpenDSS dynamics mode is used to simulate the distribution system dynamics.

### 3.1.2 Problem Statement – Need for Dynamic T&D Co-Simulation Platform

The distribution-connected dynamic loads such as single-phase induction motors are known to affect the transmission system stability in the form FIDVR. Increased penetration of DERs displaces the conventional synchronous generators and influences the transmission system response to transient events. At high penetrations, losing the DERs increases the stress on the transmission systems to stabilize the grid. Analyzing the transmission and distribution systems separately does not capture these interactions. Also, the fault ride-through requirements of DER based on IEEE 1547-2018 requires to study the T&D systems together to analyze the coupling impacts. The existing standard requires defining the characteristics, and modes of inverter-based generation to participate in the ride-through events in the transmission systems. In order to study the mutual effects, T&D systems are modeled using co-simulation approach. A loosely coupled (LC) approach is used due to the very small-time step in dynamic simulation mode.

### 3.1.3 Specific Contributions

The following specific contributions are made in this part of the project:

1. *Transmission & Distribution System simulation:* A positive-sequence dynamic transmission power flow is developed in PSAT and a distribution dynamic model with induction motors is developed in OpenDSS.
2. *IEEE 1547-2018 Standard Ride Through Requirements:* New interconnection standard requirements are studied and implemented in OpenDSS smart inverter model.
3. *Loosely coupled co-simulation framework:* A framework to loosely couple the T&D networks at each iteration is developed in PSAT. The proposed iterative method results in a co-simulation for the T&D system whose functionalities are comparable to that of the stand-alone unified T&D model.

### 3.1.4 Chapter Organization

Chapter 3 of the report is organized as follows.

- Section 3.2 discusses the new interconnection standard 1547-2018 and voltage ride-through requirements for a transient event in the transmission system. Different categories of DERs, operational regions, and their performance requirements based on the voltage are detailed. Dynamic voltage support from the standard is briefly discussed.
- Section 3.3 presents modeling details of T&D systems to support DER interconnection studies. It details the positive-sequence transmission system dynamic model in PSAT to run the transmission system dynamic power flow. It also provides information about the OpenDSS simulator used in creating the distribution system model.
- Section 3.4 presents the development of T&D loosely coupled dynamic co-simulation platform.
- Section 3.5 presents the preliminary results from the PSAT transmission model

## 3.2 IEEE 1547-2018 Interconnection Standard

The traditional power grid was designed for power to flow from the transmission to distribution systems. The distribution network was traditionally not designed to accommodate the active generation and storage. With the integration of DERs, utilities are concerned about the safety, utilization, and integration of these new resources. Owing to these concerns, IEEE 1547-2003 interconnection standard was developed with the consensus of industry, research, and academic partners on interconnecting the DER's to the grid. Later it was amended in 2014 to redefine the DER voltage and frequency response to abnormal conditions by participating in voltage regulation. In 2018, DER requirements such as ride through, dynamic support to contain the stability issues on BES were included. Even though the new interconnection standard defines several capabilities that DERs should possess, only voltage ride-through specifications are studied in this work.

### 3.2.1 Voltage Ride-Through

The DER response to the abnormal conditions (transient or fault) is divided into three categories viz. I, II, and III (Figure 3.1) to support the stability of BES. DER shall have the capability to perform: 1) Voltage ride-through 2) Frequency ride-through 3) Rate of change of frequency (ROCOF) ride-through 4) Voltage phase angle ride-through and 5) Voltage unbalance ride-through. All category performance requirements shall be met at the point of common coupling (PCC) unless there is zero sequence discontinuity between PCC and DER. In that case, point of DER connection (PoC) is the standard requirement applicability. Additional exceptions to the applicability are listed in [57]. Category I capabilities are very minimal, which most of the technologies existing today possess. DER's classified as Category II & III support the BES needs during the disturbances.

Each category has defined operation regions based on the voltage at PCC or PoC comparing to circuit nominal voltage, as shown in Table 3.1. All operation regions for various categories with clearing times is shown in Figure 3.2.

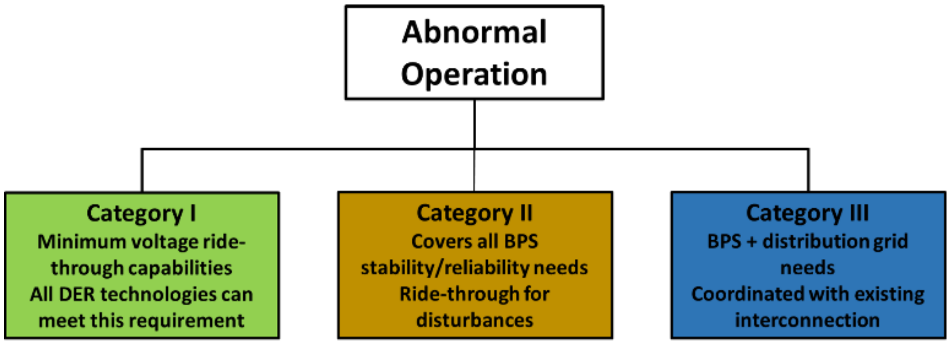


Figure 3.1 DER abnormal performance categories

Table 3.1 DER voltage ride-through regions

| Operation Type | Category I (pu) | Category II (pu) | Category III (pu) |
|---|---|---|---|
| Permissive (above $V_{nom}$) | $1.10 < V_{nom} \leq 1.20$ | $1.10 < V_{nom} \leq 1.20$ | $1.10 < V_{nom} \leq 1.20$ |
| Continuous | $0.88 \leq V_{nom} \leq 1.10$ | $0.88 \leq V_{nom} \leq 1.10$ | $0.88 \leq V_{nom} \leq 1.10$ |
| Mandatory | $0.70 \leq V_{nom} < 0.88$ | $0.65 \leq V_{nom} < 0.88$ | $0.50 \leq V_{nom} < 0.88$ |
| Permissive (below $V_{nom}$) | $0.50 \leq V_{nom} < 0.70$ | $0.30 \leq V_{nom} < 0.65$ | N/A |
| Cease to Energize | $V_{nom} < 0.50$ | $V_{nom} < 0.30$ | $V_{nom} < 0.50$ |

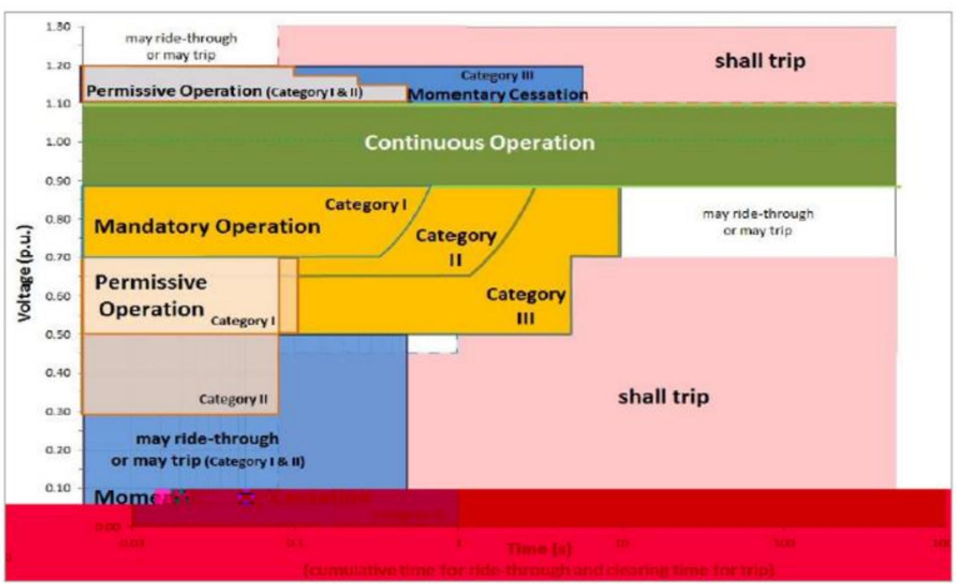


Figure 3.2 DER voltage ride-through categories

### 3.2.2 Pre-Conditions for Voltage Ride-Through

DERs designed to participate in voltage disturbances shall meet the performance category I, II, and III requirements provided the observed measurements such as frequency and exported power are within the pre-defined range. In case the measured quantities are out of range, ride-through requirements don't apply to any category and DERs may cease to energize and trip without any limitations. Pre-conditions for voltage disturbance are as follows [57]:

1) Measured voltage during voltage disturbance should fall in between ride-through operating region parameters for category I, II, and III, as shown in Table 3.1.
2) The measured frequency at PCC or PoC should fall between 57 Hz and 62 Hz ($57 < f < 62$)
3) Ride-through requirements should not exceed DER designed capabilities
4) Net active power exported across the PCC maintained at a value less than 10% of aggregated DER nameplate rating prior to any voltage disturbance
5) Active power demand is equal to, or greater than 90% of the pre-disturbance aggregate DER active power is shed within 0.1 s of when the DER ceases to energize and trips.

### 3.2.3 Dynamic Voltage Support

Voltage depression over the entire network during transient events such as fault can be improved by providing dynamic voltage support in the form of reactive power injection from DER. Effectiveness of the dynamic support depends on the X/R ratio of the system looking from distribution [62]. The new standard allows the DER to have the capability of dynamic voltage support during low voltage or high voltage ride-through regions for all categories. Support functionality can only be used outside of continuous operation zone and during mandatory or permissive operation zones. It should not cause the DER to drive towards cessation during the ride-through regions. To test the effect of providing voltage support during transient events, DERs will be modeled to inject reactive/active current depending on the topology of the distribution system.

## 3.3 Transmission & Distribution Modeling

Traditionally, the transmission systems are modeled in positive sequence and distribution systems in a three-phase representation. For this study, distribution load at the substation is assumed to be balanced and hence unsymmetrical fault analysis such as a single line-to-ground (SLG), double phase-to-ground are not simulated. Distribution system software tools may not have full capability of dynamic simulations like transmission model. In this paper, only induction motor load is assumed to be a dynamic device. Open source stand-alone programs, PSAT and OpenDSS, are used to model transmission and distribution networks.

### 3.3.1 Bulk Energy System (BES)- Transmission

PSAT is a MATLAB toolbox for electric power system analysis and control. PSAT kernel is the power flow routine which takes care of state variable initialization for further static and dynamic analysis. It includes Continuation Power Flow (CPF), Optimal Power Flow (OPF), Small Signal Stability Analysis (SSSA), and Time Domain Simulations (TDS) [60].

### A. Transmission System Dynamic Modeling in PSAT

Transmission dynamic model is a set of non-linear differential-algebraic equations (DAE) as follows:

$$\dot{x} = f(x, y, p)$$
$$0 = g(x, y, p)$$

where $x$ is the set of state variables, $y$ is the set of algebraic variables, $p$ are independent variables, $f$ and $g$ are differential and algebraic equations respectively. DAE's in the dynamic model for transmission systems consists of generators, exciters, and governors. The network is represented only by algebraic equations. Together they form DAE for the whole system.

IEEE 9 bus is used as the transmission system with three synchronous generators, six lines and three loads (see Figure 3.3a). Generators are modeled with governors (Type 2)[2] and exciters (Type 2). Loads are represented as constant impedance Since the transmission is modeled in positive sequence, only symmetrical faults are possible in PSAT. Faults in the network are cleared after the chosen protection response time. It is assumed that faults are cleared, and the line has reclosed successfully.

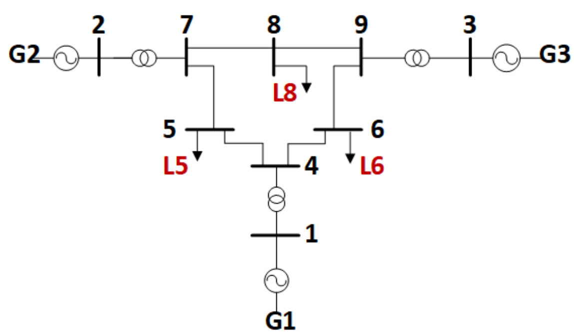


(a)

(b)

Figure 3.3 a) IEEE 9-bus test system b) EPRI Ckt-24 distribution system

### B. Transmission System Unbalanced Dynamic Model in PSAT

The assumption that the system is balanced at T&D interface is not always valid considering the proliferation of single-phase PV installations in distribution. To investigate the inverters dynamic support for unsymmetrical faults such as SLG, DLG, LL faults, transmission system needs to be represented in three-phase detail. Due to the lower modeling complexity and high computing efficiency, three-sequence model is chosen as developed in [58]. For future work, the PSAT source code will be modified to calculate the negative and zero sequence networks. The loss of inverters in single phase or two phases is reflected at the interface of T&D.

[2] PSAT has only two exciter and two governor models

### 3.3.2 Distribution Network Modeling

The dynamic solution in OpenDSS is similar to the power flow solution with very small-time step. Loads are treated as sinks of power with no dynamics, whereas generator and motors are simulated as elements with dynamics. Generator model computes its terminal currents using the voltage source, adjusted for the new phase angle computed by the integration steps, rather than a specified power and power factor as it is modeled in a power flow solution. Power from the generator will depend on system conditions which might be the result of a disturbance. Base power flow is performed to initialize the dynamic simulation mode. This is to initialize the state variables of various dynamic elements to match the power flow. Solar based DERs are modeled as inverters along with controls to change the operational modes. PV penetration is based on the number of customers. Ckt24 is used as the distribution system model, see Figure 3.3b. System voltage is 34.5 kV comprised of 3,885 customers with the residential load at 87%. The peak load of the network is 52 MVA. Induction motor is modeled as 15% of peak load to represent the dynamic loads. Aggregated PV modeled to represent the distributed solar is 12% of the peak load.

## 3.4 Dynamic T&D Co-Simulation Platform

Transmission & Distribution (T&D) are modeled intrinsically different in stand-alone programs by interfacing at the substation bus (PCC). Our previous research in the steady-state analysis used the tightly coupled interface between the systems [63]. Iterative coupling was required due to the larger time step (1 sec) in quasi-static simulations. In dynamic analysis, the time step is smaller (milliseconds), and interactions can be captured by loosely coupling the systems (Figure 3.4). At each time step, t, bus voltages and bus angles obtained from transmission systems solver (PSAT) are given as input to the distribution system source. Active and reactive power flows at the interface bus obtained from distribution solver (OpenDSS) are given as load input to the transmission to solve for next time step t+1. The entire process is repeated by exchanging the voltage and power between T&D. Time step $t$ chosen should be the less than the smallest time constant of both T&D.

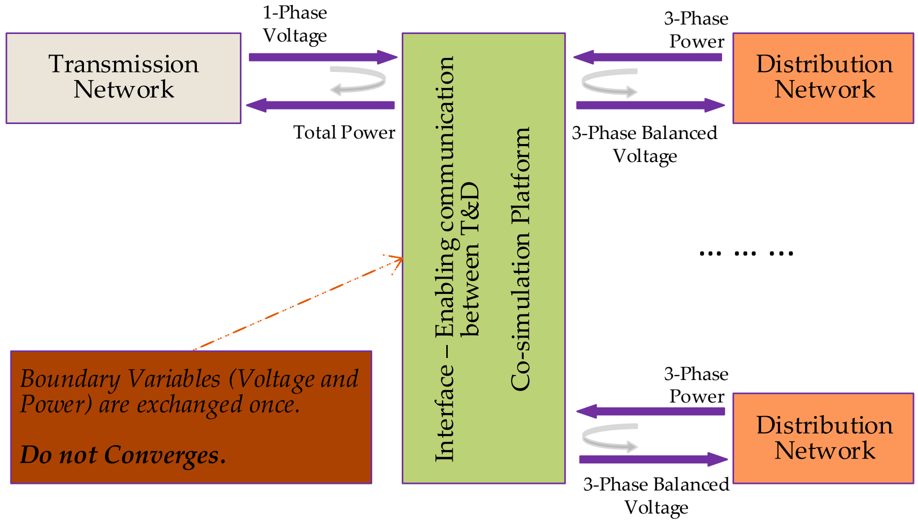


Figure 3.4 Loosely coupled co-simulation framework

### 3.4.1 Voltage Ride-Through Modeling in OpenDSS

Smart inverter controls modeling is used to emulate the advanced inverter functions such as volt-watt, volt-var, and fixed power factor. It is possible for the inverters in different locations to operate in different modes. All inverter functions are modeled based on the functions described in [64]. In Volt-Watt function, voltage points are defined based on inverter category in Table 3.1. By varying the different range of settings, sensitivity analysis on transmission can be performed. Example characteristics for the volt-watt curve is shown in Figure 3.5. The slope of the line (highlighted in red) defines the system ramping. Other functions are defined in a similar way as volt-watt.

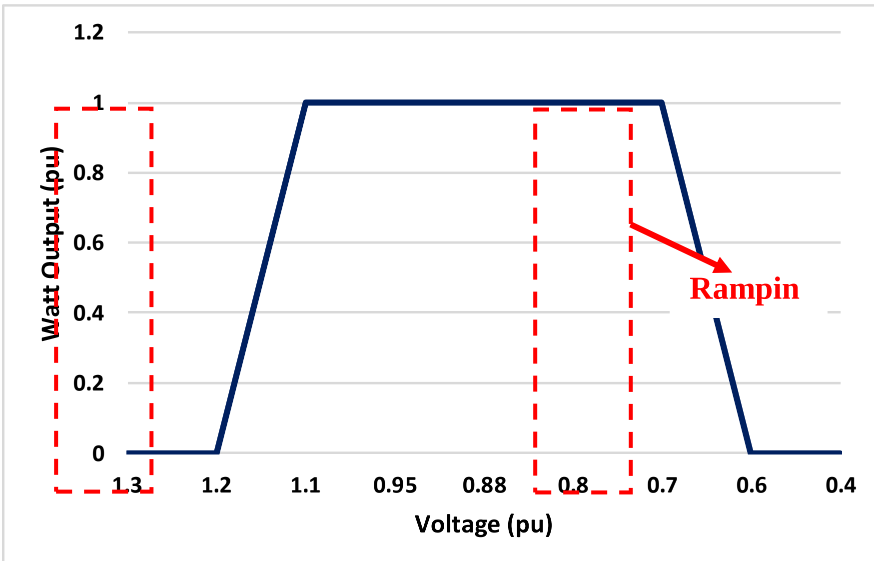


Figure 3.5 Volt-watt curve

In OpenDSS, fig. 3.5 is defined as follows:

New XYCurve.examplevoltwattcurve npts = 7 Yarray = (0.0,1.0,1.0,1.0,1.0,1.0,0.0) XArray = (0.6,0.7,0.8,0.88,0.95,1.1,1.2)

### 3.4.2 Fault Analysis

Assessing the system robustness to imminent disturbances is an important component of system analysis. Severe disturbances (bolted fault) in the form of three-phase faults will show the dynamic response of the system. In the dynamic simulation, loads are all converted to constant impedances. The simulation time step of 0.00125 s has been used with a total simulation time of 3 s. A small time step is chosen due to the induction machine time constants in OpenDSS. To designate the categories and determine the settings for different inverter categories, a sensitivity analysis using T&D dynamic co-simulation has to be performed. By staging the different faults, the effect on transmission system will be known.

## 3.5 Analysis and Results

### 3.5.1 Fault simulation studies using the dynamic transmission system model

PSAT accepts symmetrical faults at three-phase buses. Three-phase fault and breakers are defined in the model to clear the fault after a pre-defined time. During the fault dynamics, synchronous machines accelerate with the increase in rotor angle and current. Severe disturbances in the form of three-phase faults will show the dynamic response of the system. In the dynamic simulation, loads are converted to constant impedances. The simulation time step of 0.05 s has been used with total simulation is 20 s. Gen #1 is the slack bus generator.

***Case - 1:***

At 1.0 s, a three-phase fault is applied at Bus #6. Breakers open to clear the fault after 50ms. Fault is approximately equidistant to all the three generators. Rotor speeds of three generators are shown in Figure 3.6a. Rotors oscillate around 1 Hz and settle down at higher frequency. Voltage oscillations are small after the fault is cleared at 1.2 sec, as shown in Figure 3.6b. Voltages of buses near Bus #5 show similar signature as the generator voltages as shown in Figure 3.6c.

***Case - 2:***

A three-phase fault is applied at bus #5 closest to Gen #2 at 1s. The fault is cleared after 50ms by opening the breaker. Rotor oscillations shown in Figure 3.7a is compared to the fault on Bus #6. Slack bus swings more than other generators even though fault is closer to Gen #2. Generator voltages take more time to settle down and the results is presented in Figure 3.7b. Faulted Bus #5 does not come back to pre-fault voltages as shown in Figure 3.7c.

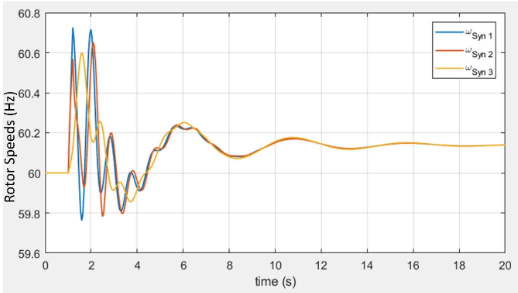


(a)

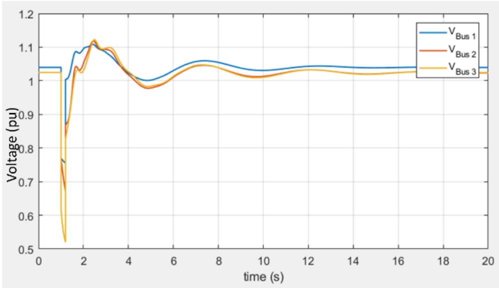


(b)

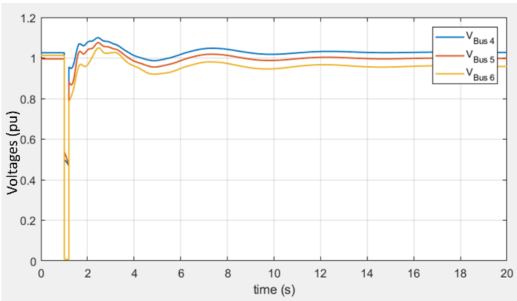


(c)

Figure 3.6 Results for Case-1 fault simulation a) Rotor speeds of generators b) Voltages of generator buses in transmission c) Voltages of the 9-bus transmission system

In this report, we focused on simulating the positive sequence dynamic model for the transmission system during a disturbance and understand the oscillations at the generators and other buses of the system. The future fault simulation work in this direction would be to 1) simulate the three-sequence dynamics of the generators in the 9-bus model, 2) include ZIP loads and (induction motor) IM load dynamics in the distribution system modeling and simulation, and 3) design and implement IEEE 1547-2018 right through standard requirements for the fault analysis.

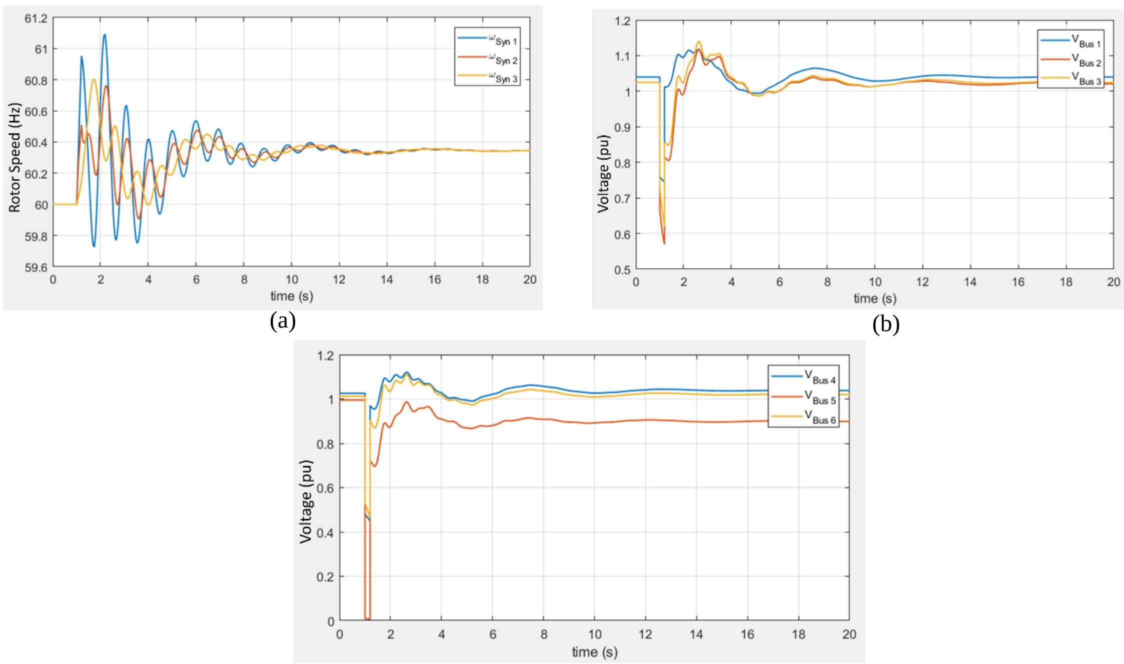


Figure 3.7 Results for Case-2 fault simulation a) Rotor speeds of generators for a fault on bus #5 b) Generator bus voltages for fault on bus #5 c) Bus voltages of the 9-bus transmission system

## 3.6. Conclusion

This part of the report focused on preliminary work on a dynamic T&D co-simulation platform to investigate the impacts of DERs on bulk grid stability during transient events such as faults. This platform provides the path to study the impacts and configure the settings of DERs based on their impact during a transient event. To demonstrate the framework, we model IEEE 9-bus transmission test system in PSAT as positive sequence dynamic model and EPRI distribution test circuit, ckt-24, in OpenDSS, solved using dynamic mode. Induction motors are modeled in the distribution grid to represent FIDVR, and smart inverters are included to emulate the IEEE 1547-2018 interconnection standard fault ride-through requirements. Simulation results are shown for three-phase faults. The modeling of smart inverter controller for PVs in OpenDSS dynamics mode is in progress. This work will be extended to include the negative and zero networks for transmission systems to simulate the unsymmetrical faults.

## References


[1] https://emp.lbl.gov/projects/renewables-portfolio

[2] Kevin Eber and David Corbus, "Hawaii Solar Integration Study: Executive Summary," NREL Report, NREL/TP-5500-57215, June 2013.

[3] "Stochastic Analysis to Determine Feeder Hosting Capacity for Distributed Solar PV." 1026640. Palo Alto, CA: Electric Power Research Institute (EPRI).

[4] Anamika Dubey and Surya Santoso, "Electric Vehicle Charging on Residential Distribution Systems: Impacts and Mitigations," IEEE Access, vol.3, no., pp.1871-1893, Nov. 06, 2015.

[5] Anamika Dubey et al., "Understanding Photovoltaic Hosting Capacity of Distribution Circuit" in the proceedings of the IEEE Power & Energy Society General Meeting, July 26-30, 2015, Denver, CO.

[6] Anamika Dubey et al., "Analytical Approach to Estimate Distribution Circuit's Energy Storage Accommodation Capacity," 2016 IEEE ISGT, Sept 6-9, Minneapolis, MN.

[7] DOE, Grid Modernization Multi-Year Program Plan (Nov 2015).

[8] P. Evans, "Verification of Energynet® methodology," California Energy Commission, CEC-500-2010-021, Dec. 2010.

[9] D. P. Chassin et al., "GridLAB-D: An Agent-Based Simulation Framework for Smart Grids," J. Appl. Math., vol. 2014, pp. 1–12, 2014.

[10] Ciraci, Selim, et al. "FNCS: a framework for power system and communication networks co-simulation." *Proceedings of the symposium on theory of modeling & simulation-DEVS integrative*. Society for Computer Simulation International, 2014.

[11] K. Anderson, J. Du, A. Narayan, and A. E. Gamal, "GridSpice: A Distributed Simulation Platform for the Smart Grid," in *IEEE Transactions on Industrial Informatics*, vol. 10, no. 4, pp. 2354-2363, Nov. 2014.

[12] B. Palmintier *et al*., "IGMS: An Integrated ISO-to-Appliance Scale Grid Modeling System," in *IEEE Transactions on Smart Grid*, vol. 8, no. 3, pp. 1525-1534, May 2017.

[13] B. Palmintier, D. Krishnamurthy, P. Top, S. Smith, J. Daily, and J. Fuller, "Design of the HELICS high-performance transmission-distribution-communication-market co-simulation framework," *2017 Workshop on Modeling and Simulation of Cyber-Physical Energy Systems (MSCPES)*, Pittsburgh, PA, 2017, pp. 1-6.

[14] Balasubramaniam, K., and S. Abhyankar. "A combined transmission and distribution system co-simulation framework for assessing the impact of Volt/VAR control on the transmission system." Power & Energy Society General Meeting, 2017 IEEE. IEEE, 2017.

[15] Balasubramaniam, K., S. Abhyankar., and B. Cui. "Load Model Parameter Estimation by Transmission-Distribution Co-Simulation." (manuscript submitted and accepted).

[16] Q. Huang and V. Vittal, "Integrated transmission and distribution system power flow and dynamic simulation using mixed three-sequence/three-phase modeling," IEEE Transactions on Power Systems, vol. 32, no. 5, pp. 3704–3714, 2017.

[17] Huang, Qiuhua, et al. "A Comparative Study of Interface Techniques for Transmission and Distribution Dynamic Co-Simulation." arXiv preprint arXiv:1711.02736 (2017).

[18] K. A. Birt, J. J. Graffy, J. D. McDonald, and A. H. El-Abiad, "Three-phase load flow program," in *IEEE Transactions on Power Apparatus and Systems*, vol. 95, no. 1, pp. 59-65, Jan. 1976.

[19] J. Arrillaga and B. J. Harker, "Fast-decoupled three-phase load flow," in *Proceedings of the Institution of Electrical Engineers*, vol. 125, no. 8, pp. 734-740, August 1978.
[20] B. -. Chen, M. -. Chen, R. R. Shoults, and C. -. Liang, "Hybrid three-phase load flow," in *IEE Proceedings C - Generation, Transmission and Distribution*, vol. 137, no. 3, pp. 177-185, May 1990.
[21] Xiao-Ping Zhang, "Fast three-phase load flow methods," in *IEEE Transactions on Power Systems*, vol. 11, no. 3, pp. 1547-1554, Aug. 1996.
[22] K. L. Lo and C. Zhang, "Decomposed three-phase power flow solution using the sequence component frame," in *IEE Proceedings C - Generation, Transmission and Distribution*, vol. 140, no. 3, pp. 181-188, May 1993.
[23] X. -. Zhang and H. Chen, "Asymmetrical three-phase load-flow study based on symmetrical component theory," in *IEE Proceedings - Generation, Transmission and Distribution*, vol. 141, no. 3, pp. 248-252, May 1994.
[24] M. Abdel-Akher, K. M. Nor and A. H. A. Rashid, "Improved three-phase power-flow methods using sequence components," in *IEEE Transactions on Power Systems*, vol. 20, no. 3, pp. 1389-1397, Aug. 2005.
[25] IEEE 9-bus Transmission Test System." [Online Available: http://www.kios.ucy.ac.cy/testsystems/index.php/dynamic-ieee-testsystems/ieee-9-bus-modifed-test-system].
[26] IEEE 39-bus Transmission Test System." [Online Available: http://www.kios.ucy.ac.cy/testsystems/index.php/dynamic-ieee-testsystems/ieee-39-bus-modifed-test-system].
[27] Bam, Lokendra, and Ward Jewell. "Power system analysis software tools." *IEEE Power Engineering Society General Meeting, 2005*. IEEE, 2005.
[28] Dugan, Roger C. "Reference guide: The open distribution system simulator (OpenDSS)." *Electric Power Research Institute, Inc* 7 (2012): 29.
[29] Distribution Test System: EPRI Ckt 24", [Online Available: http://sites.ieee.org/pes-testfeeders/resources/].
[30] Joshua Stein, Clifford Hansen, and Matthew J. Reno, “The variability index: a new and novel metric for quantifying irradiance and PV output variability,” No. SAND2012-2088C. Sandia National Laboratories, 2012.
[31] Dubey, Anamika, Pisitpol Chirapongsananurak, and Surya Santoso. "A Framework for Stacked-Benefit Analysis of Distribution-Level Energy Storage Deployment." *Inventions* 2.2 (2017): 6.
[32] Basso, Thomas. IEEE 1547 and 2030 standards for distributed energy resources interconnection and interoperability with the electricity grid. No. NREL/TP-5D00-63157. National Renewable Energy Laboratory (NREL), Golden, CO., 2014.
[33] Dugan, Roger C., Thomas S. Key, and Greg J. Ball. "Distributed resources standards." IEEE Industry Applications Magazine 12.1 (2006): 27-34.
[34] Liangzhong, Y. A. O., et al. "Challenges and progress of energy storage technology and its application in power systems." *Journal of Modern Power Systems and Clean Energy* 4.4 (2016): 519-528.
[35] Nunan, Virgil. "Energy Storage and Power Grid Reliability: Evidence from US Electric Utilities." (2018).

[36] Miller, Rae-Anne, Bala Venkatesh, and Daniel Cheng. "Overview of FERC Order No. 755 and proposed MISO implementation." *Power and Energy Society General Meeting (PES), 2013 IEEE*. IEEE, 2013.

[37] Sakti, Apurba, Audun Botterud, and Francis O'Sullivan. "Review of wholesale markets and regulations for advanced energy storage services in the United States: Current status and path forward." *Energy policy* 120 (2018): 569-579.

[38] Xu, Bolun, et al. "A comparison of policies on the participation of storage in us frequency regulation markets." *Power and Energy Society General Meeting (PESGM), 2016*. IEEE, 2016.

[39] Chen, Hong, et al. "PJM Integrates Energy Storage: Their Technologies and Wholesale Products." *IEEE Power and Energy Magazine* 15.5 (2017): 59-67.

[40] Campbell, T., and T. H. Bradley. "A model of the effects of automatic generation control signal characteristics on energy storage system reliability." *Journal of Power Sources* 247 (2014): 594-604.

[41] Sun, Yanan, et al. "Application of energy storage systems for frequency regulation service." *Smart Grid Communications (SmartGridComm), 2017 IEEE International Conference on*. IEEE, 2017.

[42] Xu, Bolun, et al. "Optimal battery participation in frequency regulation markets." *IEEE Transactions on Power Systems*33.6 (2018): 6715-6725.

[43] Kim, Young-Jin. "Experimental study of battery energy storage systems participating in grid frequency regulation." *Transmission and Distribution Conference and Exposition (T&D), 2016 IEEE/PES*. IEEE, 2016.

[44] Yu, Jie, et al. "Large Scale Control Strategy for Electric Vehicle Cluster Storage Participating in Frequency Regulation." *2017 IEEE 7th Annual International Conference on CYBER Technology in Automation, Control, and Intelligent Systems (CYBER)*. IEEE, 2017.

[45] Lazarewicz, Matthew L., and Alex Rojas. "Grid frequency regulation by recycling electrical energy in flywheels." *Power Engineering Society General Meeting, 2004. IEEE*. IEEE, 2004.

[46] Milano, Federico. "PSAT, Matlab-based Power System Analysis Toolbox." (2002).

[47] IEEE 9-bus Transmission Test System." [Online Available: http://www.kios.ucy.ac.cy/testsystems/index.php/dynamic-ieee-testsystems/ieee-9-bus-modifed-test-system].

[48] IEEE 39-bus Transmission Test System." [Online Available: http://www.kios.ucy.ac.cy/testsystems/index.php/dynamic-ieee-testsystems/ieee-39-bus-modifed-test-system].

[49] Dugan, Roger C. "Reference guide: The open distribution system simulator (opendss)." *Electric Power Research Institute, Inc* 7 (2012): 29.

[50] Distribution Test System: EPRI Ckt 24", [Online Available: http://sites.ieee.org/pes-testfeeders/resources/].

[51] Dubey, Anamika, and Surya Santoso. "On estimation and sensitivity analysis of distribution circuit's photovoltaic hosting capacity." *IEEE Transactions on Power Systems* 32.4 (2016): 2779-2789.

[52] Joshua Stein, Clifford Hansen, and Matthew J. Reno, "The variability index: a new and novel metric for quantifying irradiance and PV output variability," No. SAND2012-2088C. Sandia National Laboratories, 2012.

[53] Cheng, Yunzhi, et al. "Dynamic available AGC based approach for enhancing utility-scale energy storage performance." *IEEE Transactions on Smart Grid* 5.2 (2014): 1070-1078.

[54] “BES,” NERC. Available: https://www.nerc.com/pa/RAPA/Pages/BES.aspx

[55] IEEE Standard for Interconnecting Distributed Resources with Electric Power Systems," in *IEEE Std 1547-2003* , vol., no., pp.1-28, 28 July 2003.

[56] IEEE Standard for Interconnecting Distributed Resources with Electric Power Systems - Amendment 1," in *IEEE Std 1547a-2014 (Amendment to IEEE Std 1547-2003)* , vol., no., pp.1-16, 21 May 2014.

[57] IEEE Standard for Interconnection and Interoperability of Distributed Energy Resources with Associated Electric Power Systems Interfaces," in *IEEE Std 1547-2018 (Revision of IEEE Std 1547-2003)* , vol., no., pp.1-138, 6 April 2018.

[58] Q. Huang and V. Vittal, “Integrated Transmission and Distribution System Power Flow and Dynamic Simulation Using Mixed Three-Sequence/Three-Phase Modeling,” *IEEE Transactions on Power Systems*, vol. 32, no. 5, pp. 3704–3714, Sep. 2017.

[59] R. Venkatraman, S. K. Khaitan, and V. Ajjarapu, “Dynamic Co-Simulation Methods for Combined Transmission-Distribution System and Integration Time Step Impact on Convergence,” *arXiv:1801.01185 [cs, math]*, Jan. 2018.

[60] Q. Huang *et al.*, “A Comparative Study of Interface Techniques for Transmission and Distribution Dynamic Co-Simulation,” in *2018 IEEE Power & Energy Society General Meeting (PESGM)*, Portland, OR, 2018, pp. 1–5.

[61] F. Milano, “An Open Source Power System Analysis Toolbox,” *IEEE Transactions on Power Systems*, vol. 20, no. 3, pp. 1199–1206, Aug. 2005

[62] Boemer, J. C. (2016): On Stability of Sustainable Power Systems. Network Fault Response of Transmission Systems with Very High Penetration of Distributed Generation. PhD diss. Delft University of Technology, Delft, The Netherlands. Intelligent Electrical Power Grids.

[63] Y. N. Velaga, A. Chen, P. K. Sen, G. Krishnamoorthy and A. Dubey, "Transmission-Distribution Co-Simulation: Model Validation with Standalone Simulation*," 2018 North American Power Symposium (NAPS)*, Fargo, ND, 2018, pp. 1-6.

[64] Modeling High-Penetration PV for Distribution Interconnection Studies: Smart Inverter Function Modeling in OpenDSS, Rev. 2. EPRI, Palo Alto, CA: 2013. 3002002271